MINERALOGY AND PETROLOGY OF THE BUCK CLAIM LITHIUM PEGMATITE, BERNIC LAKE, SOUTHEASTERN MANITOBA

A Thesis

Presented to

The Faculty of Graduate Studies

The University of Manitoba

In Partial Fulfillment

of the Requirements for the Degree

Master of Science

by

PAUL G. LENTON

1979

MINERALOGY AND PETROLOGY OF THE BUCK CLAIM LITHIUM PEGMATITE, BERNIC LAKE, SOUTHEASTERN MANITOBA

BY

PAUL G. LENTON

A dissertation submitted to the Faculty of Graduate Studies of the University of Manitoba in partial fulfillment of the requirements of the degree of

MASTER OF SCIENCE

ABSTRACT

A study of the mineralogy, textural zoning and geochemical characteristics of the Buck claim pegmatite dike in southeastern Manitoba was undertaken to obtain data to use in interpreting the petrological and geochemical evolution of the dike.

The dike is a sheet-like body of 1 to 10 m variable thickness and a known extent of 0.4 km north-south and 2.0 km east-west. It is intruded into metamorphosed rocks of upper greenschist to lower amphibolite facies, in the Bird River greenstone belt of the English River subprovince (westernSuperior Province). The dike forms a culmination at the point of the only known surface exposure, a small open-cut trench. The dike dips gently away from the surface exposure to the east and west.

Internal zonation is well developed in the dike, although zone distribution is assymetric. The sequence of zones downward in the pegmatite is: a thin border zone of saccharoidal albite ± quartz; a quartz-albite-muscovite-beryl-tourmaline wall zone; a cleavelandite-microcline perthite-quartz-muscovite-lithian muscovite-beryl-amblygonite intermediate zone; and a quartz-rich core zone containing microcline perthite, triphylite, amblygonite, petalite, pollucite and apatite. Similar zones exist below the core except for the absence of a lower border zone.

The Buck pegmatite belongs to the Bernic-Rush Lake cogenetic swarm of which the Tanco pegmatite is the most famous member. Based on geochemistry and mineralogy the Buck dike can be included in the

classification of pegmatites most enriched in Li, Rb and Cs. The dike shows a progressive inward enrichment in Li, Rb, Cs and Be, and decreasing concentrations of Ca and Fe. The dike is rich in volatile elements, particularly F and B. Rare element minerals found in the dike include tantalite-columbite, beryl, pollucite and cassiterite.

Based on mineralogical, chemical and textural studies it is evident that the dike crystallized totally from a supercritical aqueous fluid without the direct involvement of a silicate melt phase. Subsequent to formation most of the primary assemblage of the dike was altered during an extensive phase of albitization. Hydrothermal and supergene alteration and deposition are evident as late stage processes of limited extent.

A pressure of about 3.0 Kbars and a maximum temperature at the beginning of crystallization of about 650^{o}C are inferred from mineralogical evidence.

ACKNOWLEDGEMENTS

This study was conducted under the guidance of Dr. P. Černý of the Department of Earth Sciences, University of Manitoba. Financial assistance during the study was obtained from operating grants allocated to Dr. P. Černý. The author is indebted to Dr. A. C. Turnock and Dr. H. Gesser of the University of Manitoba and Mr. B. Bannatyne of the Manitoba Department of Mines, Resources and Environmental Management for critical reading of the manuscript. Mr. J. Macek (Manitoba Department of Mines, Resources and Environmental Management) aided in optical determinations. Mrs. B. Lenton drafted the figures and Mrs. J. Poole typed the manuscript.

Permission to enter the Buck claim and to sample the pegmatite was granted by International Mogul Mines Ltd. (Lithium Corporation of Canada). Permission was also given to use the diamond drilling records.

TABLE OF CONTENTS

TABLE OF CONTENTS (Contd.)

TABLE OF CONTENTS (Contd.)

LIST OF TABLES

LIST OF TABLES (Contd.)

LIST OF FIGURES

LIST OF FIGURES (Contd.)

LIST OF FIGURES (Contd.)

LIST OF FIGURES (Contd.)

LIST OF FIGURES (Contd.)

CHAPTER 1

INTRODUCTION

General statement

The Buck pegmatite dike, located in the Precambrian shield of southeastern Manitoba, is an excellent example of a layered differentiated pegmatite. It falls within the general classification as Li, Rb, Cs enriched pegmatite.

While the dike, averaging 6 to 10 m in thickness, is small compared to the nearby massive Tanco pegmatite, it still represents an excellent case for detailed study. Zoning is well developed in the body, although somewhat assymmetric.

The dike is well exposed in a 6 m by 25 m two level open cut trench. All zones of the dike are exposed in the trench which runs roughly parallel to the strike of the body. There is no exposure of the pegmatite away from the area of the trench, but extensive diamond drilling by the Lithium Corporation of Canada has outlined the shape and extend of the body.

CHAPTER 2

LOCATION AND GENERAL GEOLOGY

A Location and access

The Buck pegmatite is located about 190 km ENE of Winnipeg, close to the Manitoba-Ontario boundary (Fig. 2-1). The dike crops out 0.5 km east of the east end of Bernic Lake. The walk from Bernic Lake to the trench is easily accomplished over dry fairly flat ground. Bernic Lake is accessible by float plane or by road from Lac du Bonnet. The final section of road down to Bernic Lake is a private access road for the use of which permission must be obtained from the Tantalum Mining Corporation of Canada Limited. A boat is required for access from the Tanco mine, which is located on the northwestern shore of Bernic Lake. Lac du Bonnet has a float plane base and is accessible from Winnipeg by provincial highways and by rail connection.

B Previous work

The Buck pegmatite, located in the center of the Buck mining claim, has a varied history of exploration and development spanning 50 years of sporadic work. Exploration at the east end of Bernic Lake was confined to three adjacent mining claims, the Buck, Coe and Brilliant (now known as Pegli numbers 1 and 2). Work on the Buck claim is linked closely with the Coe and Brilliant claims. The first record of staking in the Buck claim area was in 1926 when Pegli number 2 was staked. Shortly after this in 1926 the Buck and Coe claims were staked. Initial

Fig. 2-1 Location map showing the position of the Buck pegmatite dike.

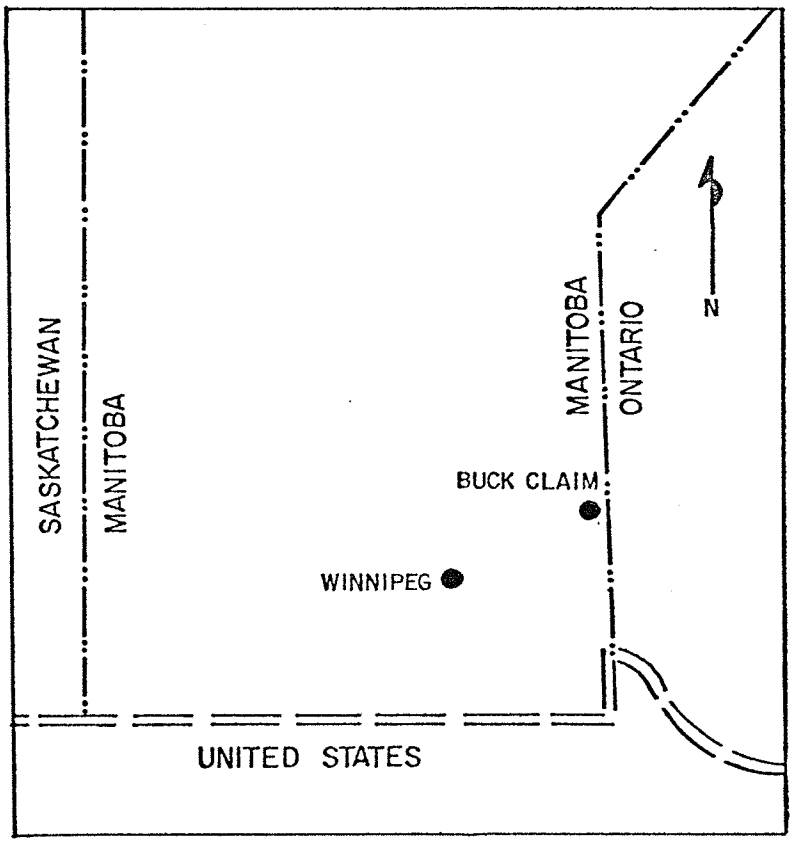

staking was by private individuals but the claims were signed over to the Lithium Corporation of Canada Ltd. in 1934. The three claims were leased by the Lithium Corporation of Canada Limited in 1947 and the lease was renewed in 1968.

From 1934 to 1955 work on the Buck claim consisted of about 600 feet of diamond drilling in 11 drill holes, surface mapping and the opening of a 2 level trench approximately 25 m long by 8 m wide in the exposed portion of the main Buck pegmatite. Approximately 150 tons of rock from the trench were hand sorted and stockpiled in bins at the south end of the quarry. Much of this material remains today at the locality.

In 1956 assessment reports were filed under claims grouping certificates for the Buck-Coe-Pegli Group for 45 drill holes with a total footage of 14,578 feet (445m). Extensive assays for lithia content were done on the split core. At a later date the remaining core was quartered and assayed for tantalum content (personal communication, B. Bannatyne).

The Buck claim was still valid in 1976 and was held by the Lithium Corporation of Canada Limited.

The Buck claim pegmatite was noted by Springer (1950) and Davies (1957) during regional mapping programs but no specific work was done on the pegmatite.

Some surface mapping and sampling was done on the Buck pegmatite in 1972 by the Manitoba Mineral Resources Division (Bannatyne, 1972).

C General geology of the surrounding rocks

The Buck pegmatite occurs in the Archean Bird River greenstone belt in the Western Superior geological province of the Canadian Shield. The Bird River greenstone belt separates the Manigotagan-Ear Falls gneiss belt and the Winnipeg River batholithic belt (Beakhouse, 1976). Together these belts form the English River subprovince (the mobile zone of Wilson, 1976) (Fig. 2-2).

Bird River greenstone belt

The Bird River greenstone belt is an east-west trending belt of metamorphosed volcanic and sedimentary rocks. The belt is bounded by the Maskwa Lake, Marijane Lake and Lac du Bonnet batholiths. The belt has been subdivided by Crouse, Černý, Trueman and Burt (1972), into five subareas (Fig. 2-3).

Subarea 1 consists of mafic lavas and volcanoclastic sediments. It has undergone polydeformation and metamorphism to greenschist facies grade.

Subarea 2 consists of metamorphosed basalt, tuffs and Algoman type iron formations. It has been intruded by gabbro, the ultramafic-gabbroic Bird River sill (Trueman and Macek, 1971), quartz-feldspar porphyry dikes and pegmatite dikes. The rocks form a simple east-trending synclinorium and are metamorphosed to greenschist facies grade.

Subarea 3 is comprised of layers of felsic volcanic and volcanoclastic rocks and metaconglomerate interlayered with felsic to mafic metavolcanic rocks overlain unconformably by metaconglomerate

Fig. 2-2 The western Superior geologic province showing the subdivision into subprovinces. The location of the Buck pegmatite is shown in the English River mobile zone. The subprovince boundaries used are taken from Černý and Trueman (1978).

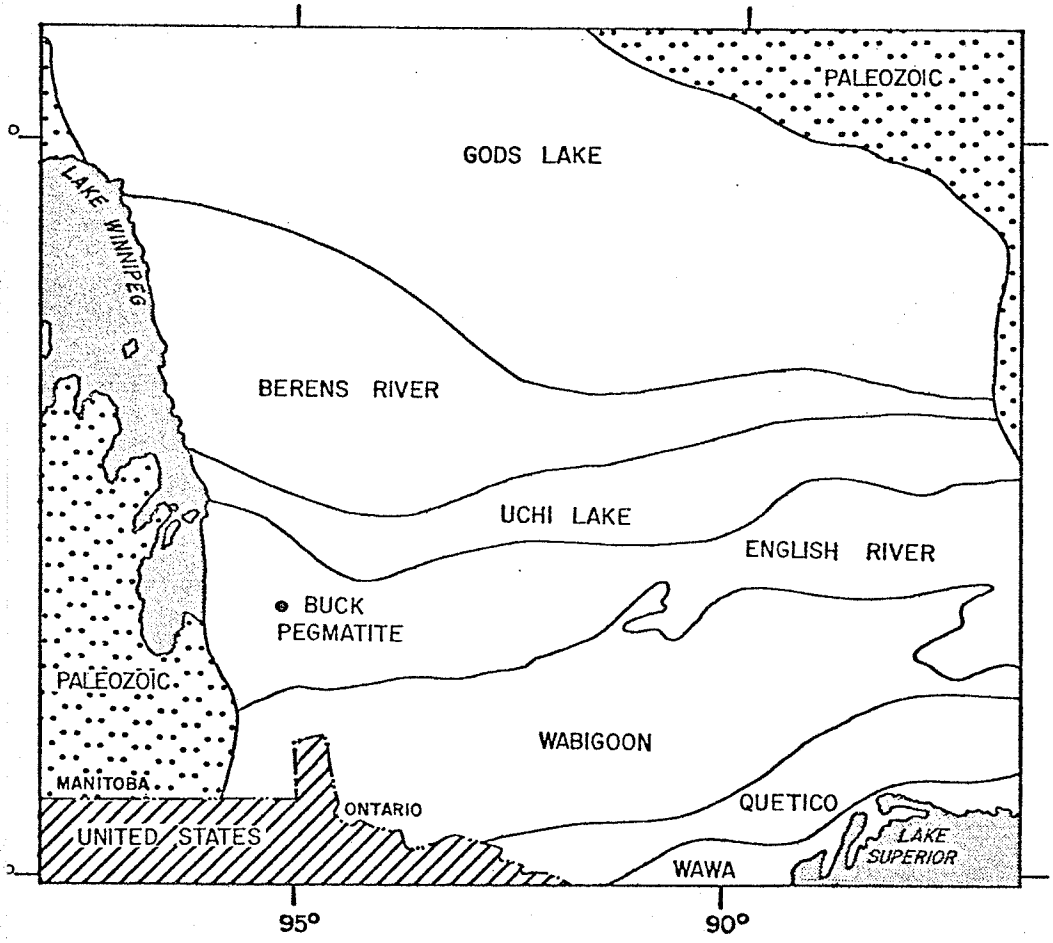

Fig. 2-3 Geologic map of the Bird River greenstone belt showing the subdivision of the belt. The numbers refer to the subareas defined by Trueman as described in the text. The figure is from Černý, 1976.

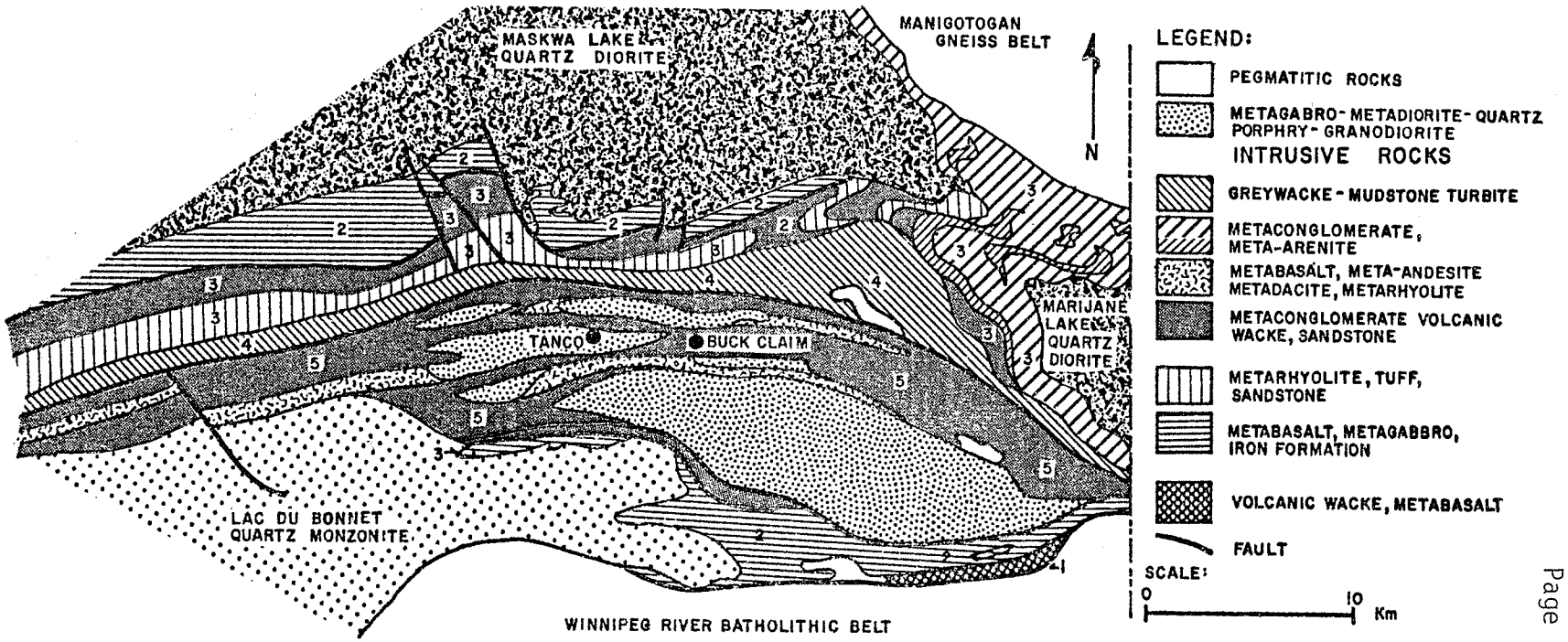

and lithic arenite. The rocks have undergone polydeformation and metamorphism to upper amphibolite facies grade.

Subarea 4 consists of greywacke-mudstone turbidites with interbedded iron formation. These are the youngest rocks in the belt and rest unconformably on the rocks of subareas 1,2,3 and 5. Subarea 4 has undergone little deformation. The rocks were metamorphosed to lower amphibolite facies grade and subsequently retrogressed.

Subarea 5 is equivalent to subarea 3 in age but has been separated because of the presence of synvolcanic stocks of gabbro, diorite, quartz-feldspar porphyry and granodiorite.

Of the batholiths that bound the Bird River greenstone belt, the Maskwa Lake and Marijane Lake quartz diorite-granodiorite plutons appear to have been emplaced synchronously with the development of the tectonic foliation of the layered rocks of the greenstone belt (McRitchie, 1971). The Lac du Bonnet quartz monzonite has been shown to be younger than the other botholiths (McRitchie 1971, Penner and Clark 1971, Farquharson 1975). Farquharson's Rb/Sr age for the Lac du Bonnet intrusive is 2680± 91 m.y.

The Buck pegmatite lies within a sequence of mafic metasedimentary rocks of subarea 5 (Fig. 2-4) with minor mafic metavolcanic rocks. The rocks in contact with the dike are homogeneous hornblende-plagioclase (quartz) amphibolites. The amphibolite is well foliated in the vicinity of the open trench but layering is generally not apparent.

Fig. 2-4 Geologic map of the Bernic Lake area. The positions of the Tanco pegmatite and Buck pegmatites are indicated. The map was adapted from Crouse et al., 1979.

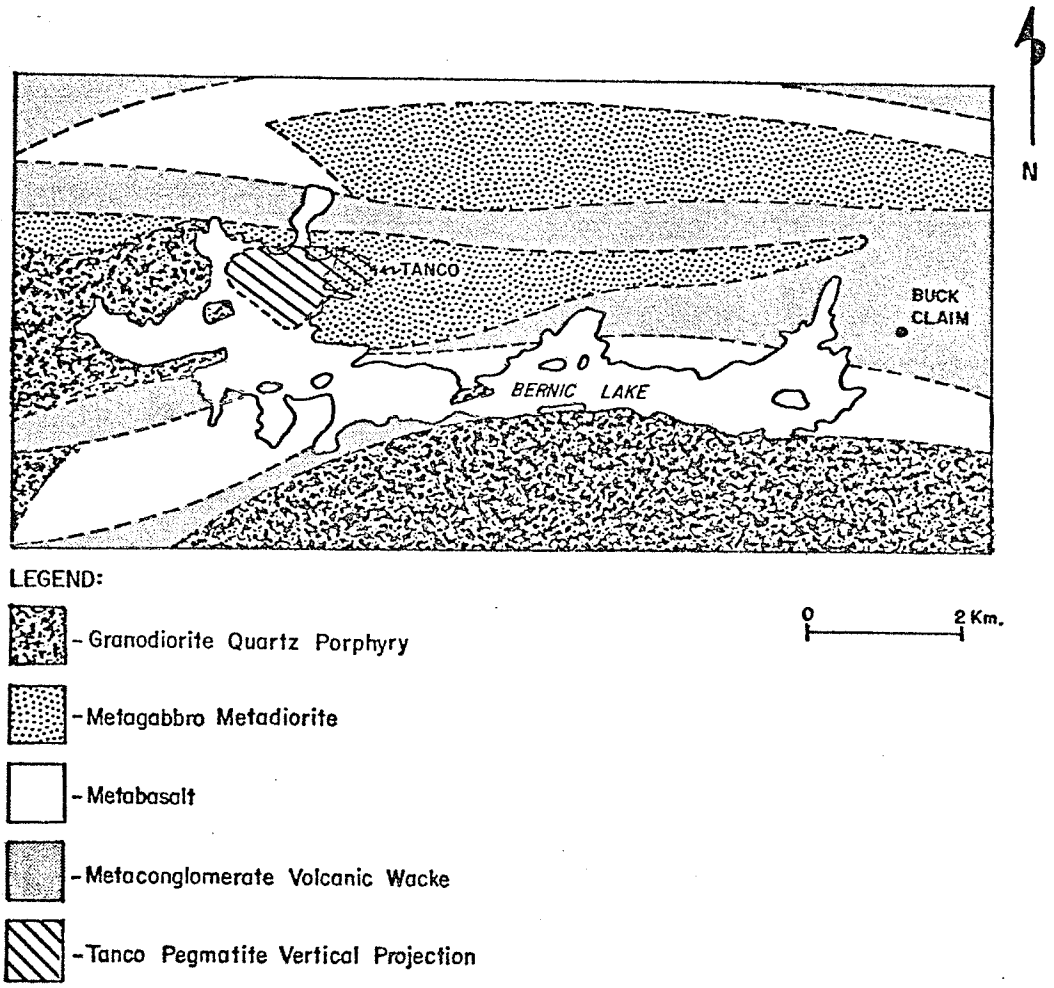

Genetic affiliation of the Buck pegmatite dike

Pegmatite bodies are rarely isolated features, but generally occur in swarms within a geologic district. Černý and Turnock (1971) have classified the various pegmatites of Southeastern Manitoba into cogenetic swarms on the basis of mineralogy and petrochemical similarities. Under this classification the Buck dike is included in the Bernic-Rush Lake Group, of which the Tanco Pegmatite is the largest and best known member.

The source of the fluids from which the pegmatites crystallized is uncertain. The whole process is currently under study as a part of a Department of Regional Economic Expansion subsidiary agreement between the Government of Canada and the Province of Manitoba. Under this program Černý and Trueman (1978) used, as a working hypothesis, the differentiation of the Lac du Bonnet batholith into adjacent bodies of pegmatitic granite. The residual fluids left from the crystallization of the pegmatitic granites formed the pegmatite aureoles. More recently geochemistry suggests partial melting of rare-element-enriched sediments as the process generating pegmatitic granites directly, with the pegmatite aureoles fractionating from them (Černý, Goad and Trueman, 1978).

CHAPTER 3

EXPERIMENTAL METHODS

A Selection and Preparation of Samples

A systematic collection of samples was gathered during a series of short field trips during 1972 and 1973.

These samples fall roughly in two groups; systematically collected suites of minerals that commonly occur either throughout the pegmatite body, or within specific zones, and minerals that had rare occurrences or could not be identified in the field. In the first group would fall the feldspars, beryl, micas, tourmalines, lithium phosphates and apatites. The second group consists of oxides, alteration products, saccharoidal albite samples and unusual occurrences of the major minerals.

In addition to the mineralogical samples taken from the pegmatite body, there was systematic sampling of the country rock at the contacts and at various intervals away from the pegmatite. These samples were thin sectioned to check for contact metasomatic features in the country rock.

Mineral samples that were collected systematically were referenced to their physical location within the open trench and to their position with respect to the mineralogical zoning of the entire pegmatite body. Because both the hanging wall and the footwall of the pegmatite are exposed it was possible to take a reasonably complete cross section of samples.

The selection of samples for analysis was based on attaining

the maximum of chemical and physical data possible in a cross section of the pegmatite body. Because the purpose of this study was to derive a petrologic interpretation of the pegmatite, the type of analysis used for each mineral group was chosen on the basis of the type of data concerning the chemistry and physical characteristics of the pegmatite body as a whole that each mineral was capable of yielding.

Sample preparation was done manually. Samples were chosen for their purity and lack of alteration. After hand crushing the mineral concentrates were made by hand picking under a binocular microscope. Final comminution for chemical analysis and x-ray study was done in an agate mortar and pestle.

B Chemical Analysis

Chemical analysis was done in the Rock Analysis Laboratory of the University of Manitoba by K. Ramlal, R. M. Hill and R. J. Chapman.

Samples analysed for alkakies, alkali earths, iron and lead were totally dissolved in acid and the determinations made on a Perkin-Elmer Atomic Absorption unit. Absorption curves were made using prepared standards on each determination. Alumina content was determined using a Philips X-ray Fluorescense Unit.

C X-ray Diffraction Studies

All x-ray diffraction work was done using a Philips X-ray diffractometer, Philips X-ray powder cameras and a Philips Gandolfi camera. The diffractometer was not monochromated and used an analog output. Where accurate absolute values were necessary the powder mounts

included an internal standard of either annealed fluorite or quartz.

The type of x-ray analysis used varied with the mineral species involved.

(1) Feldspars

Three types of feldspars were examined by x-ray methods; plagioclase, mainly cleavelandite, perthitic microcline, and small crystals of adularia taken from fissures in the core zone. Each plagioclase was x-rayed twice. The first pattern was used to determine the obliquity by the method described by Bambauer et al. (1967) based on the position of the (131) and ($1\bar{3}1$) reflections. The second sample was mixed with $KBrO_3$ and x-rayed according to the method of P. M. Orville (1967) using the plagioclase ($\bar{2}01$) and the $KBrO_3$ (101) reflections to determine the amount of orthoclase in solid solution.

Similarly the potassium feldspar was x-rayed to determine obliquity according to the method of Goldsmith and Laves as described by Orville (1967) based on d(131) and d($1\bar{3}1$) and the amount of albite in solid solution in the potassium feldspar phase as described by Orville (1967).

The adularia was x-rayed according to the methods of Wright and Stewart (1968) in order to refine the unit cell parameters. Powder smear mounts were made containing 1 part in 4 of synthetic annealed fluorite (a_o= 5.4620 at 25°C) as an internal standard. This sample was run on a diffractometer with CuK_{α_1} radiation from 57° to 10° 2θ. Two separate trials, each consisting of three runs on the diffractometer were made. The data of three runs was averaged giving two independent

sets of accurate 2θ values for the adularia. Unit cell parameters, based on the two independent sets of 2θ values, were refined using the computer program developed by Evans, Appleman and Handwerker (1963). The results with the lower standard errors were chosen as representative.

A preliminary attempt to study the adularia using Buerger precession photographs indicated complex zoning and twinning in the crystals, as was confirmed optically. Because of the complexity of the problem compared to the amount of useable data to be derived, single crystal x-ray investigations were abandoned.

(2) Micas

A selection of samples representing all the morphological types of micas in the pegmatite were x-rayed using a 114.6 mm Debye-Scherrer/Straumanis Camera. Careful measurements were made on the resulting films to determine the structural polytypes present. All powder samples were prepared by filing the sample to avoid distortion or destruction of the structure.

(3) Tourmalines

A total of 11 samples of tourmaline, representing a cross section of the occurrences in the pegmatite, were x-rayed to determine precise unit cell parameters.

Powder smear mounts of tourmaline containing 1 part in 6 of annealed fluorite (a_o= 5.4620 at 25°C) as an internal standard were x-rayed on a diffractometer. The samples were run from 12° to 70° 2θ CuK_{α_1} twice. The samples were then reground and remounted and run

twice again. The corrected, indexed d-spacings were averaged and the unit cell parameters refined using the computer program devised by Evans, Appleman and Handwerker (1963).

(4) Tantalite

The identical techniques used to refine the unit cell parameters of the tourmaline were applied to 3 chip samples taken across a single zoned crystal of tantalite. The only difference was that the samples were run on the diffractometer 3 times consecutively without being reground and remounted between runs. The mounts were rotated 180^{o} between diffractometer runs.

(5) Amblygonite-montebrasite series

A total of 72 samples were selected from the amblygonite-montebrasite group to be x-rayed. These represent 46 random samples and 26 specifically located samples.

The technique of indirect determination of fluorine content presented by Černá, et al. (1973) was used. This involved running powder smear mounts on a diffractometer from 26^{o} to 29^{o} 2Θ CuK_{α_1}. The angular distance between the $\bar{1}01$ reflection and the $1\bar{2}1$, $\bar{1}10$, $0\bar{2}1$, 011 and 120 reflections can be related graphically to the weight percent fluorine in the sample.

(6) General Identification

Any mineral that could not be recognized in hand sample was x-rayed. Where sufficient sample was present, a diffractometer was

used to identify the mineral. When only a small amount of material was available a powder x-ray camera was used. In the special case of single grains in thin sections, the grains were picked out of the thin section with a needle and identified using a Gandolfi Camera.

D Optical Studies

(1) Refractive index determination

Refractive indices were determined using the Becke line method on crushed fragments in standard Cargille immersion liquids. The light source for the microscope was monochromated using either a 5890 Å sodium lamp, or a 5890 Å interference filter. All immersion liquids were checked with an Abbe refractometer illuminated with a sodium lamp.

In situations where the optical orientation of mineral grains was difficult to control, i.e. in the absence of a strong cleavage, the grains were mounted in well slides and the refractive index determination made on a universal stage.

(2) Thin sections

Thin sections were cut for two reasons:

(a) to study texture, alteration and zoning of different mineral species within the pegmatite.

(b) to check for metasomatic alteration in the amphibolite country rocks.

CHAPTER IV

SHAPE, STRUCTURE AND ZONING OF THE BUCK PEGMATITE

A Shape of the pegmatite and its relation to the country rocks

The Buck pegmatite is one of a series of subparallel sheet-like dikes intruding metasedimentary and metavolcanic rocks at the east end of Bernic Lake. Based on extensive exploration work done by the Lithium Corporation of Canada Limited, including trenching and 56 diamond drill holes, a fairly comprehensive picture of the shape of the dike has been determined. The diamond drilling established a known extent of the dike in a north-south direction of approximately 0.4 km. A single hole drilled by Canol Metal Mines in 1961 encountered the Buck dike approximately 2 km west of the trench in the Buck claim (P. Černý, pers. comm.).

The pegmatite studied is the middle pegmatite of 3 shallow dipping sheets that strike in a general north west direction. While the lower, thicker dike appears to be a very uniform flat sheet-like body, the Buck pegmatite is irregular or contorted (Fig. 4-1). As the pegmatite is not foliated or tectonicly deformed the irregular shape must be a reflection of the fracture or zone of weakness it intruded. The isopach map, Fig. 4-2, shows that thickness varies considerably over short distances. The thickness decreases rapidly to the east, and the pegmatite was not found in drill holes 100 m east of the open trench. A generalized north-facing cross section, Fig. 4-3, shows the irregular nature and the boot shaped termination at the location of the trench.

The layered amphibolitic country rock strikes east-west,

Fig. 4-1 Elevation contours (at 10 foot intervals) on the upper contact of the pegmatite. The reference elevation is a datum plane 10 feet below Bernic Lake water level. The map is based on information obtained from 23 drill holes.

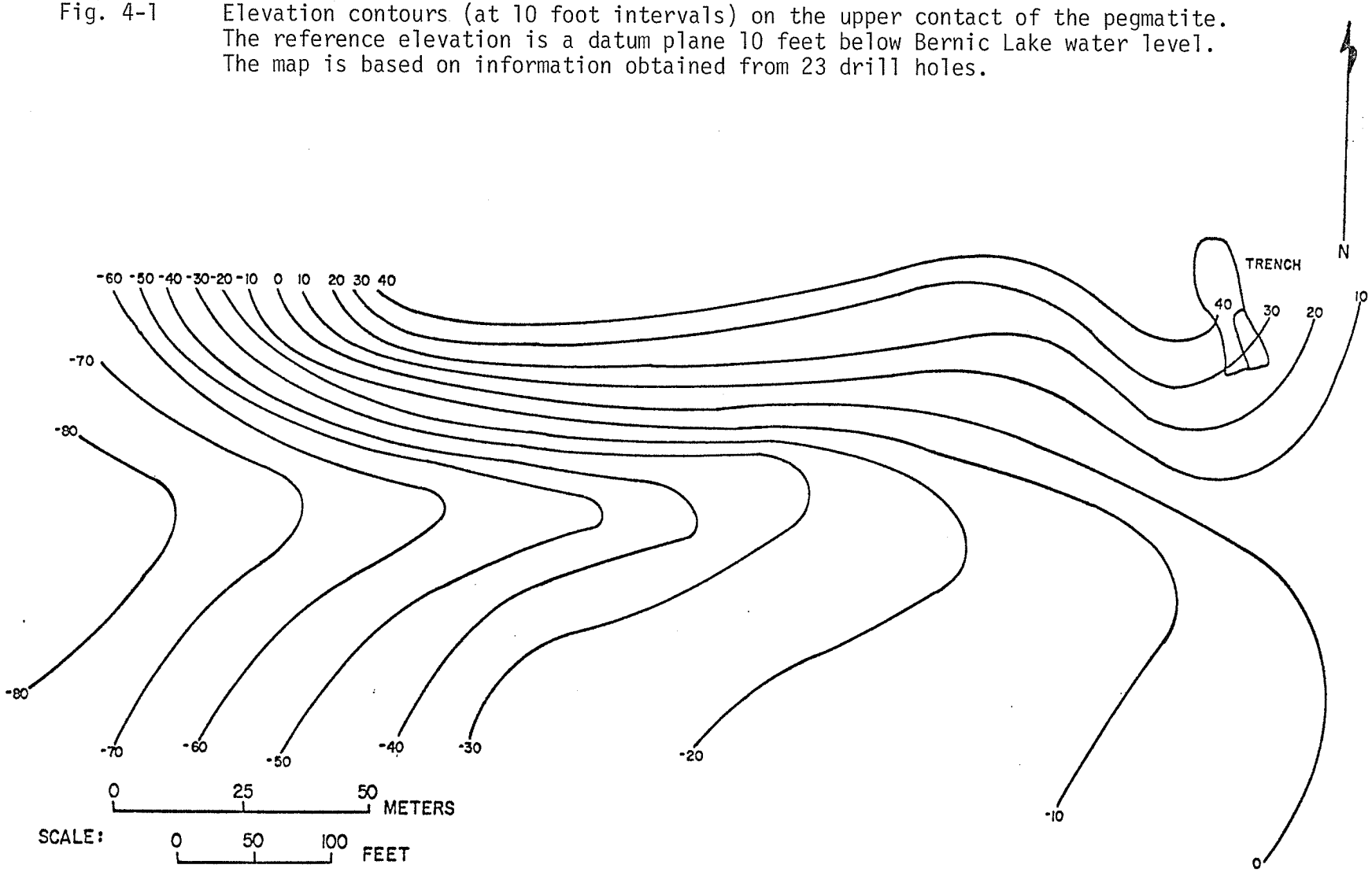

Fig. 4-2 Interpretive isopach contour map of the Buck pegmatite. The contour interval is 2 feet. Note the irregularity of thickness and the rapid thinning of the dike to the east and south. The map is based on information obtained from 23 drill holes.

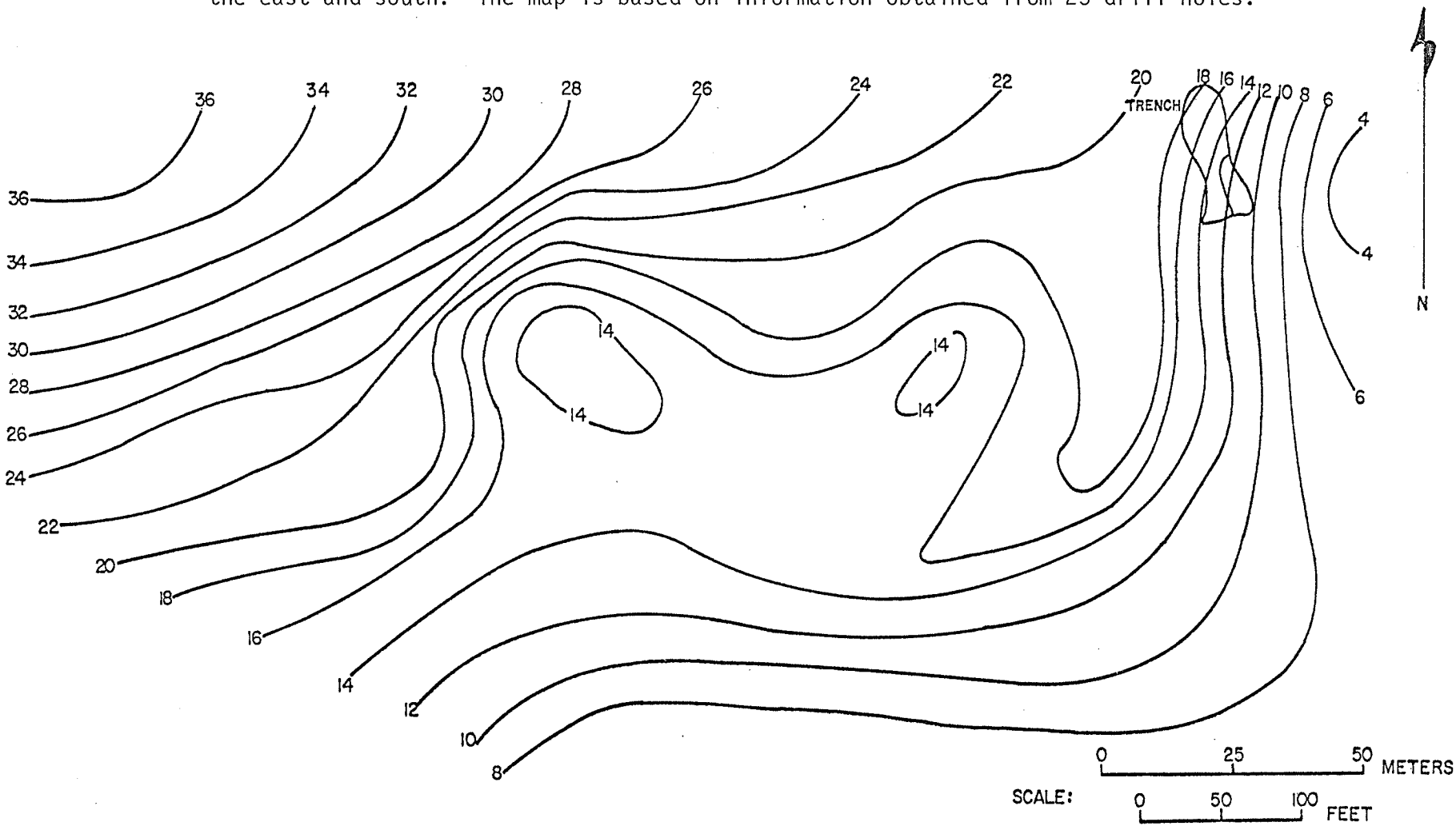

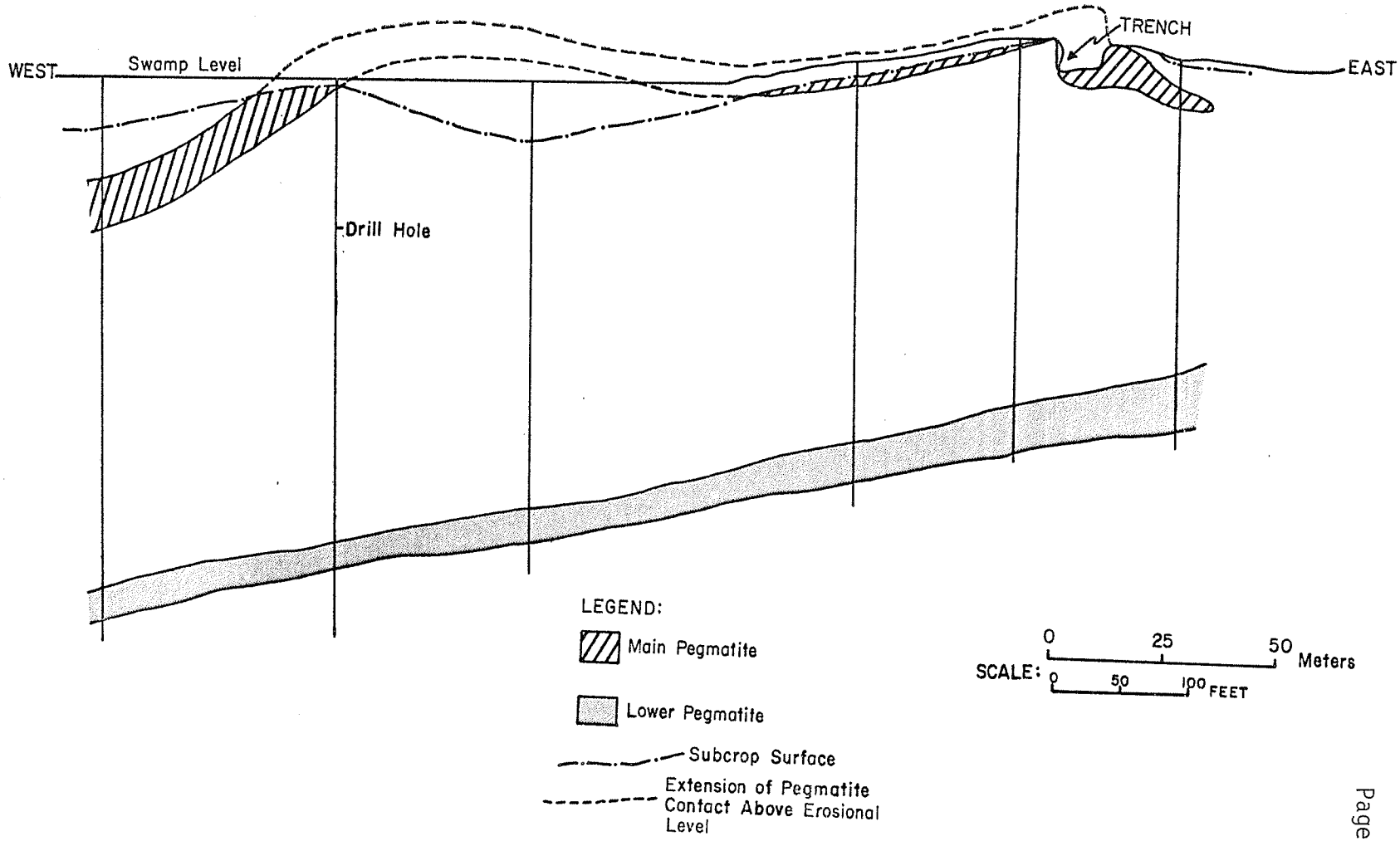

Fig. 4-3 Interpretive cross section of the Buck pegmatite based on drill hole data and surface mapping of the trench.

dipping steeply to the north so the layering is crosscut by the pegmatite. Intrusion appears to have been a passive feature. There is no deformation of the hanging wall contact and no inclusions of country rock were found in the upper part of the pegmatite. The footwall of the pegmatite is exposed only on the west edge of the trench. Here the contact is vertical following the downward offset of the pegmatite. In this part of the dike many small inclusions of amphibolite are caught up in the pegmatite. Although the inclusions are within the pegmatite, Fig. 5-40, they form an agmatite of angular fragments showing no evidence of extensive lateral transport.

Although no extensive mapping was done away from the pegmatite, the presence of a strong westward dipping shallow joint-fracture set was noted. This fracture set was also identified on the shores of Bernic Lake. These dilation fractures are probably the weakness zone along which the three parallel pegmatite dikes intruded. The offset in the pegmatite at the east end may be due to an early steeply dipping shear which may in part be responsible for the extensive brecciation of the amphibolite along the lower contact of the dike.

B Zoning

The pegmatite is well differentiated with mineral zoning easily mappable in the trench. Although the upper and lower halves are not mirror images of each other, there is a rough symmetry across the pegmatite. The zones, as shown in Fig. 4-4, are:

Exomorphic zone - E

Intrusion of the pegmatite resulted in very little metasomatic alteration of the country rocks. The typical hornblende-plagioclase-

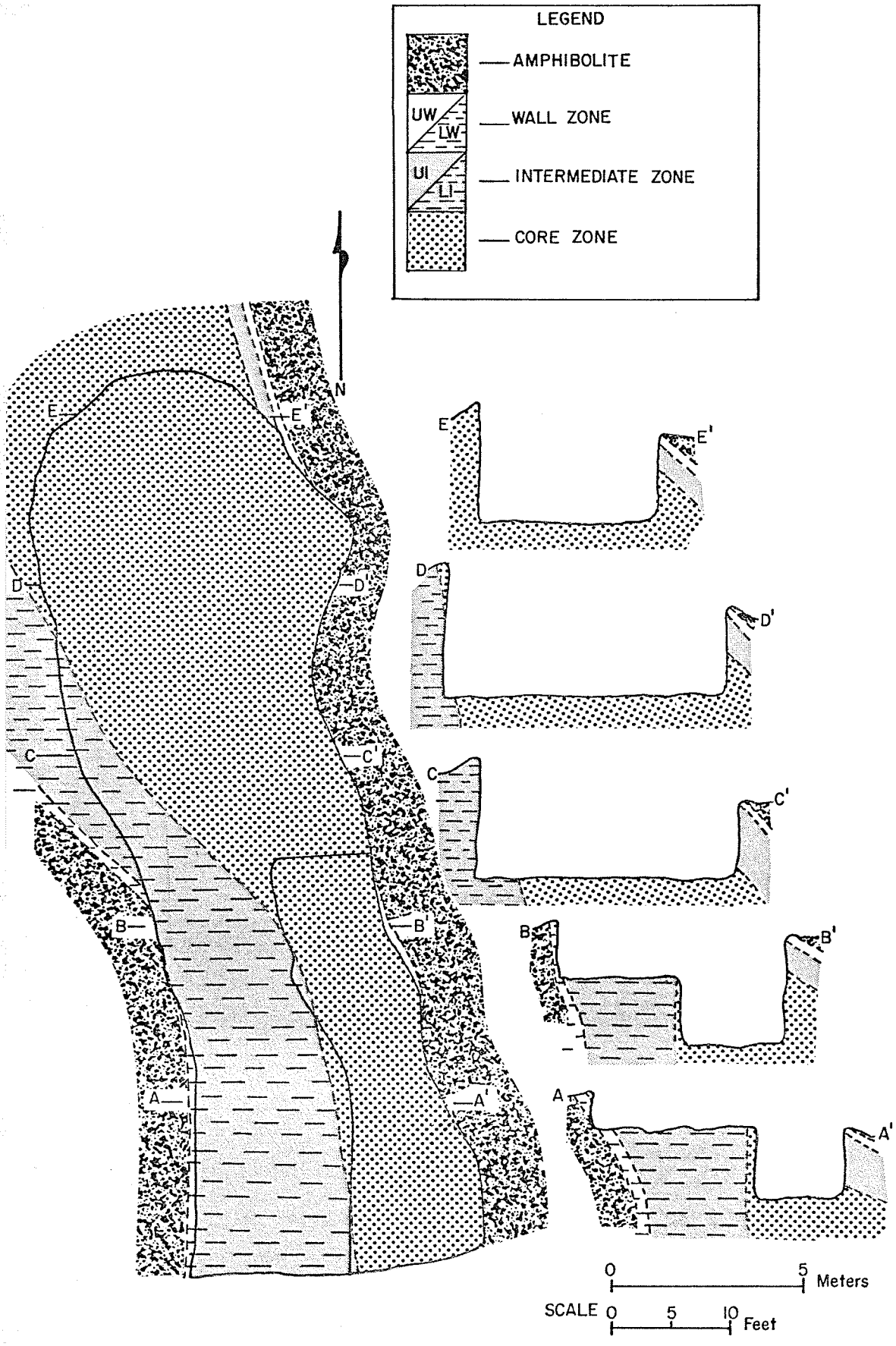
LEGEND
AMPHIBOLITE
UW
LW
WALL ZONE
UI
LI
INTERMEDIATE ZONE
CORE ZONE
N
E
E'
D
D'
C
C'
B
B'
A
A'
0
5
Meters
SCALE 0
5
10
Feet

quartz assemblage of the amphibolite is altered to a biotite-epidote-chlorite-sericite-quartz assemblage for a distance of 1 to 2 cm from the contact. Other retrogressive features are restricted to the edges of small fractures near the pegmatite. Small crystals of dark indigo tourmaline were found 3 m above the pegmatite, and traces of holmquistite were found in fractures up to 8 m above the pegmatite.

Border zone - B

A continuous 5 mm layer of saccharoidal albite found along the hangingwall contact.

Upper wall zone - UW

A 30 cm layer dominated by large tapering crystals of black tourmaline growing normal to the pegmatite contact. The tourmalines are surrounded by quartz, albite and muscovite.

Upper intermediate zone - UI

Mainly composed of pink cleavelandite and quartz, this zone contains beryl, muscovite, lithian muscovite, microcline and amblygonite. The thickness ranges from 1 to 2 m.

Core zone - C

The broad central zone is massive quartz containing large block crystals of microcline, amblygonite, lithiophilite-triphylite and spodumene-quartz aggregates pseudomorphous after

petalite. Symmetry exists in this zone. The lithiophilite-triphylite is concentrated in the middle of the zone; the amblygonite, microcline and petalite pseudomorphs are located along the upper and lower edges of the core.

Lower intermediate zone - LI

Located below the C zone it has essentially the same mineralogy as the UI zone although the lower zone is thicker than the upper zone.

Lower wall zone - LW

The lower wall zone is twice as wide as the UW zone. Although the mineralogy is similar to the UW zone the texture is considerably different consisting of fine saccharoidal albite containing stubby tourmaline crystals and numerous xenoliths. There is no equivalent to the B zone on the lower contact of the pegmatite.

C Mineral distribution and textural relations within the zones

The zones of the pegmatite are based on gross textures and mineral distributions. The characteristic minerals and associated textures for each zone are listed in Table 4-1. While some minerals occur in several zones, they may have a characteristic abundance or scarcity in some zones. Figure 4-5 shows schematic distributions for 9 major minerals.

Table 4-1 Mineral distribution and textures in the Buck Pegmatite. See Table 4-2 for mnemonic codes for minerals.

Zone	Major Minerals	Accessory Minerals	Textural Relations
B	AB,QZ		fine grained (0.02 mm) saccharoidal albite
		TM	doubly terminated 1-3 mm crystals in saccharoidal albite
		GR	0.5 mm corroded crystals - rare
		MV	irregular flakes throughout saccharoidal albite
UW	TM		10 to 30 cm tapering crystals, commonly radiating
	AB,QZ		grey platy albite with QZ between plates surrounding TM
	MV		flat plates intergrown with albite
		AM,BR	anhedral crystals no more than 1 cm across; surrounded by AB-MV near TM tips
		TL	acicular crystals included in TM
		AP	anhedral crystals throughout the zone
UI	AB (CV)		globular radiating masses
	QZ		clear irregular masses and interstitial fillings; often fractured and veined by late pink AB
	MV		randomly oriented hexagonal plates
	LM-LP		closely associated with CV, either in the cores of radiating masses or over the surfaces of spherical aggregates
	MC		irregular blocks penetrated by AB veinlets
	AM		subhedral blocks surrounded by QZ-CV; surfaces in contact with CV corroded

Table 4-1 Mineral distribution and textures in the Buck Pegmatite. (Cont'd.) See Table 4-2 for mnemonic codes for minerals.

Zone	Major Minerals	Accessory Minerals	Textural Relations
		sodic MB	surrounded by radiating fans of CV
		BR	randomly distributed in QZ-AB-MV
		VD	fractured columnar crystals included between MV sheets; occasionally flat bladed crystals
		TL	euhedral crystals and irregular masses in CV; clay-like alteration in CV around TL
		AP	irregular blue masses in CV-QZ-MV
		LL-TP	irregular grains finely dispersed in AB
C	QZ		represents the bulk of C zone-irregularly fractured with late stage minerals crystallized as crusts in fractures
	MC		large blocks of perthitic MC floating in QZ
	AM		pendant columns rooted in CV of zone UI and surrounded by QZ or as blocky crystals floating in QZ
	LL-TP		large irregular aggregates floating free in QZ
	PL		totally altered to green clay; associated with QZ-AB-LM
	PT (QZ-SD)		SD-QZ pseudomorphs of PT floating in QZ, veined by late LM
		AP	massive monomineralic veins in fractures in the QZ; euhedral crystals and drusy crusts in fractures
LI	QZ AB(CV)		texturally the same as the UI zone
	MC		only remnants remaining; heavily altered to AB

Table 4-1 Mineral distribution and textures in the Buck Pegmatite. (Cont'd.) See Table 4-2 for mnemonic codes for minerals.

Zone	Major Minerals	Accessory Minerals	Textural Relations
	AB aplite		veins of saccharoidal AB+QZ+AP in fractures
	AM		small blocky crystals surrounded by CV
	MV-LM		textures similar to UI but micas are less abundant
		BR	irregular or tapering crystals in AB-QZ-MV
		AP	irregular blue masses in QZ+AB
		TL	small wedge shaped crystals in AB,QZ+AP
		VD	included in sheets of MV
LW	AB,QZ		most of the lower wall zone is medium grained to saccharoidal albite with irregular masses of QZ
	TM		subhedral or irregular black TM scattered randomly through fine grained AB
	MV		small plates randomly oriented in AB
		AP	the saccharoidal albite is rich in fine grained colorless AP

Table 4-2 Mnemonic codes for the minerals discussed in this paper.

AB	albite
AD	adularia
AM	amblygonite
AP	apatite
BR	beryl
CV	cleavelandite
LL	lithiophilite
LP	lepidolite
LM	lithian muscovite
MB	montebrasite
MC	microcline
MV	muscovite
PL	pollucite
PT	petalite
QZ	quartz
SD	spodumene
TD	tetrahedrite
TL	tantalite
TM	tourmaline
TP	triphylite
VD	verdelite

Fig. 4-5 A schematic representation of the relative distribution of 11 major minerals in the pegmatite. This diagram shows the general trends of mineral distribution but is not meant to imply absolute quantities of minerals.

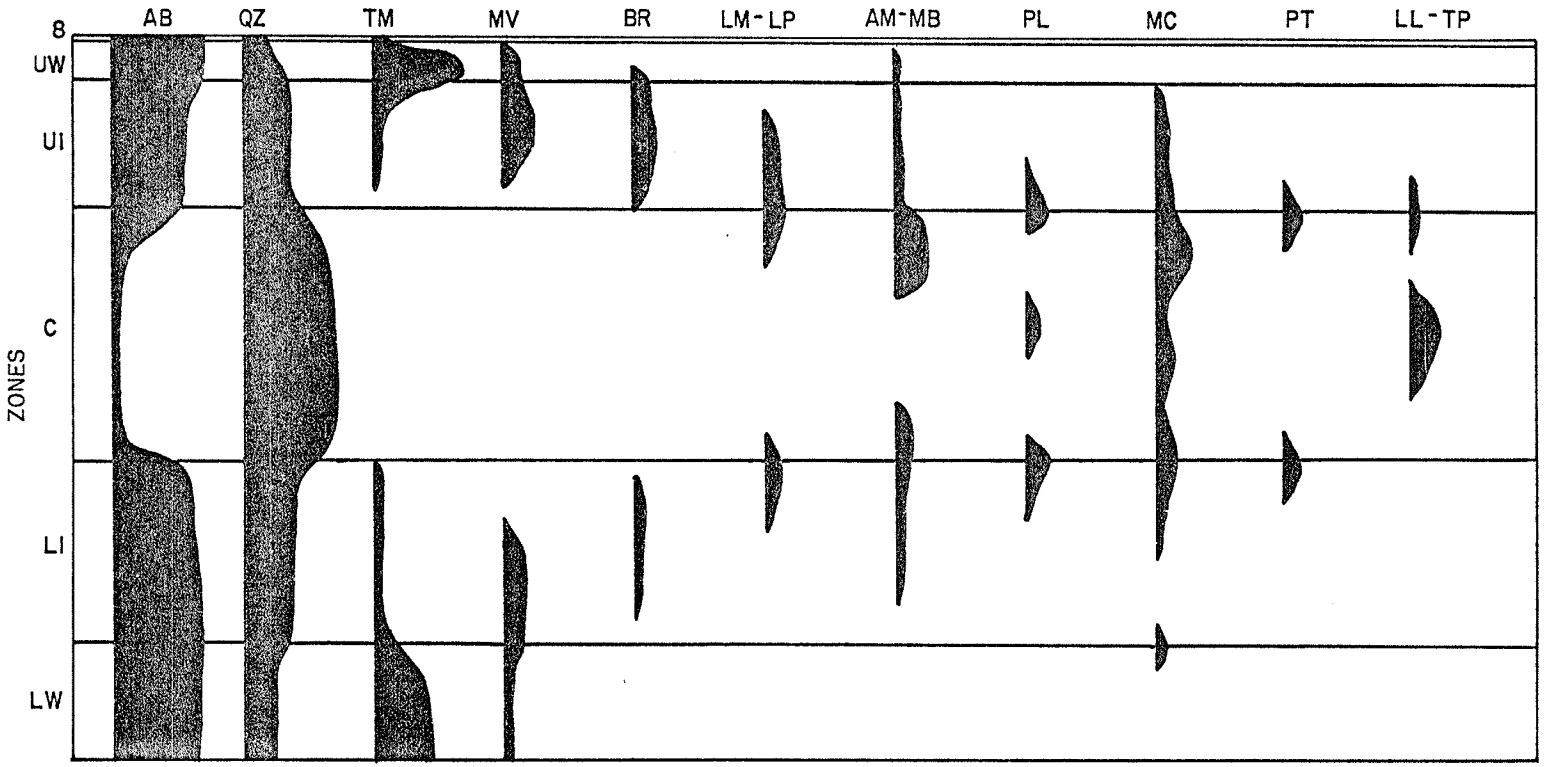

CHAPTER V

DESCRIPTIVE MINEROLOGY

A General statement

During the course of this study most of the mineral phases in the pegmatite were studied. The extent of work committed to each mineral or mineral group in general reflects the contribution the resulting data can make towards a petrogenetic interpretation of the Buck pegmatite dike. The following sections are not intended as a complete classical descriptive mineralogical study of all phases present.

The following descriptions include chemical, optical, x-ray and textural data. Each section contains a summary of data for a particular mineral or mineral group. Conclusions to be drawn from this data will be found in later chapters.

B Potassium feldspar

Potassium feldspar, $(K,Na,Rb,Cs,Ca)\ AlSi_3O_8$, occurs in two forms in the Buck pegmatite. The most common form is blocks of perthitic microcline distributed through much of the interior of the dike. The second form, adularia, is restricted to rare late occurrences in crystal-coated fractures in the quartz core. Adularia will be discussed later in this section.

Large mottled blocky crystals of microcline, Fig. 5-1, are found throughout the core zone and in the intermediate zones. The UW zone contains no K-feldspar, but remnants of one highly altered crystal were found at the top edge of the LW zone. In general the microcline

Fig. 5-1 A blocky crystal of perthitic microline (rusty red) in the upper part of the quartz core zone.

crystals in the core zone are unaltered, whereas the crystals in the intermediate zones are moderately altered. The typical alteration of the K-feldspar involves albitization accompanied by the growth of a lithian muscovite along the boundary between the microcline and albite (Fig. 5-2). The mica produced during the alteration is a brownish plumose lithian muscovite moderately enriched in Li,Rb and Cs (cf. LM-mica, Chapter V, section D).

All the microcline examined contained albite as a second phase. The albite can occur in any of 5 forms, Fig. 5-3, as either an exsolved phase in a perthite or as discrete crystals or veinlets of albite. The veinlets of albite are mixed with mica and quartz representing late alteration of the microcline. The discrete subhedral crystals (type 4, Fig. 5-3) of albite are of uncertain origin, but because of their random orientation and the cross-cutting nature of the exsolved albite it is likely they represent inclusions of primary albite trapped in the microcline during its crystallization. The typical texture of the perthitic microcline is illustrated in Fig. 5-4.

Chemical variations

Sixteen samples of microcline were analysed for alkali elements, calcium and lead (Table 5-1). Of these the first 10 were collected by the author from recorded locations, while the 6 samples designated BC-C-1 were collected by P. Černý and although they come mainly from the core and UI zones no exact locations were noted for the samples. Samples BC-67-I and BC-68-O are from the same "crystal", respectively from its interior and from its outer edge. The individual

Fig. 5-3 Five forms taken by albite in microcline crystals.

Fig. 5-2 A block of microcline (mottled pink and white) partially altered to albite (reddish orange). The black lines between the microcline and the albite are aggregates of lithian muscovite and quartz.

1. String Perthite
   (a) En Echelon
   (b) Spotted

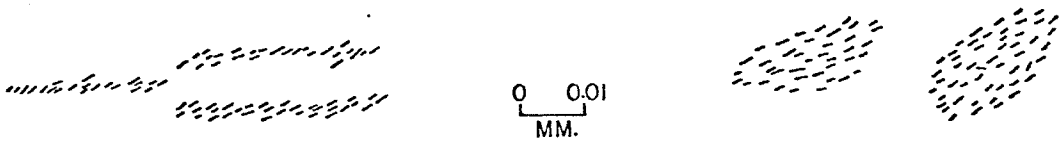

2. Flame or Plume Perthite in 2 Directions

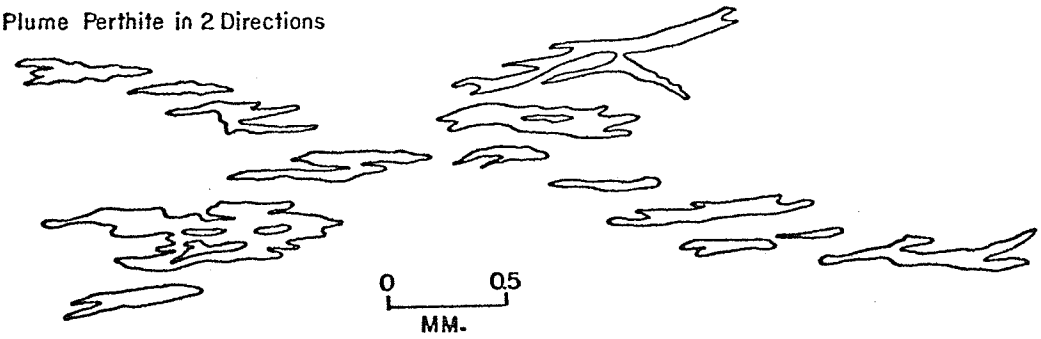

3. Patch Perthite
   (a) Alone
   (b) With String Perthite

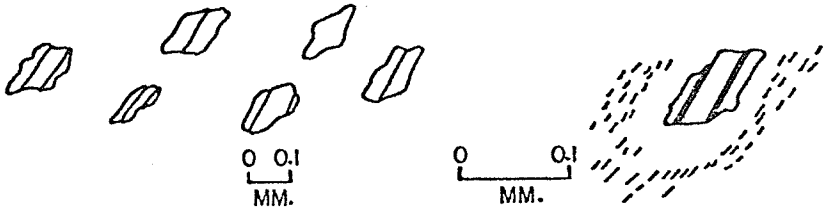

4. Subhedral Grains of Non-Perthitic Albite
   (a) Alone
   (b) Combined with Types I and 2 Perthites

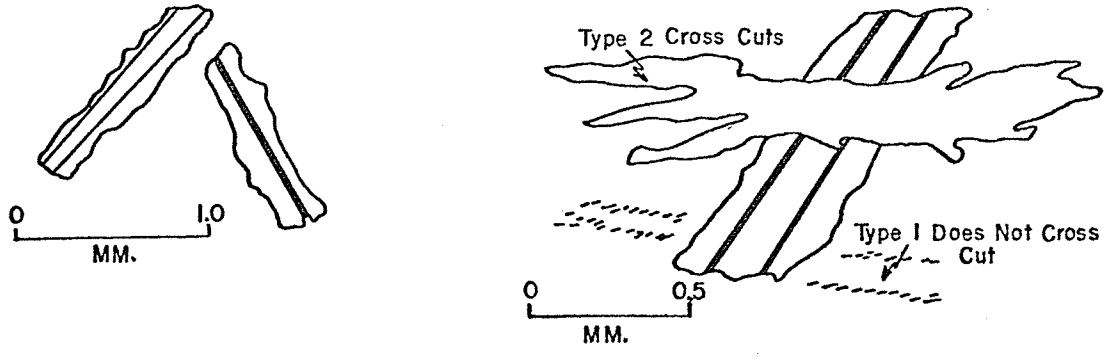

5. Cross Cutting Veinlets of Late Albite

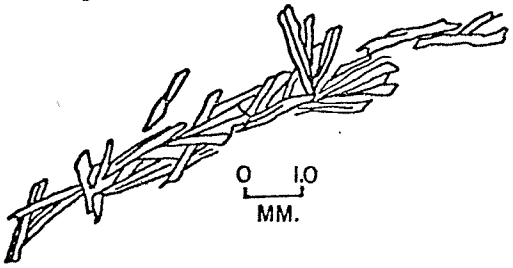

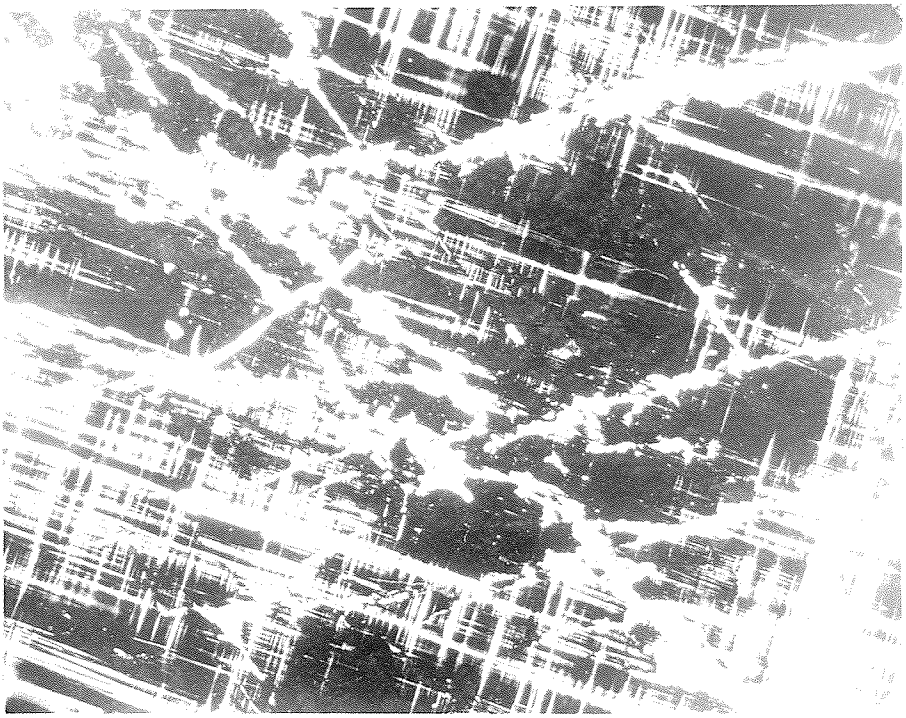

Fig. 5-4 A microphotograph of perthitic microcline showing grid twinning and a complex pattern of albite stringers following mainly the (1$\bar{1}$0) and (1$\bar{1}$0) planes. Cross polarized light.

Table 5-1 Results of chemical and x-ray analyses of microcline.
The symbol Δ is the triclinicity; Δ = 12.5 (d 131 - d $1\bar{3}1$).

Sample Number	Zone Location	Wt. % K_2O	Na_2O	Rb_2O	Cs_2O	CaO	PbO	Δ	Mol % Ab_{ss} By x-ray	K/Rb	Rb/Cs
BC 17	UI	10.84	3.83	1.14	0.052	0.161	nil	0.950	3	8.6	21.3
BC 18	UI	13.88	1.80	1.12	0.059	0.043	0.0004	0.862	7	11.3	18.3
BC 19	UI	14.20	0.72	1.48	0.059	0.036	nil	0.911	4	8.7	24.2
BC 130	Top of C	13.60	1.11	1.49	0.069	0.353	0.0010	0.950	5	8.3	21.0
BC 63	C	14.33	1.27	1.28	0.078	0.208	nil	0.852	4	10.2	15.8
BC 66	C	13.25	1.81	1.28	0.065	0.037	0.0001	0.800	3	9.4	19.2
BC 67-I	C	13.19	1.55	1.57	0.092	0.018	nil	0.863	2	7.6	16.5
BC 68-0	C	14.52	1.00	1.81	0.124	0.102	0.0006	0.867	2	7.3	14.1
BC 69	C	13.14	1.41	1.66	0.104	0.025	nil	0.876	2	7.2	15.5
BC 124	LI	12.80	1.69	1.31	0.091	0.168	0.0010	0.838	2	8.9	13.9
BC-C-1		12.14	1.94	1.36	0.079	0.019	nil			8.1	16.6
BC-C-2		13.20	1.36	1.31	0.092	0.038	0.0030			9.1	13.8
BC-C-3		13.20	1.72	1.25	0.074	0.019	nil			9.6	16.3
BC-C-4		13.20	1.80	1.31	0.085	1.13	nil			9.1	15.0
BC-C-5		13.70	1.90	1.09	0.072	0.021	0.0050	0.888		11.4	14.7
BC-C-6		12.31	1.72	1.43	0.100	0.016	0.0010	0.963		7.8	13.9

feldspar components of each sample, Table 5-2 and Fig. 5-5, show the following trends:

1. The Cs and Rb-feldspar contents are higher in the center of the dike than at the edges.
2. The Or content remains roughly constant. The outermost sample, BC-17, shows a very high Ab content (32.4 mol%) and low Or content. This is probably caused by extensive veining of the sample by late albite.
3. The Ab content behaves erratically. This is caused by sampling problems; it is impossible to obtain a sample with a uniform average content of exsolved Ab and no late albite. Similarily the anorthite content follows no pattern.
4. The amount of Ab in solid solution in the K-feldspar decreases toward the core.
5. While the sample pair BC-67 and 68 shows different absolute contents of Rb-feldspar and Cs-feldspar the K/Rb and Rb/Cs ratios are roughly equal for both samples. The variation in contents of rare alkali feldspars is a reflection of the amount of albite in each mass and not indicative of a chemical zoning.

X-ray studies

The x-ray techniques of Orville (1967) were used to determine the Ab in solid solution in the K-feldspars. The obliquity values were determined according to the method of Goldsmith and Laves (1954). The significant features of the Ab solid solution have already been discussed.

The obliquity values, Δ, are a measure of the degree of deviation of the feldspar structure from the monoclinic form. The values

Table 5-2 Calculated feldspar compositions of the analysed microcline samples.

Sample	mol %					
Numbers	Or	Ab	Rb-fs	Cs-fs	An	Σ fs
BC 17	64.06	32.41	3.96	0.14	0.80	101.37
BC 18	82.03	15.23	3.89	0.16	0.22	101.53
BC 19	83.91	6.09	5.14	0.16	0.18	95.49
BC 130	80.37	9.39	5.18	0.18	1.75	96.87
BC 63	84.68	10.75	4.45	0.21	1.03	101.12
BC 66	78.30	15.32	4.45	0.17	0.18	98.42
BC 67-I	77.95	13.12	5.46	0.24	0.09	96.86
BC 68-0	85.81	8.46	6.29	0.33	0.51	101.40
BC 69	77.65	11.93	5.76	0.27	0.13	95.74
BC 124	75.64	14.30	4.55	0.24	0.83	95.56
BC-C-1	71.74	16.41	4.73	0.21	0.10	93.19
BC-C-2	78.01	11.51	4.55	0.24	0.19	94.50
BC-C-3	78.01	14.56	4.34	0.20	0.10	97.21
BC-C-4	78.01	15.23	4.55	0.22	5.61	103.62
BC-C-5	80.96	16.08	3.79	0.19	0.10	101.12
BC-C-6	72.75	14.56	4.97	0.26	0.08	92.62

Fig. 5-5 Variation in the contents of feldspar components of the K-feldspar samples across the dike.

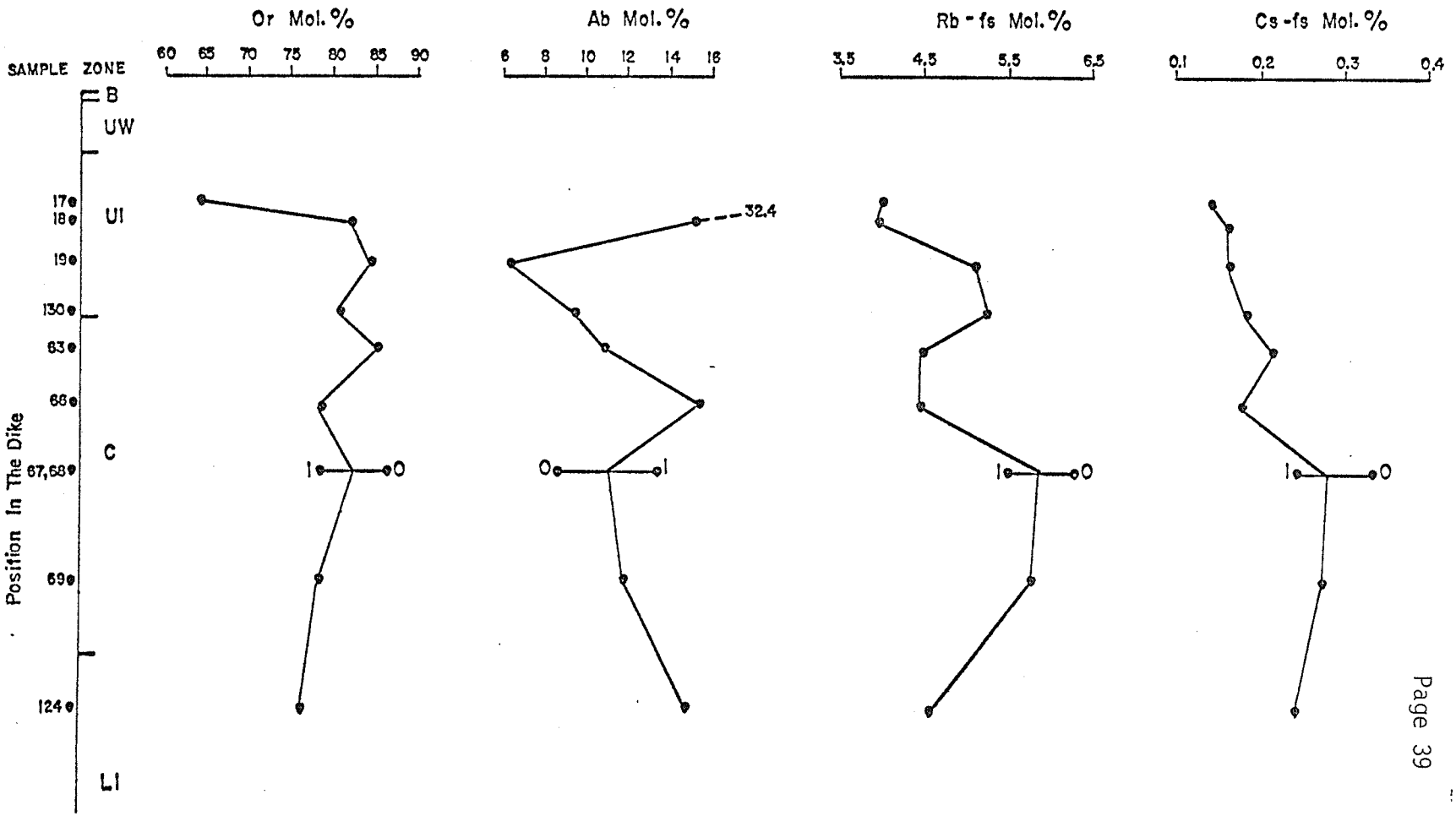

Fig. 5-5 Continued.

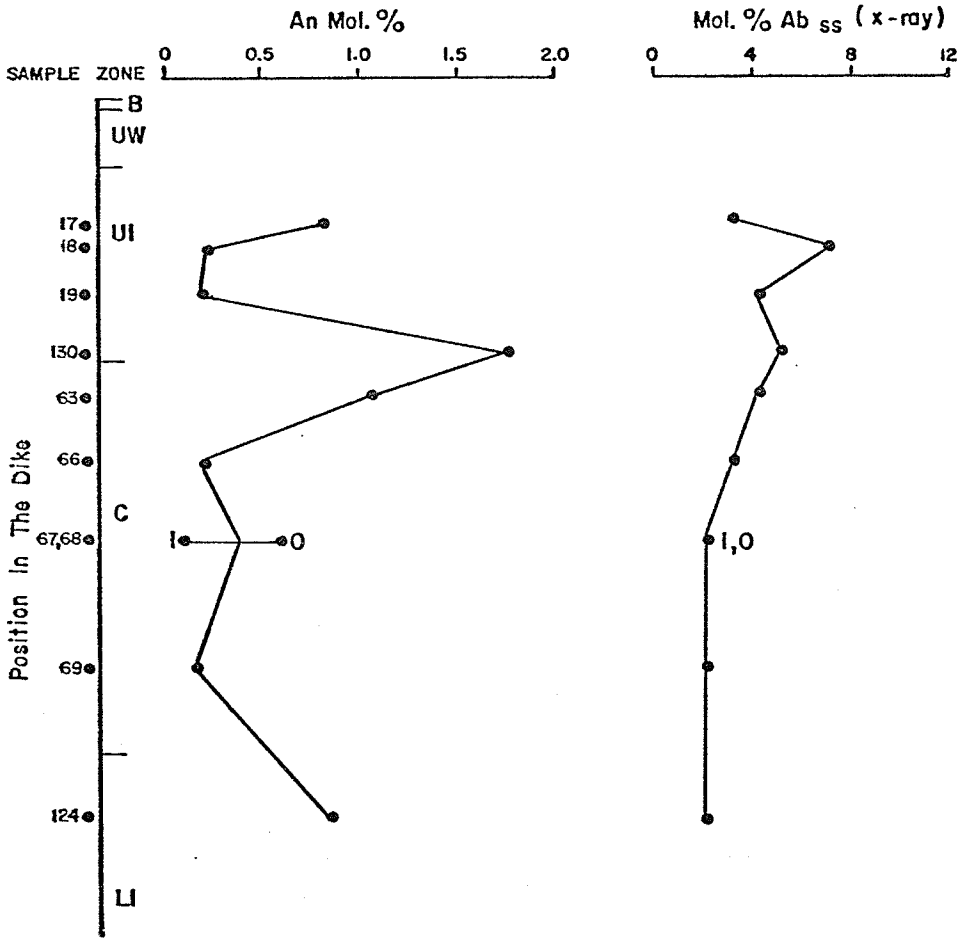

range from 0 for the monoclinic structure to 1.0 for the triclinic structure that deviates the most from the monoclinic. The deviation from monoclinic to triclinic is caused by ordering of Si and Al in the tetrahedral sites. The values of Δ for K-feldspars of the Buck dike range from 0.800 to 0.963 with a mean/standard deviation of 0.885 ± 0.050. The Δ values are close to maximum microcline and thus show a low temperature ordered structure.

Adularia

Adularia is a rare phase in the Buck dike. It occurs as tiny crystals approximately 0.5 mm across growing on open fractures in the quartz core. It is usually found adhering to the surface of the quartz among euhedral crystals of apatite. The crystals have clear colorless rims and transparent red cores or occasionally colorless cores and rims with an intermediate red zone.

Optical examination using a universal stage showed both chemical zonation and complex twinning. The dominant twin law is the Baveno law. A preliminary attempt to study this crystal by single crystal x-ray diffraction methods confirmed the complexity of the zoning and twinning. Because of the complexity of the problem the single crystal studies were abandoned as being outside of the scope of this study.

Unit cell demensions for the adularia were refined using x-ray powder diffraction methods. Because of the zonation many of the diffraction peaks were poorly formed, broad or ragged. Repeated runs on the diffractometer produced 12 reflections that were consistently well formed and produced reliable d-values. These values were used in refining the unit cell dimensions. The measured values, calculated

values and calculated cell dimensions are summarized in Table 5-3. The b and c values, when plotted against each other (Fig. 5-6) fall well outside the determined trend fields. Even using double the standard error as the uncertainty limits it is well outside the field so this deviation is not a result of experimental error. Some of the deviation may possibly be caused by strain from zoning, but the diffraction peaks used were well formed and consistent. It appears the adularia has a disordered structure similar to the high sanidine structure.

Summary

Potassium feldspar is an important phase to consider in the history of the Buck pegmatite.

The following points are significant:

1. There are two K-feldspar types in the dike; an early formed maximum microcline and a late formed high sanidine structure adularia.
2. The microcline is always perthitic and contains inclusions of albite that are probably a primary phase.
3. The microcline shows advanced alteration to albite and lithian micas. The albitization is more advanced in the intermediate zones than in the core.
4. The Rb and Cs content of the feldspars increases from the margins toward the core of the dike.
5. The amount of albite in solid solution in the microcline decreases from the margins toward the core.

Table 5-3 Observed and calculated diffraction lines and refined cell dimensions for adularia. The lines represent only the well formed peaks used in refining the cell dimensions.

h k l	I	d observed Å	d calculated Å
$20\bar{1}$	40	4.239	4.234
111	15	3.943	3.942
130	60	3.794	3.792
$\bar{2}21$	11	3.554	3.552
$\bar{1}12$	35	3.458	3.454
*220	100	3.341	3.326
$\bar{2}02$	44	3.279	3.281
002	68	3.219	3.220
131	54	2.997	2.998
$\bar{3}11$	12	2.797	2.799
$\bar{1}32$	23	2.765	2.765
$\bar{2}41$	30	2.585	2.585
$\bar{3}55$	21	1.254	1.254

* Rejected during calculation because it exceeded a 2θ tolerance level of 0.04^{o}.

$\underline{a}$ = 8.6036 ± 0.0039 Å

$\underline{b}$ = 13.0555 ± 0.0076 Å

$\underline{c}$ = 7.1648 ± 0.0019 Å

β = 116^{o} 1.81' ± 2.4'

Volume 723.14 $Å^3$ ± 0.43 $Å^3$

Fig. 5-6 Plot of b versus c cell dimensions for feldspars. The error limits marked are double the calculated standard errors. The standard field limits are from Stewart (1974).

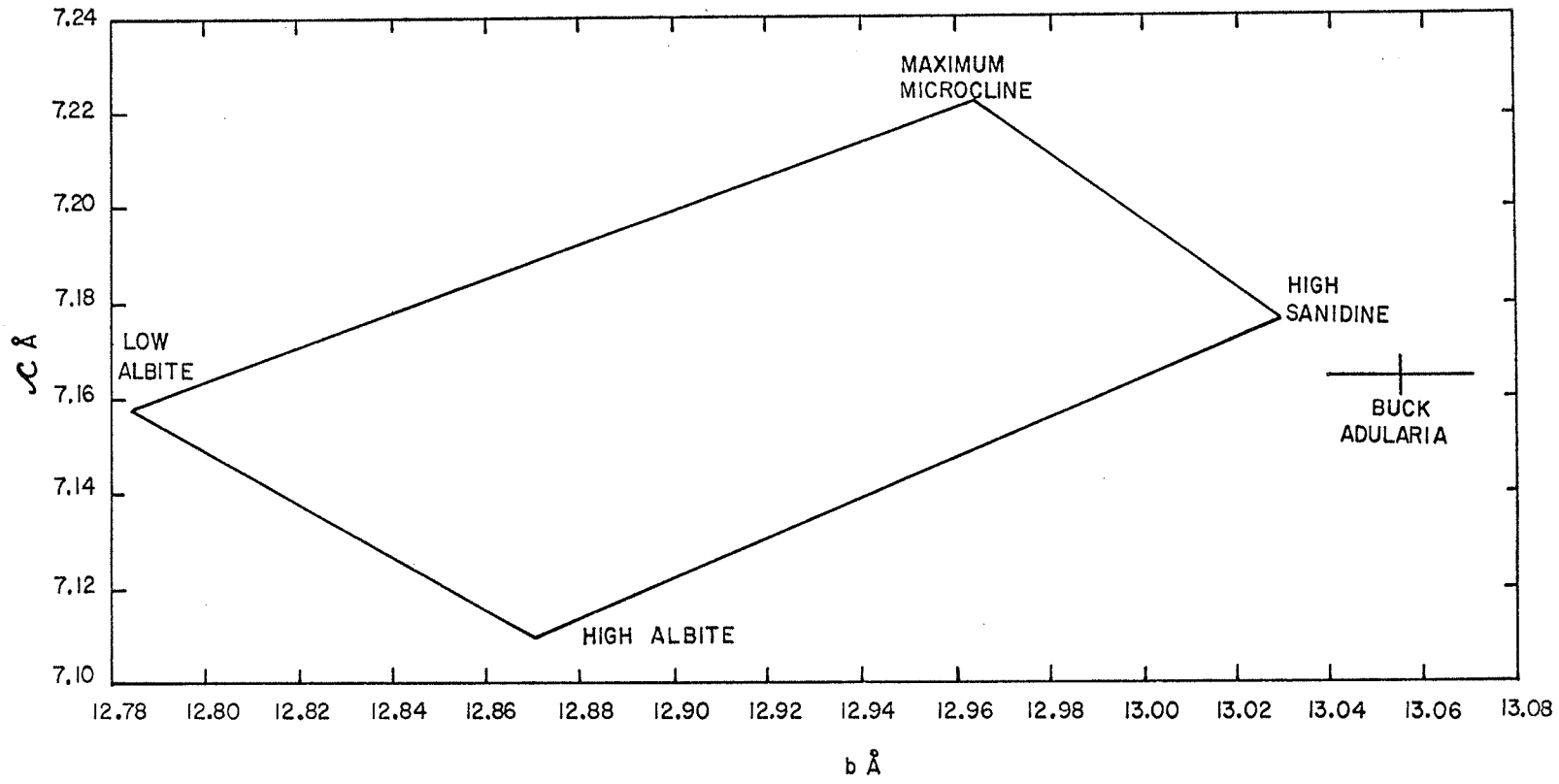

C Plagioclase

Plagioclase, $NaAlSi_3O_8$-$CaAl_2Si_2O_8$, is a ubiquitous phase in the pegmatite and in the country rocks. Other than determining optically the composition range ($An_{27}$to An_{34}) the plagioclase of the country rock was not considered in the study.

Four forms of albitic plagioclase occur in the dike:

1. Platy albite - AB

   Mottled white and grey plates of albite occuring in the wall zones. The plates are randomly oriented and often intergrown.

2. Cleavelandite - CV

   Fan shaped or globular aggregates of pink or buff radiating blades of albite, Figs. 5-7, 8 , dominate the intermediate zones of the dike. The blades often radiate from crystals of amblygonite or aggregates of lithium-rich micas.

3. Saccharoidal albite - AA

   Fine grained aggregates of lath-shaped albite with quartz, apatite, muscovite and tourmaline occur in the B and LW zones and as veins in the lower part of the LW zone. The pink saccharoidal albite consists predominantly of albite, Fig. 5-9, as randomly oriented crystals, or occasionally strongly oriented in a flow-like fabric.

4. Vein albite - VA

   Veinlets of late albite (Ab_{99} by oil immersion) fill fracture networks in the quartz masses of the UI zone ,

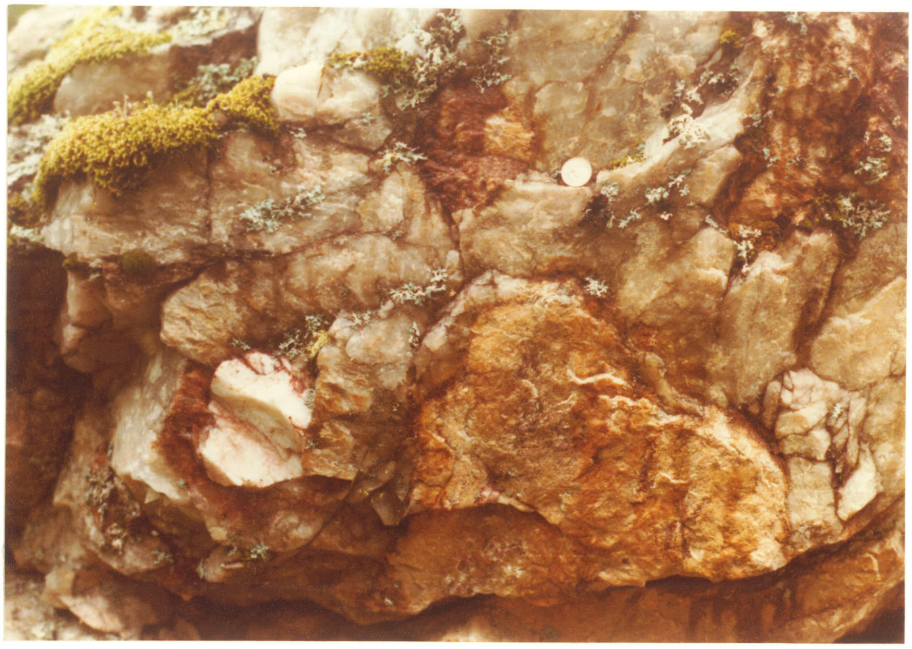

Fig. 5-7 Globular masses of beige, iron stained cleavelandite on the edge of the quartz core. The surrounding material is grey quartz; the white crystal is blocky amblygonite. Note the small purple crystals of sodic montebrasite in the center of the radiating fans of albite. The coin is 2 cm wide.

Fig. 5-8 A close-up view of a mass of cleavelandite (beige). Note the radiating texture of the blades. The dark grey material on the right side is an aggregate of lithian muscovite, quartz and apatite.

Fig. 5-9 Microphotograph of the saccharoidal albite of the LI zone. The albite crystals have well developed twins, but crystal faces are fluted and irregular. Thin section under cross polarized light.

Fig. 5-10. Although finer grained than the large masses of cleavelandite they have much the same texture.

Nine samples, described in Table 5-4, were chosen for detailed study.

Chemical variations

The nine samples were analysed for sodium, calcium and potassium contents (Table 5-5). Sample BC-36 is a very fine grained saccharoidal albite. Examination in thin section showed that it contained quartz, apatite, and micas on too fine a scale to separate. Because of the impurities in the sample, resulting in a low calculated total feldspar content and erroneous calcium and potassium contents, this sample is not included in the discussion. Sample BC-98 is also contaminated, but examination has shown the contaminant to be quartz, so the ratio of feldspars calculated is correct even though the value for total feldspars is low.

The composition of the plagioclase follows an assymetric trend across the dike (Fig. 5-11). In the B, UW and upper UI zones Ab is roughly constant while An and Or show an inverse relationship. Across the remainder of the dike An maintains a constant level and Ab and Or show erratic inverse relationships.

X-ray studies

The analysed albite samples were x-rayed to determine the structural state according to the methods of Bambauer et al. (1967). The values of $\Delta\Theta$ in Table 5-5 represent the angular difference

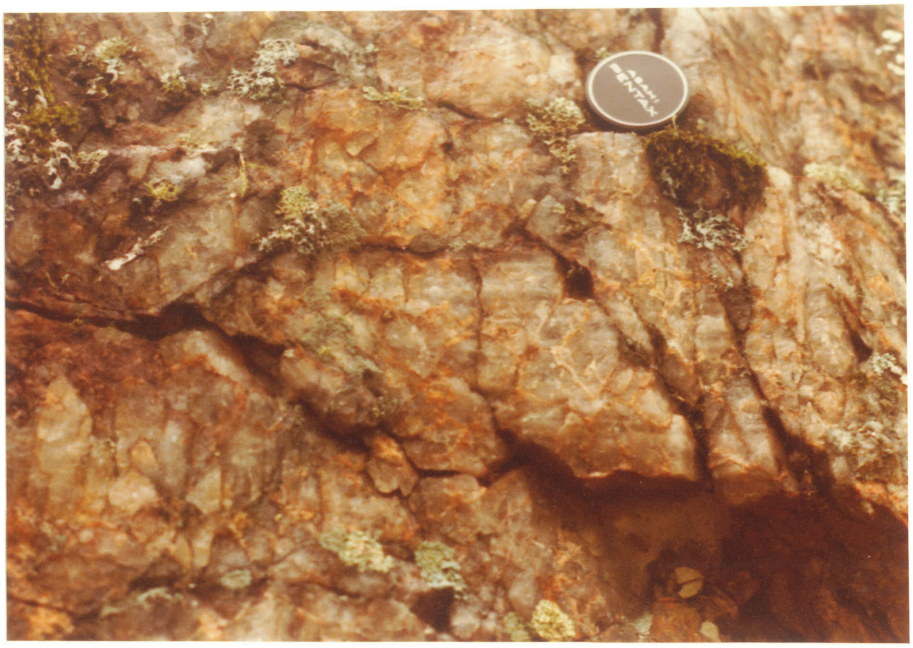

Fig. 5-10 Albite of the CV type (flesh-colored vein material) filling fractures in grey quartz. The lens cap is 52 mm wide.

Table 5-4 Description and location of analysed albite samples.

No.	Type	Zone	Description
BC-86	AA	B	fine to medium grained grey albite with QZ, TM
BC-64	AB	UW	platy medium grey albite with QZ, MV, TM
BC-57c	AB	UW/UI	platy white albite with TM, MV, QZ
BC-51	CV	UI	buff radiating blades with BR, QZ
BC-42a	CV	UI	pink radiating masses with MV, LM, QZ, VD, MB
BC-22	CV	UI	beige radiating blades with LM, AM, QZ
BC-99	CV	LI/LW	pink radiating masses with QZ, MV, AP, TM
BC-98	AB	LW	pinkish-white plates with TM, MV, QZ
BC-36	AA	LI	very fine grained saccharoidal albite - AB+QZ+MV+AP

Table 5-5 Partial chemical analysis data for albites. The Or, Ab and An contents are calculated for the samples. The values $\Delta\theta$ are $2\theta_{131} - 2\theta_{1\bar{3}1}$ (CuK_{α_1}) of Bambauer et al. (1967).

		Wt. %			mol %				
No.	Type	Na_2O	CaO	K_2O	Ab	An	Or	Σfs	$\Delta\theta^o$
BC-86	AA	10.96	0.840	0.77	92.7	4.2	4.5	101.4	1.20
BC-64	AB	10.88	0.810	0.77	92.1	4.0	4.5	100.6	1.10
BC-57c	AB	10.24	0.580	1.05	86.7	2.9	6.2	95.8	1.03
BC-51	CV	10.00	0.280	1.09	84.6	1.4	6.4	92.4	1.13
BC-42a	CV	10.16	0.130	1.24	86.0	0.9	7.3	94.2	1.03
BC-22	CV	10.16	0.250	1.85	86.0	1.2	10.9	98.1	1.15
BC-99	CV	10.96	0.063	0.90	92.7	0.3	5.3	98.3	1.15
BC-98	AB	9.92	0.105	1.12	83.9	0.5	6.6	90.7	1.09
BC-36	AA	9.12	0.340	1.06	77.2	1.7	6.3	85.2	1.12

Fig. 5-11 The compositional variation of plagioclase across the dike. The three components have been recalculated to 100 percent.

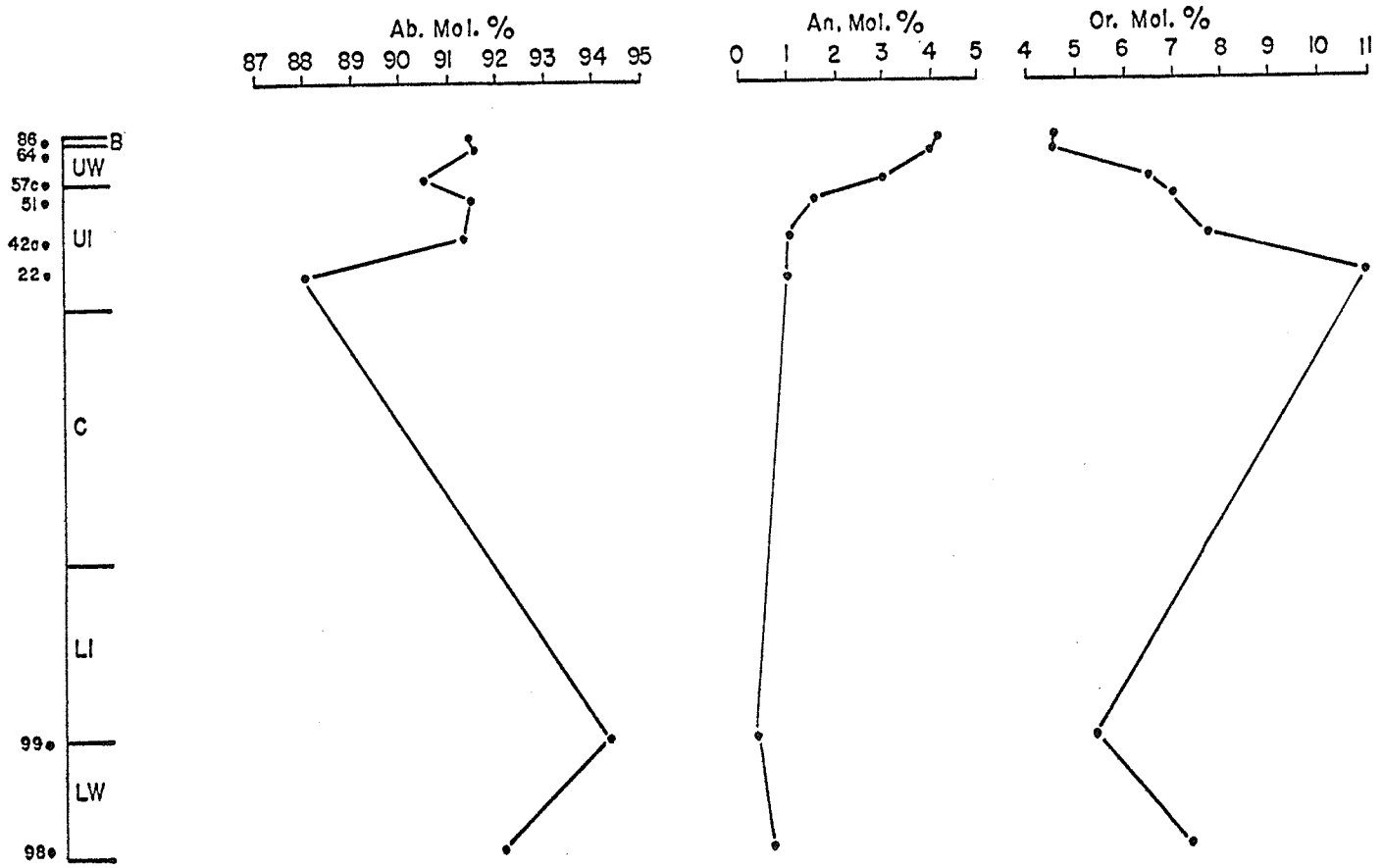

$2\theta_{131} - 2\theta_{1\bar{3}1}$ (CuK_{α_1}). Fig. 5-12 shows all the values correspond to low plagioclase. There is no apparent reason other than experimental error for 2 points to plot well below the established curve. The samples plotting below the curve do not correspond with high Or_{ss} contents. The variation in $\Delta\theta$ across the pegmatite is random.

Optical studies

The anorthite content of the albite was checked in immersion liquids using the method of Morse (1968). A comparison of An values calculated from chemical analyses and optically determined values, Table 5-6, shows a general agreement, although the optically determined values are generally somewhat lower.

Summary

Plagioclase in the Buck dike has the following properties:

1. Four textural forms are present in the dike; platy albite, cleavelandite, saccharoidal albite and vein albite.
2. The An/Ab compositional range is $\approx Ab_{95}$ to Ab_{100}.
3. The Or component increases from the margin to the core of the dike.
4. The An content decreases from the margin to the core of the pegmatite.
5. The albite is in the low structural state.

D Micas

Within the pegmatite one can distinguish five morphological forms of muscovite and lithian muscovite. These five types, differing

Fig. 5-12 A plot of $\Delta\Theta$ versus the An content of plagioclase. The curves are taken from Bambauer et al. (1967). All albites x-rayed correspond to the low plagioclase trend. The dotted line is for low plagioclase containing 4.0 mol % Or.

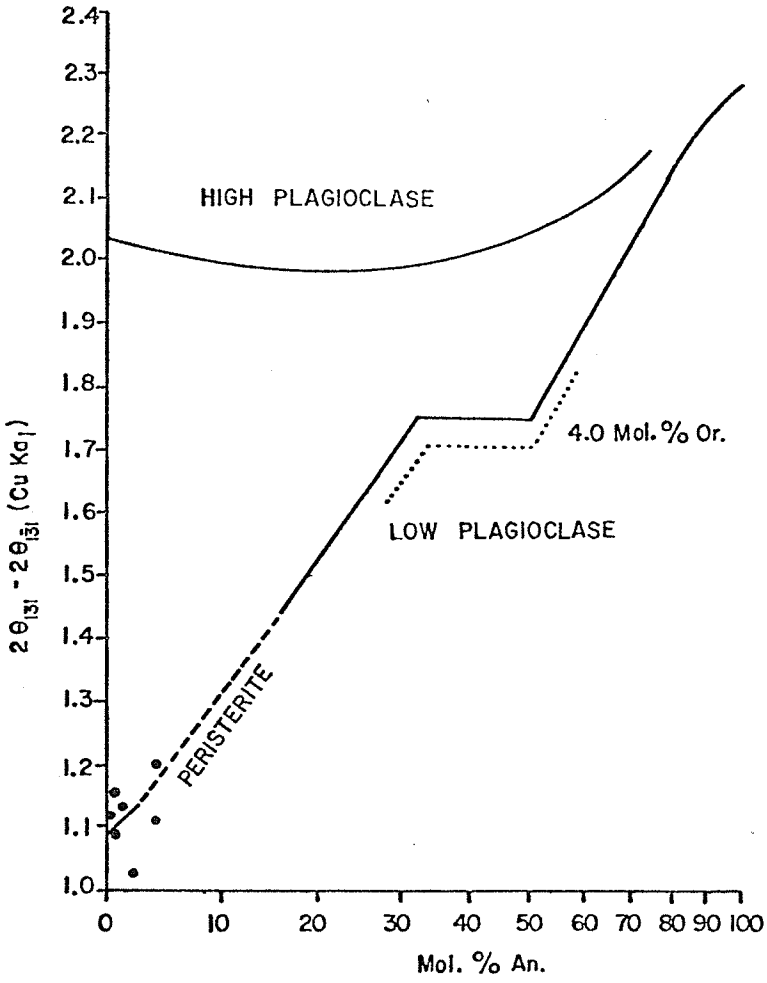

Table 5-6 Comparison of optically determined anorthite contents and anorthite contents calculated from the chemical data.

No.	mol % An (calc.)	mol % An (opt.)
BC-86	4.3	5.0
BC-64	4.2	3.0
BC-57c	3.2	3.0
BC-51	1.6	0.5
BC-42a	1.0	0.5
BC-22	1.4	-1.0
BC-99	0.3	0
BC-201	---	1.0

in morphology and color, can also be divided into two genetic types as follows:

(1) Early muscovite phases

(a) Book muscovite - M

This is the most common muscovite, consisting of transparent sheets of pale green, yellow, or pale brown $2M_1$ muscovite in hexagonal books ranging from a few millimeters to several centimeters thick and 1 to 10 cm wide.

(b) Radial or plumose brownish muscovite - LM

A silver-brown translucent $2M_1$ lithian muscovite occurring as wedge shaped radiating sheets forming spherical or occasionally feather aggregates. These spherical aggregates can reach a diameter of 3 cm.

(c) Curvilamellar or "dish-shaped" muscovite - LM-L

A less common form, it consists of curved scales of $2M_1$ lithian muscovite mixed with 1M lepidolite forming dish-shaped or occasionally globular aggregates. It is translucent, silver-white, with an occasional pink or blue tinge to it.

(2) Late muscovites

(a) Flaky muscovite - FM

Normally found as an alteration and along late fractures, this bright silver-white muscovite forms thin, randomly

oriented irregular flakes generally 2 to 3 mm across.

(b) Sugary muscovite - SM

A late alteration product, this lithian mica forms irregular saccharoidal blebs and veinlets of fine grained yellow, green or bluish grey muscovite. The grain size is normally 0.5 mm.

A total of 26 samples covering all 5 types of mica were selected for further work. The γ or γ' refractive index was determined for all 26 samples. In addition 14 samples covering the muscovite, LM, LM-L, and late mica groups were chemically analysed for Li, Na, K, Rb, Cs and Ca, and 3 for total iron as Fe_2O_3. These 14 samples plus three late muscovites were also x-rayed using a 114.6 mm Debye-Scherrer camera in order to determine the structural polytypes. Sample locations and descriptions are given in Table 5-7.

Distribution of samples

Micas are distributed throughout the upper and lower wall and intermediate zones. M-mica is the most common form present and was sampled from three levels in the dike; wall muscovites from the wall zone, intermediate muscovites from the upper portion of the intermediate zone, and interior muscovites, the innermost occurrences from the middle of the intermediate zone. The associated minerals for the muscovite zones are:

(a) wall muscovite - black tourmaline + quartz + albite ± amblygonite/montebrasite ± beryl

Table 5-7 Type, location and description of mica samples for which some analysis was done.

Number	Type	Location	Description
BC 44	M	UW	pale green flat sheets
BC 39	M	UW	greenish brown sheets
BC 108	M	UW	white to pale green
BC 41	M	UI	green to pale brown translucent
BC 42A	M	Interior of UI	pale green mica associated with LM
BC 40	M	UI	pale green sheets
BC 79	M	UI ?	pale brown - contains abundant verdelite
BC 120	M	LI (Interior)	pale amber sheets
BC 123	M	LI	pale green sheets
BC 99	M	LW	white sheet mica
BC 42B	LM	UI	silver grey flakes
BC 22	LM	UI	grey flakes
BC 79	LM	UI ?	pale brownish flakes, globular aggregates
BC 14	LM	UI ?	silver-brown curved flakes
BC 128	LM	LI	pale brown globular aggregates
BC 45	LM-L	UI	silver white curved sheets
BC 38	LM-L	UI	bluish white curved sheets
BC 43	LM-L	UI	silver-grey globular aggregates
BC 25	LM-L	UI near C	silver grey curved flakes
BC 35	LM-L	UI near C	blue-grey globular aggregates
BC 10	LM-L	Unknown	grey curved sheets
BC 81	FM	UI	grey flakes on altered amblygonite
BC 83	FM	C	randomly oriented silver-white flakes
BC 132	FM	C	white flakes from interior of amblygonite crystals
BC 119	SM	LI	fine grained grey aggregate altering petalite pseudomorphs
BC 20	SM	UI	green saccharoidal aggregate from pit 30 m north of trench

(b) intermediate muscovite - albite + quartz + beryl + amblygonite + green tourmaline

(c) interior muscovite - albite + quartz + amblygonite ± beryl + green tourmaline ± LM-mica

Only the innermost interior muscovite is associated with the lithian muscovites. The lower part of the intermediate zone contains LM and LML micas, while small amounts of lithian muscovite-lepidolite represent the only mica in the core zone. A symmetrical mirror image of these occurrences is found in the lower zones below the quartz core zone.

Two distinct varieties of muscovite appeared late in the development of the pegmatite, principally as late alterations of primary phases such as spodumene, tourmaline, and Li-phosphates. One sample of late muscovite was chemically analysed. Representative samples were examined optically and by x-ray powder diffraction photography.

The secondary mica FM associated with tourmaline and amblygonite group minerals is silvery white to pale yellow and occurs as irregular sheets in tourmaline and randomly oriented books or occasionally irregular radial aggregates in alteration veinlets in amblygonite; see Figs. 5-13, 14. The secondary mica (SM) associated with spodumene and triphylite-spodumene aggregates is a fine grained sugary blue-green to grey mica occurring as rims and alteration veinlets.

Chemistry

Examination of the analyses in Table 5-8 shows several chemical trends in the micas, which can be correlated with morphological

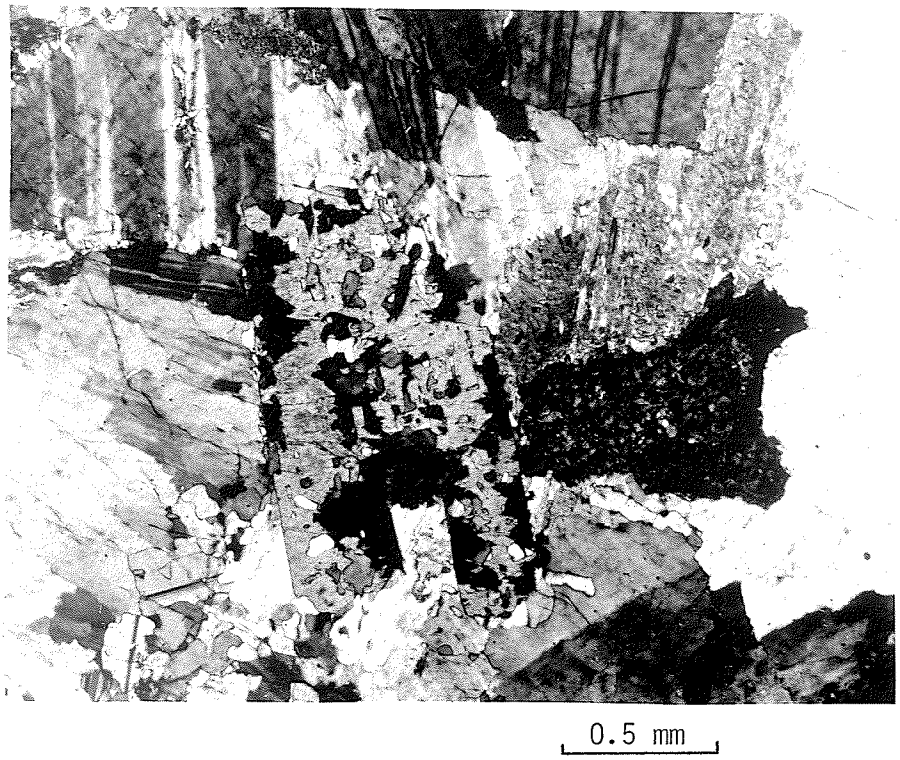

Fig. 5-13 A muscovite pseudomorph after tourmaline (ragged grey and black rectangular mass in the centre) in a quartz albite matrix; x-nicols.

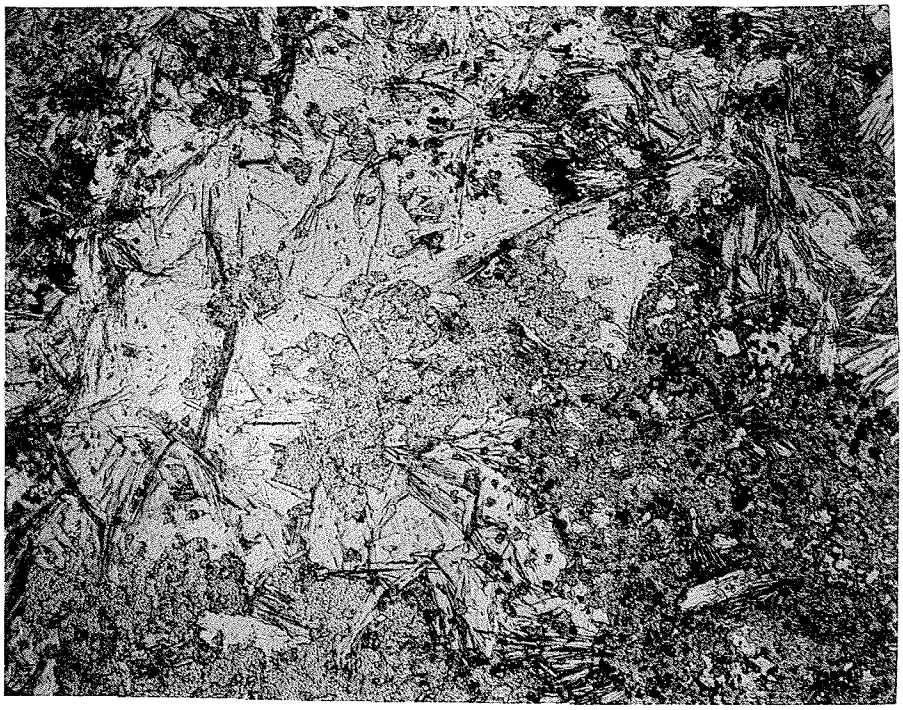

Fig. 5-14 Radial growths of muscovite (light grey with prominent cleavage lines) in an altered amblygonite crystal. The dark granular matrix is a fine grained aggregate of quartz and apatite. X-nicols.

Table 5-8 Chemical and physical data for selected muscovite samples.

Sample Number -- Type	Weight % Oxides								
	Li_2O	Na_2O	K_2O	Rb_2O	Cs_2O	CaO	Total Iron as Fe_2O_3	R.I. γ or γ'	Structural Type
BC 44-M	0.42	0.79	8.94	0.79	0.030	0.000		1.598	$2M_1$
BC 39-M								1.5905	
BC 108-M								1.597	
BC 41-M	0.44	0.58	8.30	1.03	0.042	0.004		1.598	$2M_1$
BC 42A-M	0.43	0.66	9.10	1.11	0.049	0.000		1.598	$2M_1$
BC 40-M								1.5985	
BC 79-M								1.592	
BC 120-M	0.58	0.81	8.80	1.28	0.055	0.017	1.59	1.592	$2M_1$
BC 123-M	0.54	0.82	9.20	1.14	0.054	0.010	1.54	1.5975	$2M_1$
BC 99-M	0.53	0.67	8.60	0.97	0.035	0.000		1.597	$2M_1$
BC 42B-LM	1.66	0.48	8.22	1.67	0.174	0.034		1.582	$2M_1$
BC 22-LM								1.590	
BC 79-LM	1.84	0.58	8.76	1.64	0.169	0.085		1.5825	$2M_1$
BC 14-LM	2.13	0.54	7.88	1.73	0.150	0.050		1.5885	$2M_1$
BC 128-LM	2.50	0.24	9.28	2.16	0.285	0.009	1.32	1.5815	$2M_1 >> 1M$
BC 45-LML	3.18	0.46	8.64	2.18	0.219	0.024		1.5825	$2M_1 >> 1M$
BC 38-LML								1.575	
BC 43-LML								1.589	

Table 5-8 Chemical and physical data for selected muscovite samples.

Sample Number -- Type	Weight % Oxides Li_2O	Na_2O	K_2O	Rb_2O	Cs_2O	CaO	Total Iron as Fe_2O_3	R. I. γ or γ'	Structural Type
BC 25-LML	3.13	0.56	8.64	2.15	0.222	0.017		1.5765	$2M_1 >> 1M$
BC 35-LML	2.77	0.27	8.94	2.06	0.216	0.037		1.579	$2M_1$
BC 10-LML								1.5795	
BC 81-FM								1.5725	
BC 83-FM								1.592	$2M_1$
BC 132-FM									$2M_1$
BC 119-SM								1.5845	$2M_1$
BC 20-SM	1.10	0.70	9.40	1.43	0.43	0.019			

types and with their position in the pegmatite.

Figures 5-15, 16 indicate a continuous increase of LI content from the Li-poor M muscovite, through the LM to the most lithium enriched LM-L form. Also, within the morphological groups there is a distinctly higher Li content in the samples collected from the zones beneath the central core.

Distribution of Rb (Fig. 5-15) shows a linear trend of enrichment with increasing Li content (broken line Fig. 5-15). That is, the Rb content of the micas increases steadily from the wall zone to the core. In addition, the normal muscovite shows a separate linear trend, (solid line, Fig. 5-15) of Rb enrichment from the wall to the interior, despite the Li contents of the samples being almost constant. It should be noted also that the lower sequence samples are richer in Rb as well as Li, for equivalent positions in the pegmatite, than those from the upper sequence.

Cesium shows similar enrichment trends (Fig. 5-16) to Rb. The difference between the upper and lower muscovite series is, however, not as obvious. The sample marked lower LM mica has anomalously high Rb and Cs contents, compared to the other LM mica samples. Cesium enrichment is particularly apparent and may be due to the fact that this sample is the innermost occurrence of LM-muscovite, located on the bottom edge of the core zone and thus was probably the last of the early lithian muscovites to crystallize.

The sample of greenish SM mica shows a different trend. The Rb content, (Fig. 5-15), lies very close to the linear enrichment trend of the earlier micas, however Figure 5-16 shows a higher Cs content than

Fig. 5-15 Li plotted as a function of Rb for four types of micas from the Buck dike.

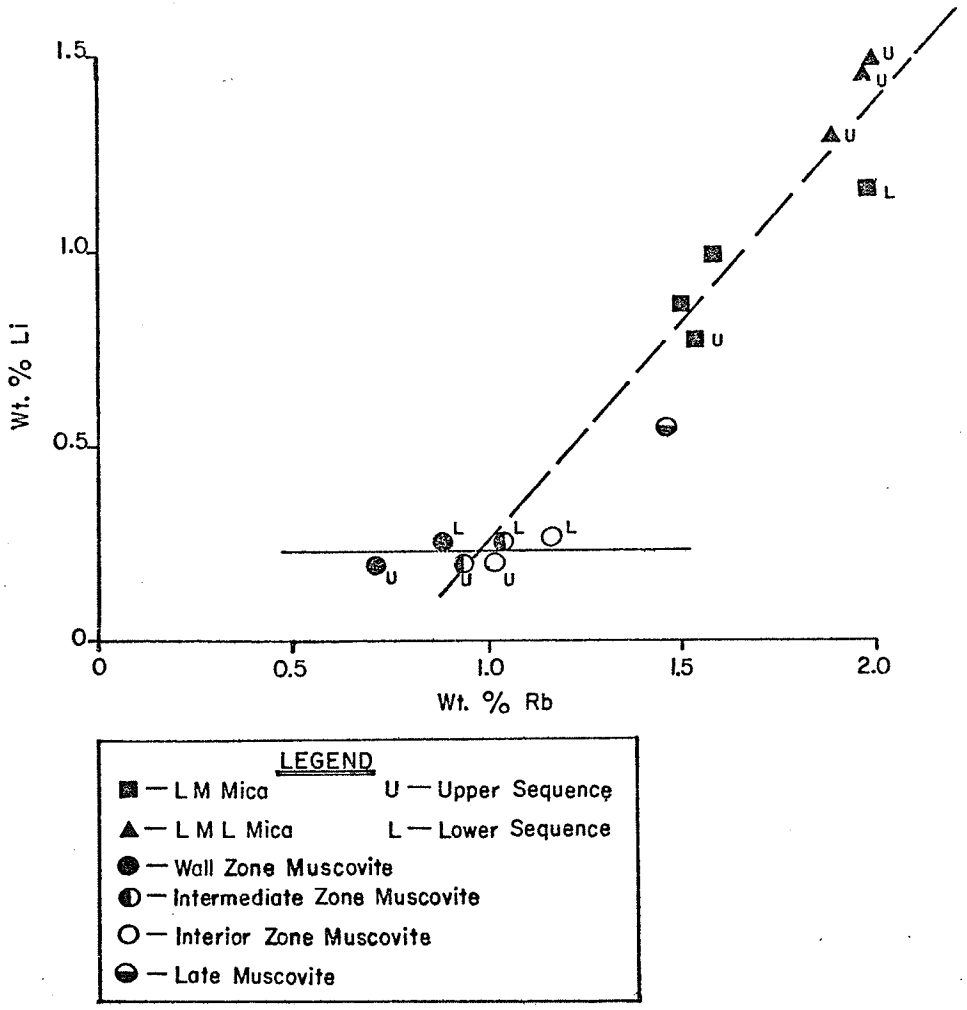

Fig. 5-16 A plot of Li versus Cs for four types of micas of the Buck pegmatite. The symbols are the same as in Fig. 5-15.

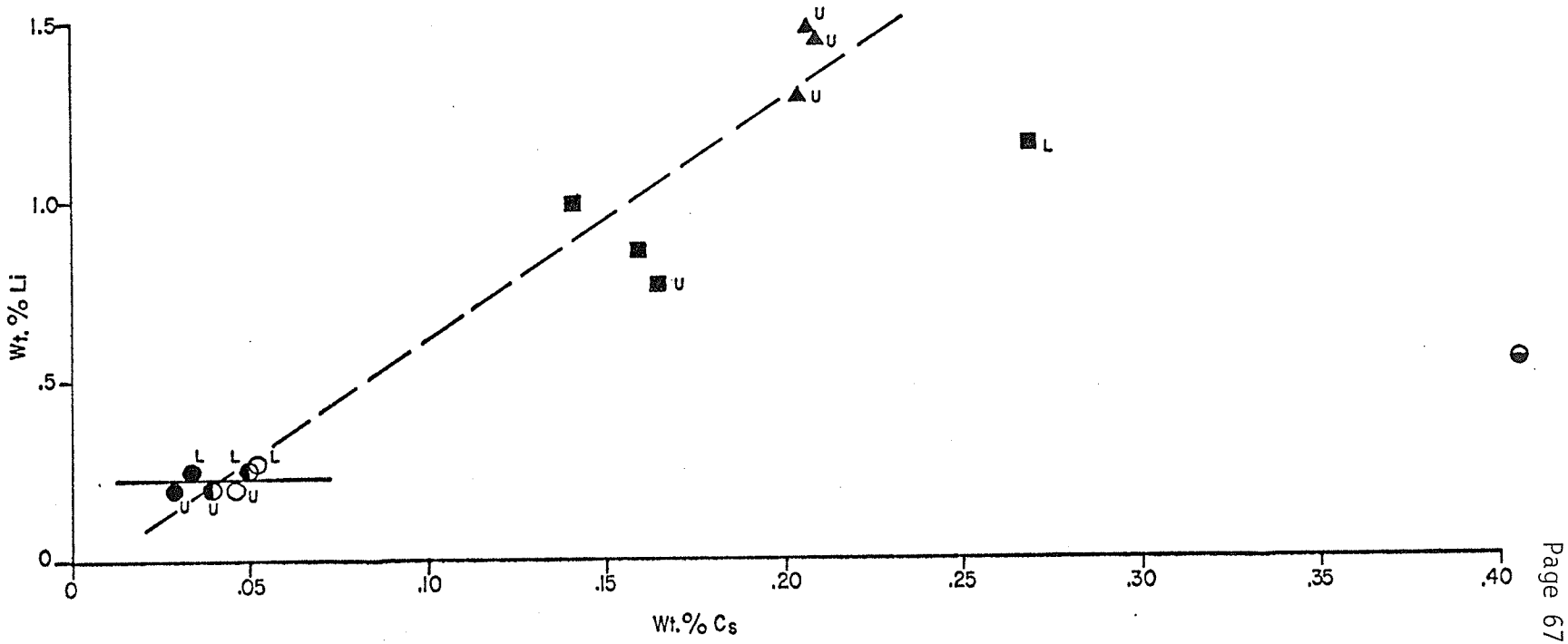

the other mica types. This sample has the highest Cs content of any mineral analysed from the pegmatite and is about 4 times higher than the maximum for the earlier mica types.

The plot of Rb versus Cs, Figure 5-17, suggests an initial rapid increase of Rb in the muscovite, with a proportionately lower rate of Cs enrichment, in the wall and intermediate zones, while deeper in the pegmatite the relative rate of Cs enrichment increases and the Rb rate decreases.

As would be expected, the Na_2O and K_2O contents decrease toward the core as the Rb and Cs increases, substituting for K and Na in interlayer sites. Calcium behaves slightly different in that the highest calcium contents occur in the LM mica while the innermost LML mica show intermediate CaO contents.

X-ray diffraction studies

In all mica samples examined by x-ray powder diffraction methods the $2M_1$ structural type was the dominant form (Table 5-8). In only three samples, two of lithian muscovite-lepidolite micas, and the LM-mica sample BC 128, is there evidence of a different polytype. All three samples have strong $2M_1$ paterns, but with 3 to 5 additional lines that correspond to the strongest distinctive reflections of the 1M (3T) polytype. The 1M lines are weak and indicate that they represent the subordinate in a mixed polytype mica.

The relationship between structural type and Li_2O content has been demonstrated by Levinson (1953) and Rinaldi et al. (1972). While there is no apparent correspondence between the quoted trends and

Fig. 5-17 Rb/Cs enrichment trend for four types of micas of the Buck pegmatite. The symbols are the same as Fig. 5-15

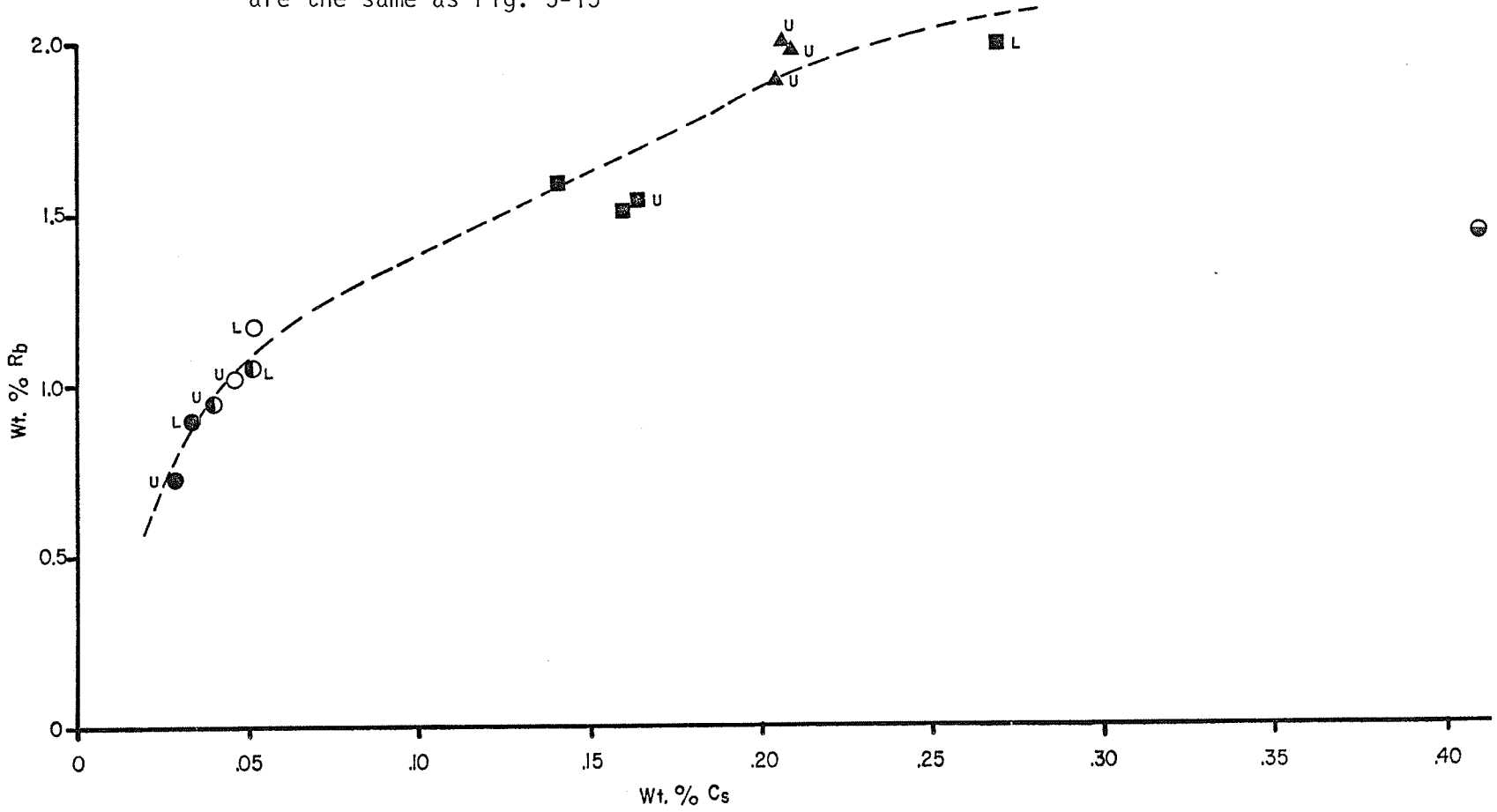

those found in the Buck samples (Table 5-9), this is a function of sample inhomogeneity. The Li_2O contents quoted here are bulk chemical values for the samples. The mixed polytype micas contain $2M_1$ muscovite and high lithium 1M lepidolite. The limits for separate phases as given in Levinson (1953) may well apply to the Buck muscovites.

Sample BC-128LM shows chemical variations and structure intermediate between the other LM samples and the LM-L samples.

Optical studies

A plot of the γ or γ' refractive index against Li_2O contents for the 13 samples for which partial chemical analyses were determined, Fig. 5-18, shows decreasing refractive indices with increasing Li_2O content. The separation of the three principal morphological forms along a linear trend is pronounced, forming 3 distinct data clusters. Sample BC 128-LM shows a refractive index intermediate between the LM and LML types. A schematic frequency plot of 21 determinations of $\gamma(\gamma')$, Fig. 5-19, demonstrates again the separation of the 3 forms.

Optical examination of all mica types showed good optical continuity within the plates of M-muscovite, while the globular and plumose growths of LML and LM mica consist of mosaics of small flakes. However, the γ refractive index was constant within any aggregate. This would suggest that even though x-ray data indicate polytypic (and thus compositional) inhomogeneity, any variation in refractive index is on a submicroscopic scale. Thus the optical data obtained would be an average value representing the bulk composition of the mica.

It should be noted that while Fig. 5-18 shows a roughly linear relationship between Li_2O content and the γ refractive index,

Table 5-9 Comparison of lithia content and structural polytype of micas.

Levinson (1953)

Wt. % Li_2O	Name and Structure Type
$<\sim$ 3.3	lithian muscovite, $2M_1$
3.40 - 4.0	transitional structure, $2M_2$+$2M_1$
4.0 - 5.1	lepidolite, $2M_2$
> 5.1	lepidolite, 1M

Rinaldi et al. (1972)

Wt. % Li_2O	Name and Structure Type
< 3.50	lithian muscovite, $2M_1$
3.50 - 3.97	mixed type, $2M_1$+1M, $2M_1$>1M
4.52	mixed type, $2M_1$+1M, 1M>2M

This Paper

Wt. % Li_2O	Structure Type
< 2.50	$2M_1$
> 2.50	$2M_1 \gg 1M$

Fig. 5-18 Plot of the wt. % Li_2O versus the γ or γ' refractive index for the 3 principal mica types.

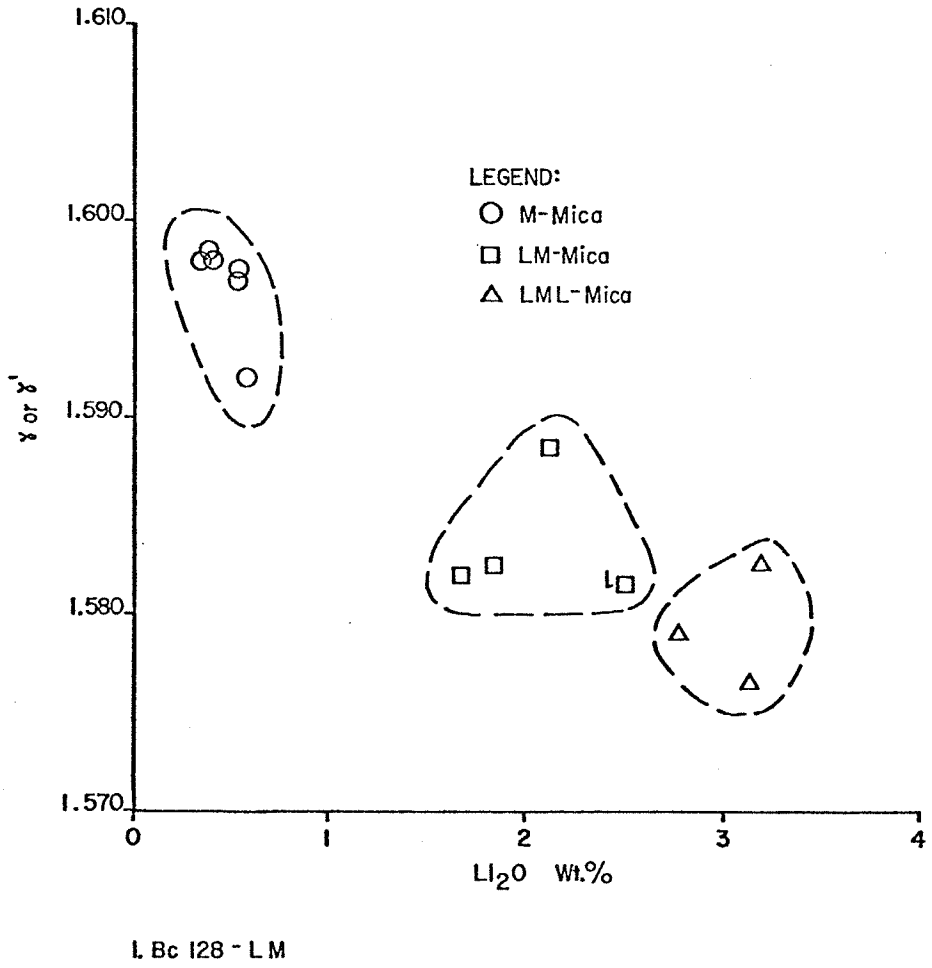

Fig. 5-19 Frequency plot of the refractive index γ or γ' for the 3 principal muscovite types. The bracketed number is the number of samples.

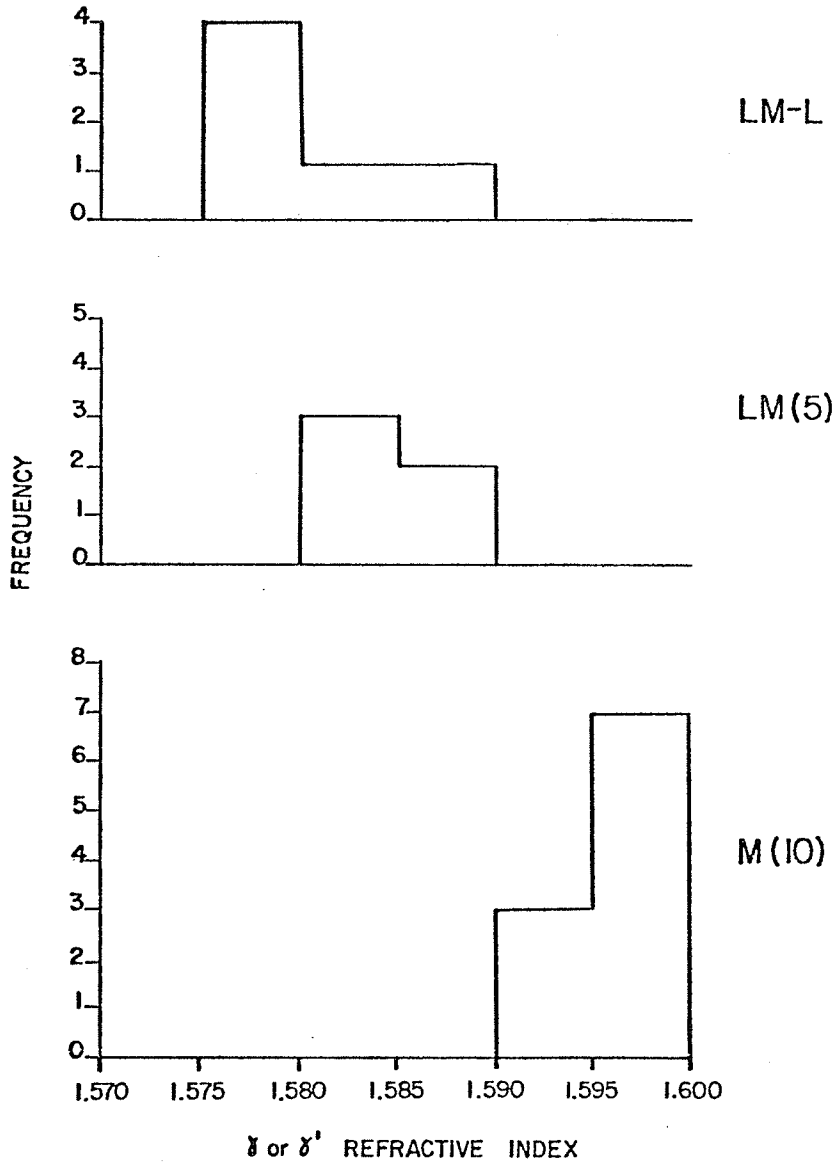

Rinaldi, et al. (1972) suggest that the F/(OH) ratio is probably responsible for most of the variation in refractive index in micas. The linear trend of Fig. 5-18 thus shows the general increases in fluorine content with increasing lithia content. Foster (1960) has shown that F and Li vary concomitantly in micas.

The structural type for all secondary micas for which x-ray photographs were taken is $2M_1$. The determinations of γ refractive indices is more ambiguous, covering the entire range from normal muscovite to LML mica.

Microscopic examination of the secondary micas shows occasional very small patches of alteration that looks like a chlorite, probably cookeite, but no reliable x-ray identification was possible because of the small size of the grains.

Summary

(1) Sheet silicates represent a ubiquitous phase within the pegmatite. The five phases studied span the entire crystallization history of the pegmatite, including the late hydrothermal alterations.

(2) The chemical variations noted in and among the different micas show a distinct spatial arrangement and thus we should assume a corresponding temporal sequence in the formation of the micas.

(3) The rare alkalis, Li, Rb and Cs show a continuous increase from the wall contacts toward the core of the pegmatite.

(4) The Rb/Cs ratio of micas decreases inward.

(5) The late micas would not be expected to follow any defineable trend. The single chemical analysis of a late mica shows a high Cs_2O content.

E Amblygonite-montebrasite minerals

Minerals of the amblygonite-montebrasite-natromontebrasite group, $(Li,Na)ALPO_4(F,OH)$, are common throughout the Buck pegmatite. They occur from the wall zone to the core as crystals ranging from a few millimeters to more than half a meter in length and show considerable chemical variation in the pegmatite.

The names amblygonite-montebrasite depend on the F/OH ratio with F exceeding hydroxyl in amblygonite. Since in this study only F is determined directly, the division between amblygonite and montebrasite will be taken as 6.5 weight percent fluorine. The name natromontebrasite refers to montebrasite for which the Na/Li ratio is greater than one (Heinrich et al., 1955). There are no occurrences of natromontebrasite in the Buck pegmatite; however, a distinct genetic group of minerals shows significantly higher Na contents than the other groups and thus, to separate this group, any sample with more than 0.25 wt. % Na_2O will be called sodic montebrasite-amblygonite.

Distribution in the pegmatite

Within the pegmatite amblygonite-montebrasite minerals can be grouped into four types as follows:

(1) Large "pendant crystals" of primary montebrasite growing from the inner contact of the intermediate zone into the quartz core, or floating free as blocks in the quartz core, are the largest crystals of the amblygonite group in the pegmatite. The crystals of translucent white to pale yellow montebrasite have rough columnar forms and range in length from 20 to 85 cm. While the crystals occasionally float free in the core zone, completely surrounded by quartz, they are more commonly rooted in masses of cleavelandite. The flat plates of albite radiate away from the montebrasite crystals. There is generally a thin skin of reddish alteration products on the surface of the crystal in contact with the cleavelandite. From each of two large columnar montebrasite crystals, five chip samples were taken along the length of the columns. These ten samples were analysed for Li_2O,Na_2O,K_2O,CaO and x-rayed using the method of Černá et al. (1973) to determine their F content.

(2) Scattered throughout the lower intermediate zone are smaller irregular to subhedral crystals of white to pale grey blocky amblygonite. Assymetrically distributed with respect to the zoning of the pegmatite, most occur in the lower intermediate zone in clusters of irregular crystals, Fig. 5-20, or as isolated masses ranging in size from 0.5 cm to 15 cm. Although not restricted to the lower intermediate zone the small blocky amblygonite crystals are less common in the upper intermediate zone. Small isolated crystals were noted as high up in the

Fig. 5-20 A cluster of blocky amblygonite crystals (white) in a coarse cleavelandite matrix. The hammer head is 17 cm long.

dike as the lower contact of the upper wall zone. The blocky amblygonite is usually surrounded by a radiating growth of cleavelandite blades, Fig. 5-21, with an assemblage of cleavelandite + muscovite + quartz + apatite ± beryl ± tourmaline. Commonly the amblygonite has veinlets of red or grey alteration.

No samples of the blocky amblygonite were analysed for alkali content, but several crystals were x-rayed to determine F content and several thin sections were made to study the alteration veinlets.

(3) Within the intermediate zone, associated with masses of radial cleavelandite, occur small elongate crystals of sodic montebrasite-amblygonite. Rarely exceeding 2 cm in diameter but commonly reaching 6 to 10 cm in length the sodic montebrasite occurs as subhedral crystals or irregular cleaveable blades. Commonly several small masses will form an aggregate with subordinate albite, quartz, lithian muscovite, lithian muscovite-lepidolite and apatite in the core of large globular masses of cleavelandite (Fig. 5-22). The sodic montebrasite-amblygonite crystals can be distinguished from the small blocky amblygonites by a faint pink coloration and a thin rusty red coating on the crystal surface. Partial chemical analyses and fluorine determinations were done for six randomly selected samples with this particular habit.

Fig. 5-21 A cluster of irregular blocky amblygonite crystals (white) completely surrounded by radiating blades of albite (brown).

Fig. 5-22 Small crystals of sodic-montebrasite-amblygonite (white with reddish-brown surface stains) in a matrix of radiating cleavelandite (beige).

(4) All amblygonite-montebrasite masses examined show some degree of F-OH exchange reactions. This is generally shown by veins and vein-networks of secondary montebrasite cutting through primary crystals.

Statistical study of variation in fluorine content

For a randomly selected collection of 53 amblygonite-montebrasite samples x-ray patterns were recorded to determine the fluorine content. Many of the samples were collected from the bins of hand sorted material and others were selected from located samples to give a cross section of determination of all types from the entire pegmatite. A frequency plot, Fig. 5-23, shows that the majority of samples have between 5.5 and 6.5 wt. % F, only 7.5% exceeded 6.75 wt. % F. This shows an average composition to be a fluorine rich montebrasite with a mean F content between 5.5 and 6.0 wt. %. The 4 values below 4.0 wt. % F are late montebrasite samples rimming alteration veinlets in the amblygonites.

Careful examination of the specimens showed slight variations in color. The color differences are very slight involving pale tints of green, yellow, grey and blue. The best method of determining these slight differences is to note the color of light transmitted through thin cleavage flakes. As figure 5-24 shows, there is a distinct consociation of color and fluorine content. While color is by no means an exact criterion, and has only been applied on this study and in the work of Černá et al. (1972) at Tanco, it may prove, with experience, to be a valuable field test during mapping of amblygonite bearing bodies. Černá (op.cit.) differentiated three colors of amblygonite-montebrasite

Fig. 5-23 Frequency of fluorine contents in 53 randomly selected samples of amblygonite-montebrasite (taken at 0.5% intervals centred at x.0 and x.5 wt. % F).

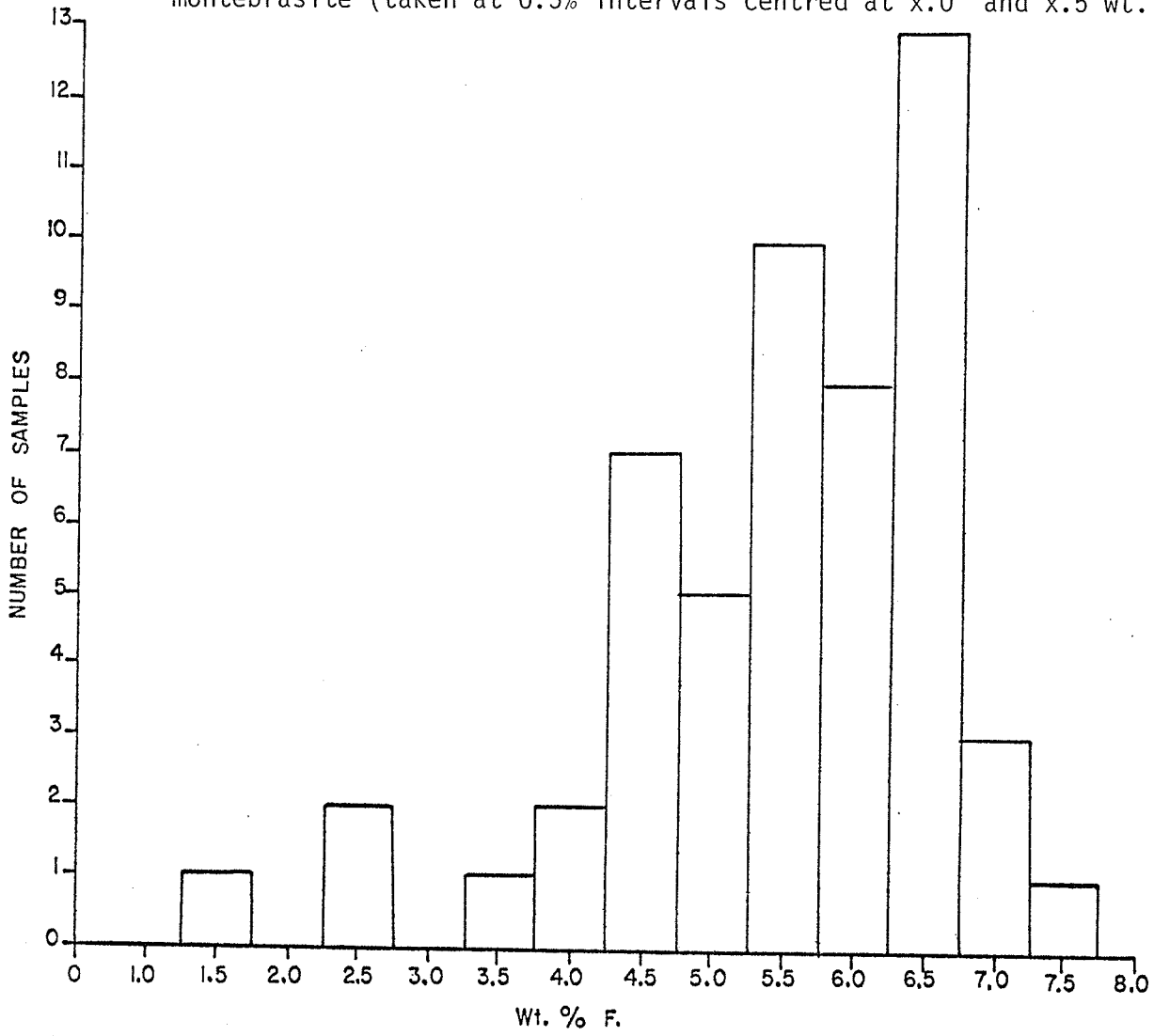

Fig. 5-24 Frequency diagrams showing the consociation of color and fluorine content for 38 randomly selected specimens.

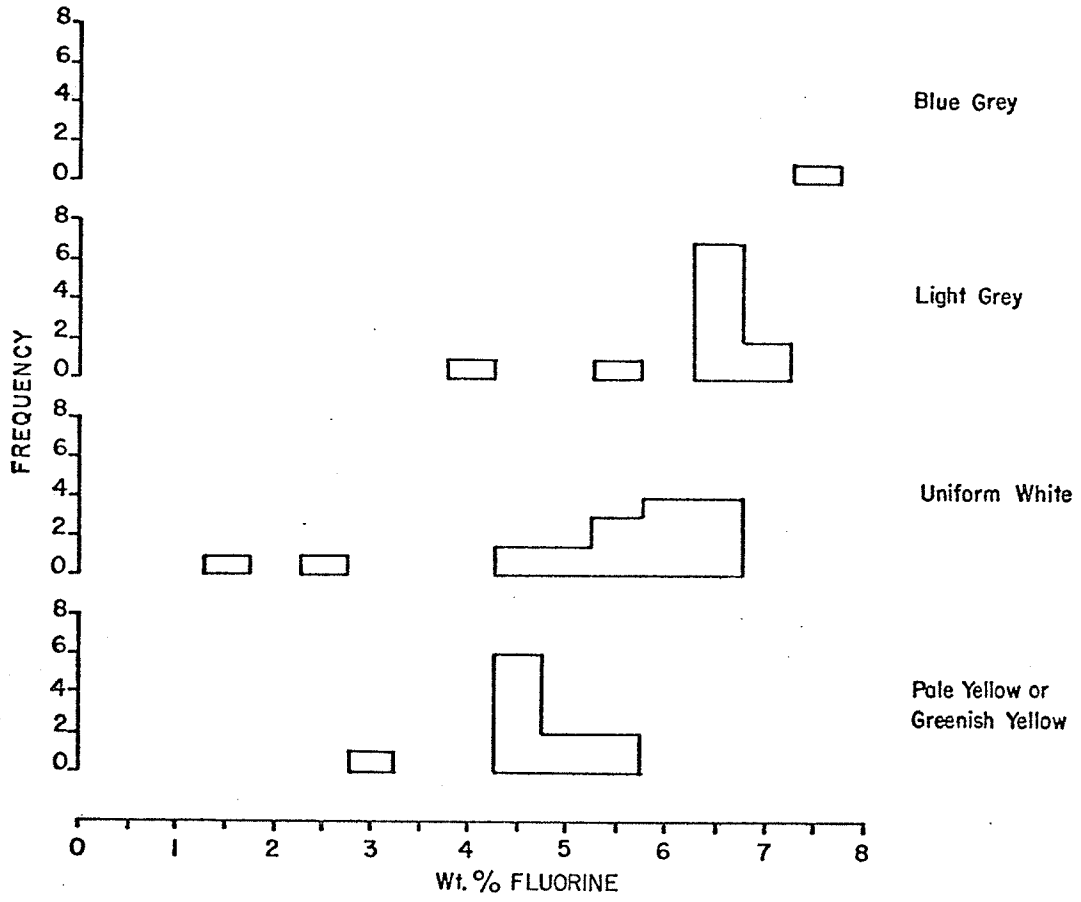

at Tanco, yellow, white and pink. While no pink specimens were noted in the Buck pegmatite, Černá's mean F contents for the yellow and white specimens correspond closely to those of the Buck pegmatite amblygonite.

Chemical variations

Blocky amblygonite "pendants"

As shown in Table 5-10 partial chemical analyses and fluorine determinations were obtained for 16 samples. The samples numbered BC 60 and BC 61 are chip samples taken from the surface of two large montebrasite crystals shown in Figs. 5-25 and 5-26. The crystals are both located on the upper edge of the quartz core and are rooted in radiating masses of cleavelandite. Crystal BC 60 is surrounded only by quartz cut by rare veinlets of creamy green massive apatite, while crystal BC 61 was in contact with a pocket of green clay (right side of photograph 5-26) that probably represents an alteration of primary pollucite. Sample locations and plots of major alkali element and fluorine contents are shown in Figs. 5-27 and 5-28. It should be remembered that Li_2O can be replaced by Na_2O, $\frac{1}{2}CaO$ or very small amounts of K_2O, thus the sum of $Na_2O + K_2O + \frac{1}{2}CaO$ shows a direct inverse to the Li_2O content. The alkalis Na_2O and K_2O have initially high values at the upper end of the crystals. This can be explained by ion exchange with the plagioclase in which it is rooted. The Na_2O and K_2O decrease down the crystal. However K_2O shows a sudden increase in the lowest sample of both crystals. Both samples BC 60E and BC 61E are from the surface of the crystal and may have undergone some potassium contamination possibly during the late metasomatic stage. Calcium behaves much more erratically, but does tend

Table 5-10 Partial chemical analyses of amblygonite-montebrasite.

Sample Number	Weight % Oxide				
	Li_2O	Na_2O	K_2O	CaO	Wt. % F By X-Ray
BC 60-A	10.15	0.282	0.006	0.179	4.5
BC 60-B	10.58	0.072	0.003	0.062	3.8
BC 60-C	10.32	0.052	0.003	0.112	5.2
BC 60-D	9.98	0.056	0.002	0.385	4.9
BC 60-E	10.02	0.076	0.004	0.211	4.8
BC 61-A	10.06	0.250	0.004	0.236	5.0
BC 61-B	9.89	0.222	0.004	0.645	5.4
BC 61-C	10.32	0.110	0.002	0.052	4.9
BC 61-D	10.28	0.114	0.002	0.258	4.3
BC 61-E	10.41	0.074	0.003	0.438	3.5
BC 2-SM	9.82	0.86	0.40	0.323	5.6
BC 5-SM	10.33	0.22	0.16	0.093	5.7
BC 7-SM	9.90	0.26	0.19	0.368	6.3
BC 11-SM	10.16	0.40	0.38	0.135	4.1
BC 12-SM	9.30	1.01	0.55	0.443	3.6
BC 13-SM	10.33	0.26	0.03	0.380	6.6

Fig. 5-25 Large columnar montebrasite-amblygonite crystal (white), number BC 60, floating in the upper edge of the quartz core. The lens cap is 54 mm wide.

Fig. 5-26 Large columnar montebrasite crystal (white with beige staining) number BC-61 floating in the upper edge of the quartz core. The lens cap is 54 cm wide.

Fig. 5-27 Chemical variations along a single crystal of montebrasite-amblygonite (sample BC-60).

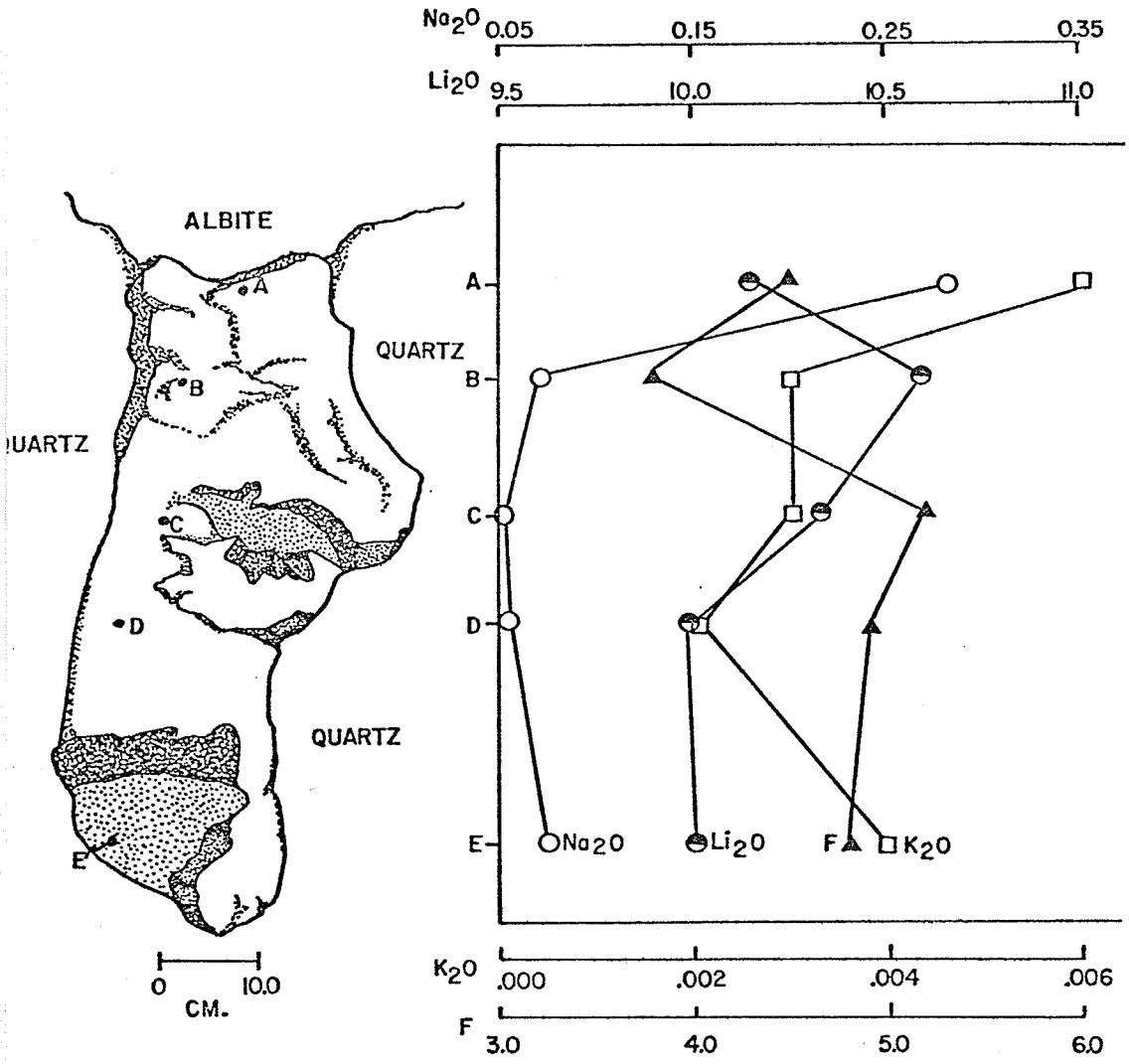

Fig. 5-28 Chemical variations along a single crystal of montebrasite-amblygonite (sample BC-61).

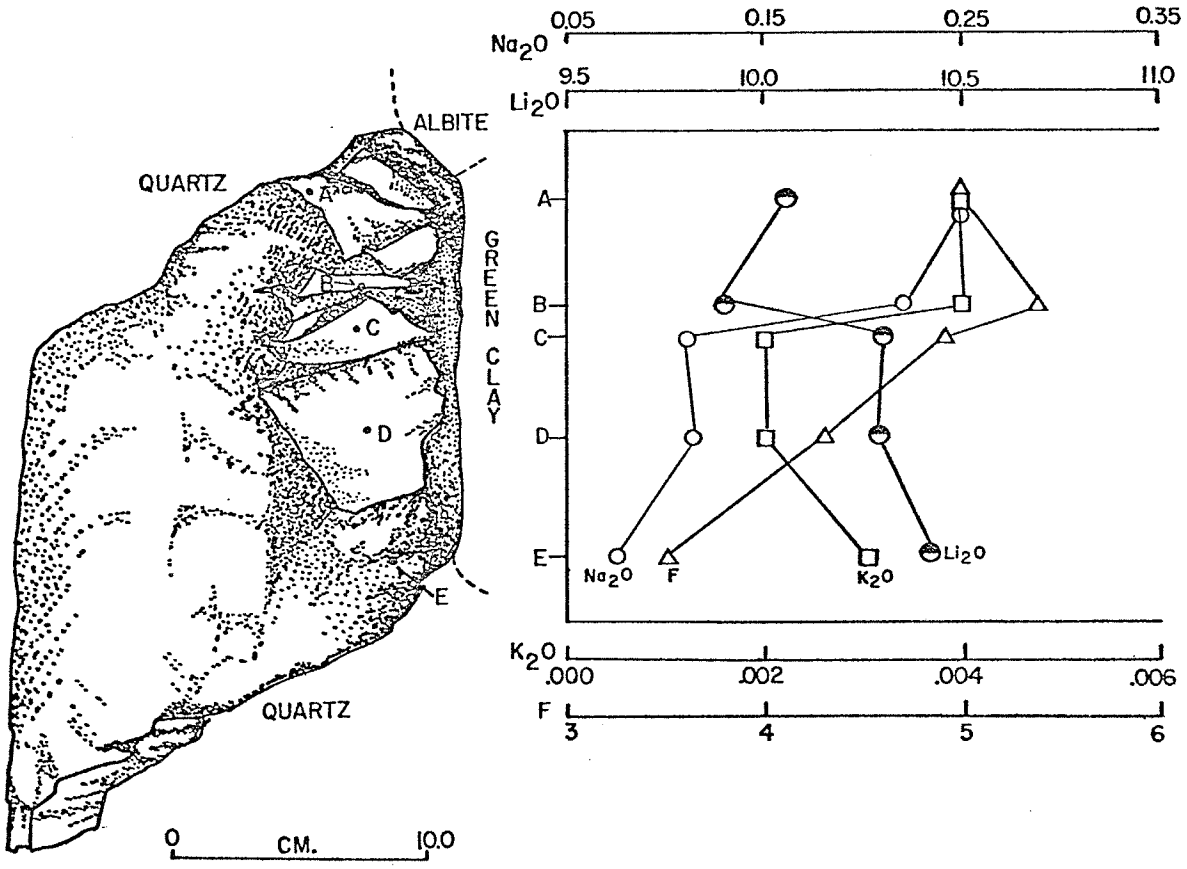

to be higher in content on the top and bottom of the crystals.

Fluorine content of the two large crystals does not show any consistent trend. While sample BC 60 shows erratic roughly constant F content, BC 61 shows a continual decrease in F down the crystal. The variable behaviour of fluorine could be caused either by actual chemical zoning in the crystal, or by irregular zones of alteration. In order to test the possibility of zoning existing in crystals a smaller blocky amblygonite crystal was cut in half and 8 samples taken across the crystal. These samples were x-rayed to determine F content and the results plotted in Fig. 5-29. The behaviour of F in this particular crystal seems to show a large scale symmetrical zoning. It should also be noted that the fluorine content of the crystal is among the highest determined for the pegmatite.

Sodic montebrasite-amblygonite

The six samples marked SM in Table 5-10 are samples with the characteristic color and location within radiating masses of cleavelandite. The soda content of these samples is 2 to 5 times higher than in the other samples analysed and the potash content is two orders of magnitude higher. The CaO content shows no significant variation. The crystals normally have thin reddish crusts on the surface which are high in apatite content. This suggests that if the crystals reacted with the albitizing fluids that Ca was caught in apatite while some Na and K substituted for Li in the montebrasite. Considerable reaction took place between these crystals and some altering fluid as shown in Fig. 5-30. This photograph shows two adjoining sodic montebrasite crystals. The

Fig. 5-29 Variation in fluorine content across a single crystal of blocky amblygonite.

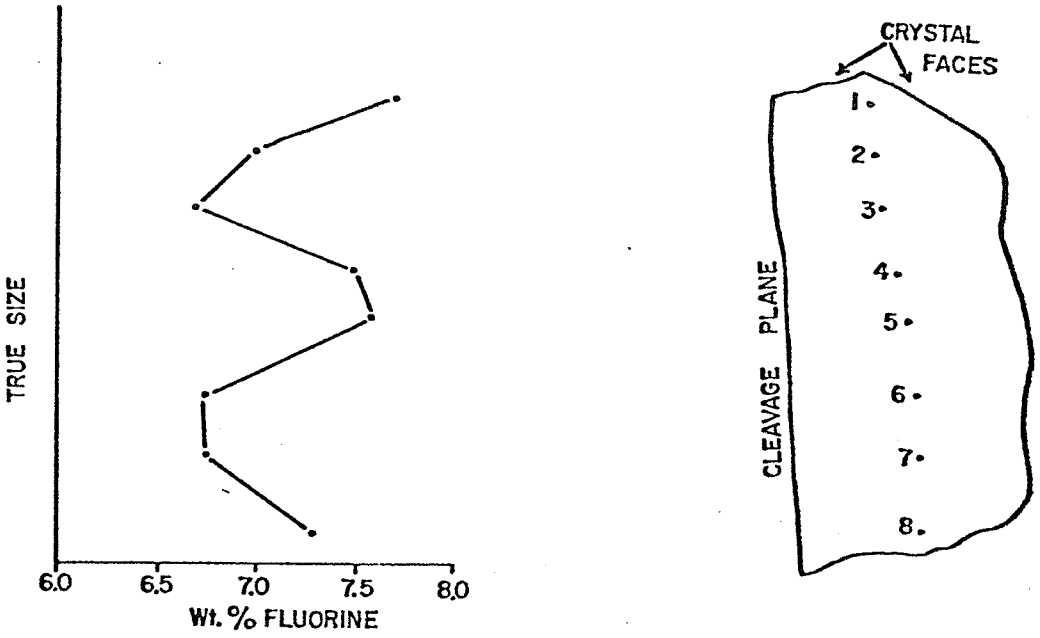

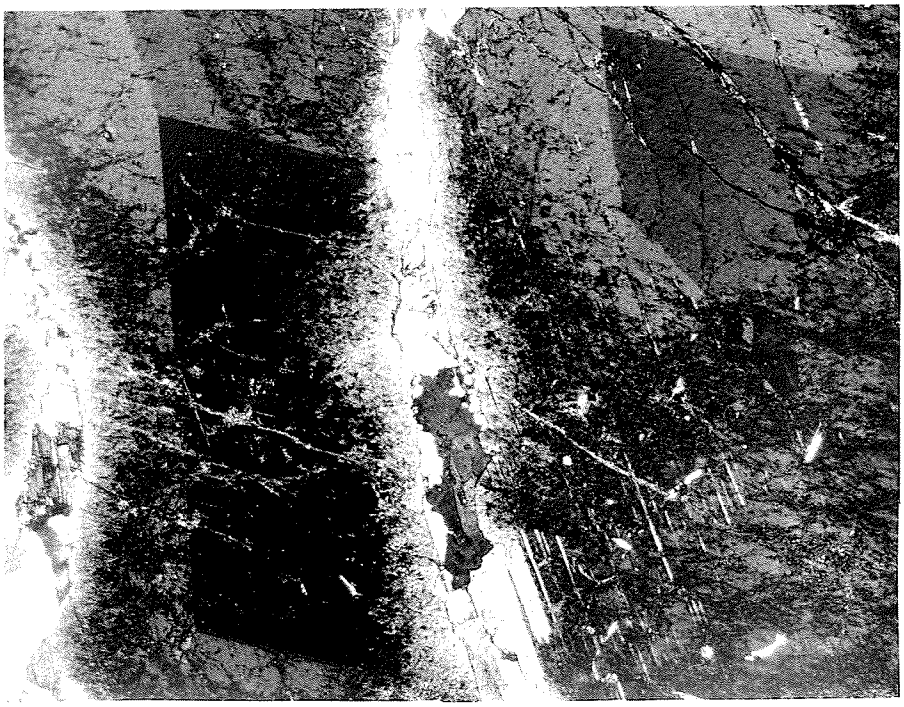

Fig. 5-30 Photomicrograph of two adjoining crystals of sodic montebrasite under cross polarized light. The two crystals are separated by a vein of quartz + apatite (white vein at centre). See text for further description.

sharply delineated dark grey core zones are optically homogeneous with a uniform extinction. The overgrowing material is zoned with the extinction radiating from the core to the rim, with twinning developing in the lower right hand section. The core thus has a uniform F/OH ratio and the OH content increases outward. The veinlets in the center and left of the photograph are late alteration veinlets with quartz-apatite core (black and dark grey) and rims of secondary montebrasite alterations (bright white). The F determinations in Table 5-10 may represent a rough average composition. The x-ray peaks used for the determinations were ragged and generally broader than in homogeneous samples.

Secondary montebrasite

All samples of the amblygonite-montebrasite group examined in thin section showed some degree of late montebrasite alteration (Fig. 5-31). Samples taken from late alteration veinlets have F contents of 1.5 to 3.1 wt. % fluorine.

Commonly the more highly altered veinlets have cores of apatite, quartz and white mica. Fluorine shows a continual increase away from the alteration veinlet, cf. Fig. 5-32.

Summary

The following facts can be summarized for the amblygonite-montebrasite group:

(1) The majority of the samples tested are montebrasites, with the statistical mean composition close to the dividing line

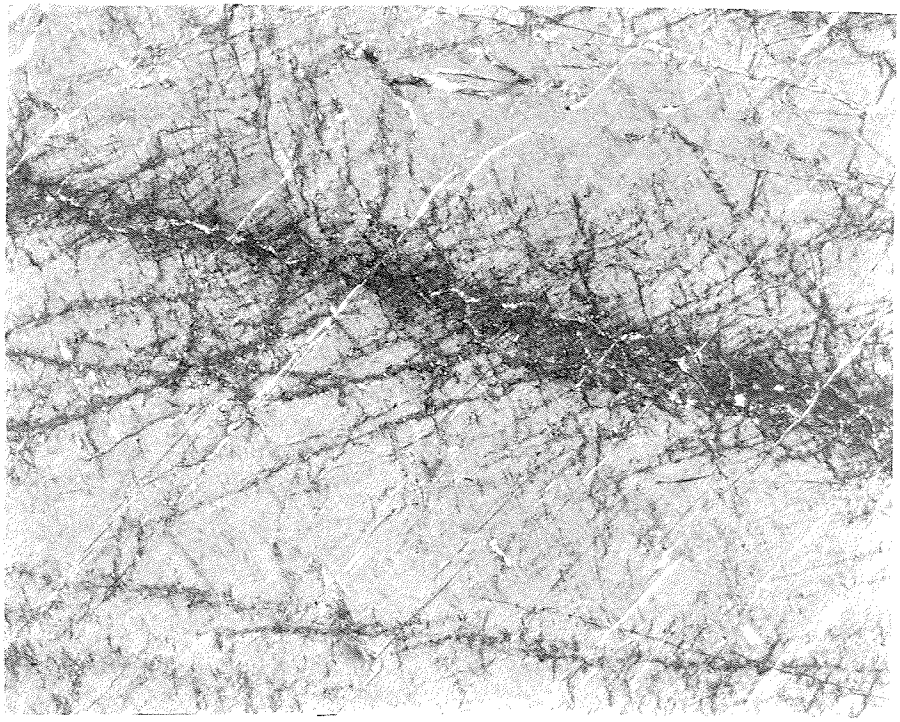

Fig. 5-31 Microphotograph, in cross polarized light, of an amblygonite grain (light grey) cut by a veinlet of secondary montebrasite (dark grey).

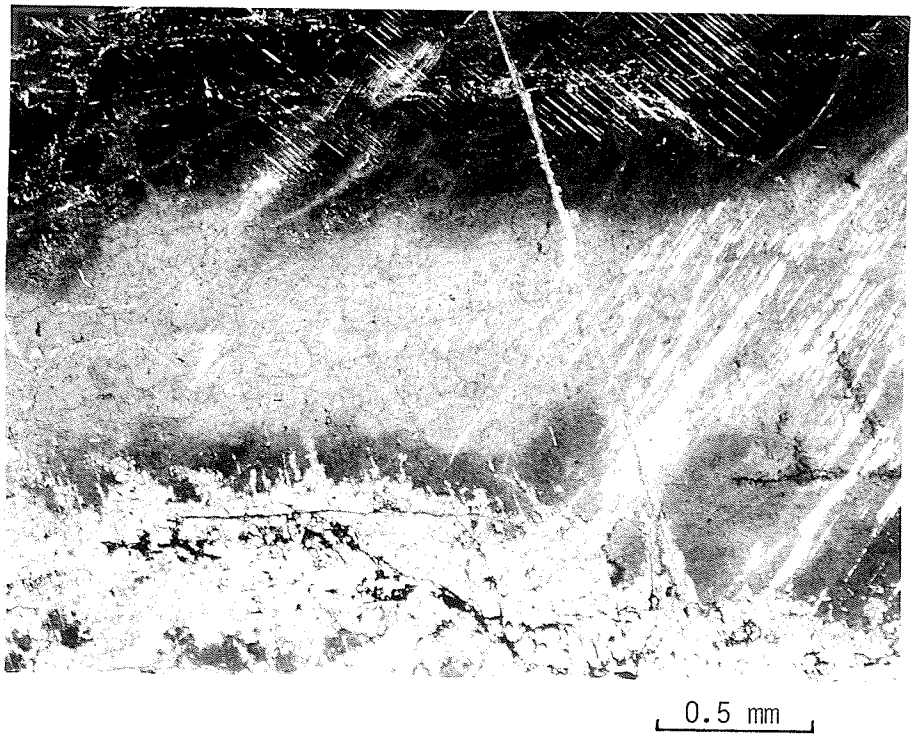

Fig. 5-32 Microphotograph, in cross polarized light, showing the gradation from primary amblygonite (dark grey, top) to secondary montebrasite (white, bottom).

between amblygonite and montebrasite which is often the fact for amblygonite bearing pegmatites.

(2) Substitution by Na and K is much less in the early large blocky amblygonites than in the small crystals of the albite zone. Alkali substitution shows a general decrease toward the core of the pegmatite.

(3) Zoning is common in the amblygonite crystals. The F/OH ratio decreases from core to rim. According to Loh & Wise (1976) this suggests the possibility of isothermal crystallization in a relatively small closed system. The one crystal tested that showed cyclic zoning could result from either isothermal crystallization with pulsed renewal of the fluid medium, or a period of isothermal crystallization causing decreasing F content followed by crystallization by decreasing temperature producing an increase in fluorine content.

(4) All crystals examined showed some degree of alteration to montebrasite. The fluorapatite generally associated with the montebrasite alteration did not equilibrate with the montebrasite (Loh and Wise, 1976).

(5) Faint colorations of the amblygonite-montebrasite minerals can be roughly related to F content.

F Triphylite-lithiophilite

Within the core zone and the UI zone minerals of the triphylite-lithiophilite group, $Li(Fe,Mn)PO_4$, are common. In the

core zone the minerals occur as large anhedral masses of deep green to yellowish-green color. Where exposed to weathering an iridescent black coating of oxide formed (Fig. 5-33). The irregular blocks of phosphate float in quartz along with blocky K-feldspar "crystals" in the approximate center of the core zone. Triphylite-lithiophilite also occurs in minor amounts in the UI zone as 1 to 8 mm irregular crystal aggregates in masses of cleavelandite. Green spodumene growing as fibrous needles is an occasional accessory in the phosphate masses in the core.

Composition

Seven chip samples representing a cross section of triphylite-lithiophilite occurrences across the core zone were checked optically to determine composition. Five samples were selected across one mass of phosphate and checked optically. The sign and magnitude of the 2V angle, dispersion, and range of n_γ were determined for crystal fragments on a universal stage in white light. The samples all fell within the range $1.690 < n_\gamma < 1.700$ which corresponds to a compositional range of 63 to 78 mol % $LiFePO_4$ (Chapman 1943, Thomssen and Anthony 1977). The compositions determined by 2V using the data of Chapman (1943) in Winchell (1951) fall in a narrow range (Table 5-11) with no apparent variation across the dike.

It should be remembered that the optical determination of the composition is only an approximation. It does not take into account other substitutions such as Mg which could have a significant content. It does, however, suffice to indicate a narrow compositional range for

Fig. 5-33 An irregular mass of triphylite floating in the quartz core. The green color of the triphylite is masked by a coating of iridescent black oxide. The red crystal above the triphylite is a blocky microcline. The lens cap is 52 mm wide.

Table 5-11 Optical properties and corresponding compositions for triphylite samples. Samples 74a to g are chip samples collected across the core while samples 77-1 to 5 are chips from a simple mass of triphylite.

No.	2V	Dispersion	mol % $LiFePO_4$
74-a	$+74^{o}$	r>v	76
74-b	$+70^{o}$	r>v	76
74-c	$+72^{o}$	r>v	76
74-d	$+75^{o}$	r>v	77
74-e	$+72^{o}$	r>v	76
74-f	$+77^{o}$	r>v	77
74-g	$+60^{o}$	r>v	75
77-1	$+66^{o}$	r>v	75
77-2	$+76^{o}$	r>v	77
77-3	$+70^{o}$	r>v	76
77-4	$+70^{o}$	r>v	76
77-5	$+75^{o}$	r>v	77

the triphylite.

Alterations of triphylite

Two classes of alteration of triphylite are identified in the pegmatite. These are tentatively called hydrothermal, late, and supergene alterations.

(1) Hydrothermal alteration involves simple alteration of triphylite to alluaudite minerals. This alteration has been identified mainly in the albite rich UI zone where small masses of triphylite are intergrown with greenish black fibrous growths of alluaudite mixed with apatite. Moore (1973) has shown that triphylite alters to alluaudite under oxidizing conditions.

(2) Supergene alteration in the zone of weathering of the pegmatite has resulted in the alteration of triphylite to masses of varicolored phosphates. The mineralogy is very complex with several phosphate phases present.

Because Fe and Mn can have different oxidation states under alteration conditions, a variety of alteration products can form. A detailed study of this process was considered as outside the realm of this particular study.

G Apatite

Apatite is present in varying degrees of abundance in all zones of the Buck pegmatite dike. The apatite can be separated into

4 types based on color, morphology and mode of occurrence.

(1) Small, colorless, irregular grains averaging less than 1 mm are dispersed throughout the dike. The apatite is particularly abundant as an interstitial material between grains of albite and tourmaline in the wall zones, but colorless apatite was found in most thin sections examined from samples throughout the dike.

(2) Irregular blebs of deep milky blue apatite ranging from single grains less than 1 mm wide to masses 2 to 3 cm wide. The blue apatite is found mainly in the intermediate zones and the upper saccharoidal albite portion of the LW zone.

(3) Veins of massive apatite from 1 to 10 cm thick (Fig. 5-34) occur in the central and upper part of the quartz core. The apatite is either pale creamy yellow or pale green. It occurs as either a massive glassy looking material in which grain boundaries are indistinguishable or as aggregates of equant tabular subhedral grains averaging 1 cm in size with some yellowish mica between grains. Minor accessory minerals in these veins include triphylite, alluaudite and tetrahedrite.

(4) Fissure coatings of apatite are abundant in late fractures in the quartz core. This apatite can have several morphologies:

(a) Colloform coatings of white apatite on quartz or overgrowing more idiomorphic crystals of apatite.

(b) Fibrous columnar crystals of apatite. The crystals form hexagonal prisms 0.2 mm wide and 2 mm long with ragged or corroded fibrous terminations.

Fig. 5-34 Veins of coarse apatite (beige) filling fractures in the quartz (white) of the core zone.

(c) Idiomorphic crystals of colorless apatite. The euhedral 0.2 to 1.0 mm crystals are often coated with thin layers of very soft white apatite with a spongy texture possibly caused by an abundance of fluid inclusions. These layers can be easily flaked off exposing the water-clear crystals underneath. There is a wide range in the development of the crystal forms of the idiomorphic apatite. The sequence of forms identified is:

(i) hexagonal dipyramids

(ii) hexagonal dipyramids with small basal pinacoids

(iii) hexagonal dipyramids with basal pinacoids and poorly developed hexagonal prisms

(iv) equal development of pyramidal, prismatic and basal pinacoidal faces

(v) hexagonal prisms with pinicoidal terminations modified by weak pyramidal faces

(vi) hexagonal prisms with basal pinacoids
This form is the least common.

Optical studies

Samples from all the above types were examined optically and n_ω determined. Many of the fissure-coating crystals showed closely spaced concentric layers of inclusion-clouded material separating thin layers of clear apatite.

All the samples examined in immersion liquids showed nearly the same n_ω values. The range for n_ω was 1.632 to 1.638 with the majority of the values near 1.634. There was no systematic variation

determined and it would appear that the composition of the apatite, as indicated by optics has a narrow range in the fluorine-rich part of the apatite composition field. However, an apatite with admixtures of OH and CO_2 in approximately equal amounts would also fall within the same range of refractive indices.

Summary

(1) Apatite occurs throughout the dike and appears predominantly as a late phase.

(2) The apatite has a narrow compositional range near the fluorine-rich member of the series.

(3) Fluid inclusions and zones of inclusions are common in the late fissure apatite but are not a prominent feature in the other forms.

H Beryl

Although beryl is not abundant in the Buck pegmatite several samples were obtained. Restricted mainly to the intermediate zone it does occur from the lower edge of the upper wall zone, in the vicinity of the tips of large columnar tourmalines, down close to the core zone. Samples of beryl from the lower intermediate zone below the quartz core are much less common, but this may represent a sampling problem rather than a distribution factor as the lower half of the pegmatite is not as well exposed at the upper half.

Beryl forms small stubby or occasionally conical crystals,

generally in masses of albite and quartz. Crystals range in size from 0.5 to 2.0 cm. All crystals examined have milky colors of white, pale yellow or pale green. Broken crystals show a granular texture and a mottled or streaky color. Minerals commonly associated with beryl are albite, quartz, muscovite, lithian muscovite, sodic montebrasite and green tourmaline. The beryls appear unaltered both in hand specimen and under optical examination.

Compositional variation

Seven samples of beryl were analysed for alkali elements and calcium,cf. Table 5-12. All samples are from the intermediate zones, with 2 samples from the lower intermediate zone below the quartz core.

Examination of Table 5-12 and Fig. 5-35 shows some general trends. Total alkalis range from 1.4 wt. % R_2O for the sample of outer beryl to 2.8 % wt. % R_2O for beryls near the core. Calcium shows a generally erratic behaviour, while potassium remains fairly constant. In general terms lithium, rubidium and cesium tend to be lower for outer beryls near the wall zone and for the beryls below the quartz core.

Classifications of beryl based on variations in alkali contents and related to the petrogenetic character of the parent pegmatites have been presented, e.g. by Beus (1960) and Černý (1975a). Based on Černý's (1975a) simplified classification the beryls of the Buck pegmatite fall between the classes of sodic-lithian beryl and lithian-cesian beryl. This corresponds to the sharp bend in the cesium enrichment trend shown in Fig. 5-36, based on a plot of Na/Li versus Cs.

Table 5-12 Alkali elements and calcium contents and n_ω for beryls. Numbers suffixed by C are near the core, by I are in the middle of the intermediate zone and by O near the wall zone. An * indicates samples below the quartz core.

Sample No.	Li_2O	Na_2O	K_2O	Rb_2O	Cs_2O	CaO	ΣR_2O	n_ω
BC 46-c	0.471	0.84	0.029	0.041	0.284	0.012	1.665	(1)
BC 48-c	0.577	0.95	0.034	0.058	0.411	0.010	2.030	(2)
BC 49-c	0.495	0.92	0.070	0.046	0.356	0.005	1.887	1.5840
BC 82-c	0.728	1.14	0.033	0.065	0.835	0.003	2.801	1.5859
BC 122-c*	0.46	0.83	0.036	0.029	0.222	0.008	1.577	1.5809
BC 110-I*	0.56	1.01	0.035	0.028	0.374	0.023	2.007	1.5823
BC 51-O	0.396	0.69	0.037	0.027	0.209	0.004	1.359	1.5799

(1) (2) For these samples n_ω was determined for the core and rim of the crystal as follows:

BC 46-c core 1.5850 rim 1.5840

BC 48-c core 1.5850 rim 1.5820

Fig. 5-35 A plot of alkali oxides, total alkalies and calcium as a function of the soda content for 7 samples of beryl.

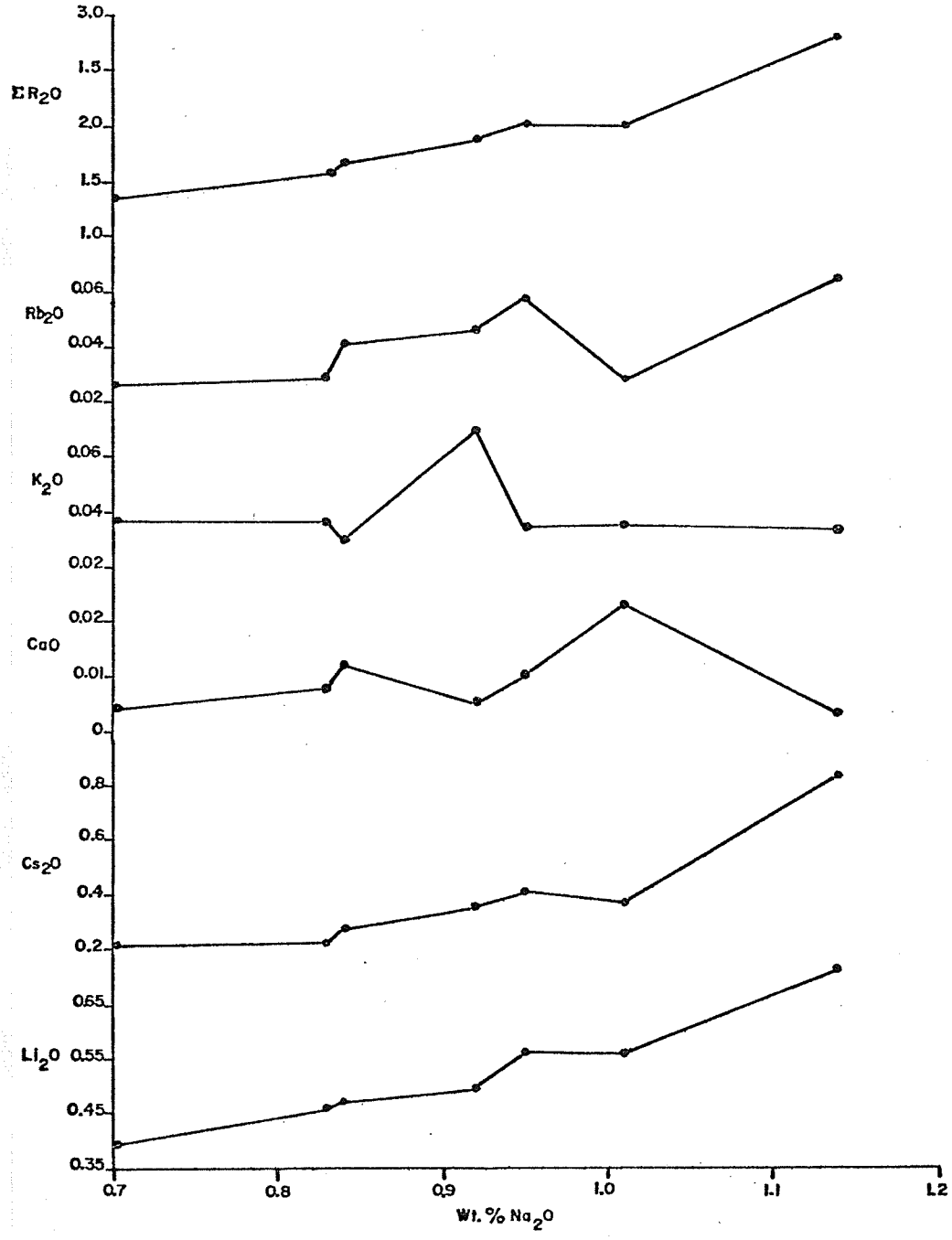

Fig. 5-36 The ratio Na/Li is plotted as a function of Cs for pegmatitic beryls. The dots represent beryl samples from the Buck pegmatite. The area enclosed by dashed lines represents the Bernic-Rush Lake pegmatite group; the solid line is the generalized trend line (figure after Černý, 1975a).

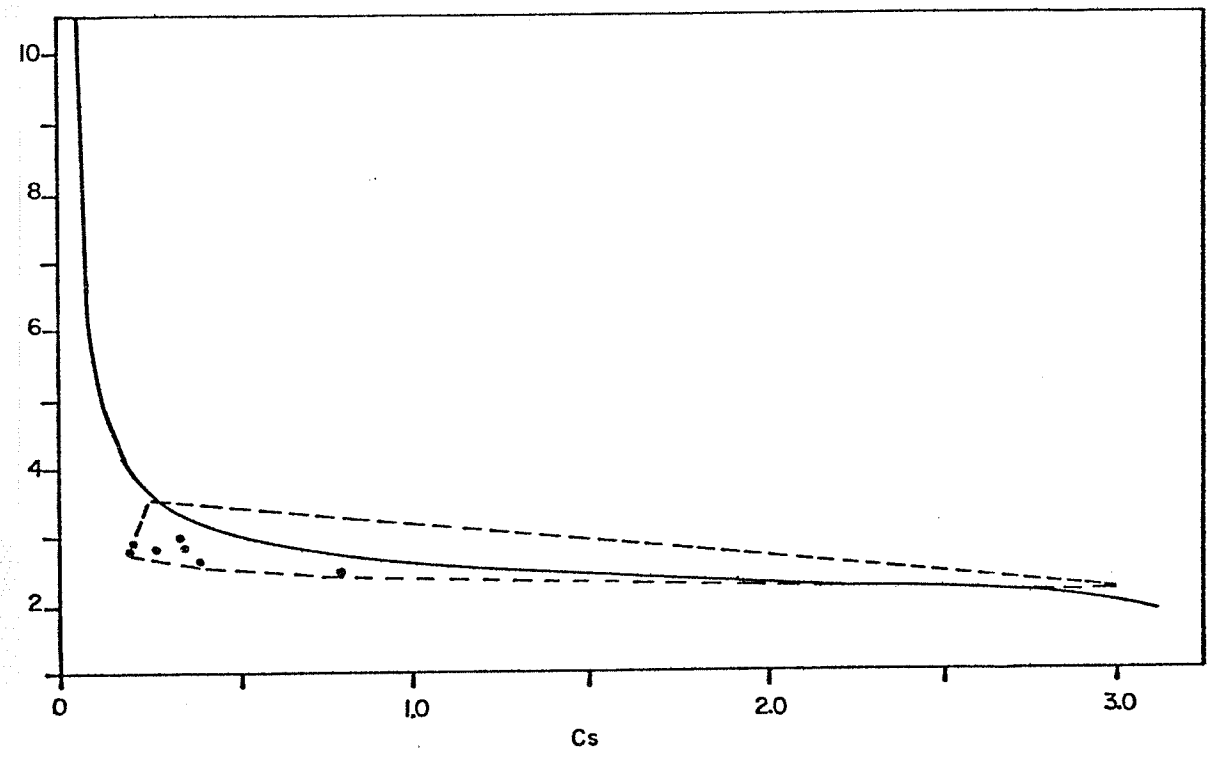

Optical variation

The $_{\omega}$ refractive index for the analysed beryls was determined by oil immersion. Černý and Hawthorne (1976) have shown that, while trying to relate n_{ω} to composition for all beryls is impossible because of the broad range of chemical substitutions possible in beryl that affect the refractive index, limiting the field to beryls from Li, Rb and Cs enriched pegmatites restricts the variables so meaningful relations can be determined. A plot of total alkalis plus calcium versus n_{ω}, Fig. 5-37, shows a consistent trend. Zoning in the crystals is the reverse of that most commonly encountered in beryl (e.g. the Tanco beryls of Černý and Simpson, 1977). That is, the cores are more enriched in alkalis having a higher n_{ω} than the rim.

Most of the beryls examined optically showed minute bubble inclusions or dusty inclusions which could be responsible for the data scatter.

Summary

The following points give some evidence toward the paragenesis of the beryl in the Buck pegmatite:

(a) Bulk composition data suggest the total alkali content of the beryl increases toward the center of the pegmatite.

(b) The beryl appears to be more abundant in the upper intermediate zone than the lower intermediate zone. This trend is in accordance with the observations of Beus (1960) on the preferred accumulations of beryl in the apical portions of differentiated pegmatites

Fig. 5-37 Plot of total alkalies plus calcium versus n_ω for beryls. The dashed trend line is from Černý and Hawthorne (1976) for beryls from Li, Rb, and Cs enriched pegmatites. The 2 pairs of points joined by solid lines represent ω values from the cores and rims of the same crystals, with the rim values marked R. Circles represent beryls from below the quartz core.

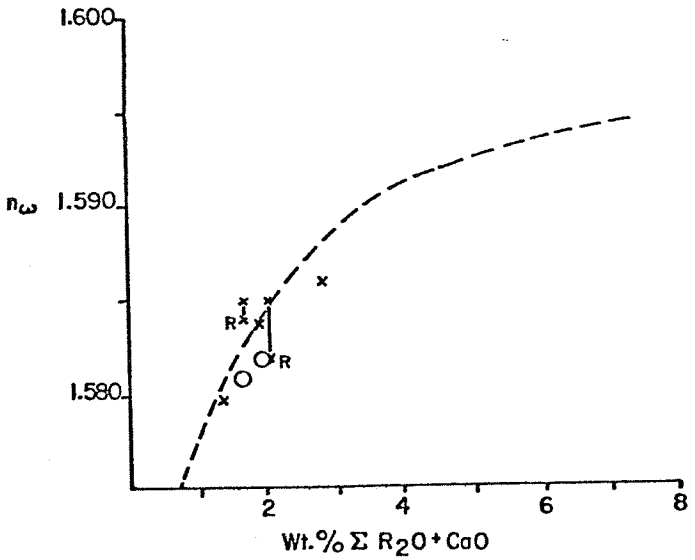

(although reverse cases such as the Tanco pegmatite are also known).

(c) Beryl is restricted to the albite-muscovite intermediate zones.

(d) The chemical zonation of the beryl is toward lower alkali content in the rims. This would indicate the fluid from which beryl crystallized was rapidly depleted in rare alkalies.

I Tourmaline

Minerals of the tourmaline group, $Na(Mg,Fe,Mn,Li,Al)_3Al_6(Si_6O_{18})(BO_3)_3(OH,F)_4$, are distributed throughout much of the pegmatite. They represent a major phase in the wall zones and an accessory mineral in the border zone and intermediate zones. Tourmaline was not found in the core zone.

Using the criteria of color, habit and location in the pegmatite 4 types of tourmaline can be distinguished:

(1) Acicular crystals 1 to 3 mm long and 0.5 to 1.0 mm wide of black tourmaline. These occur in the B zone and the outer 3 to 4 cm of the wall zones. The crystals may be doubly terminated or have ragged corroded outlines (Fig. 5-38).

(2) Large columnar crystals of bluish-black tourmaline dominate the wall zones. The tourmaline of the UW zone can reach sizes up to 5 by 15 cm. The subparallel tapering columns grow perpendicular to the hanging wall contact (Fig. 5-39). In the LW zone the crystals have a wide range of sizes up

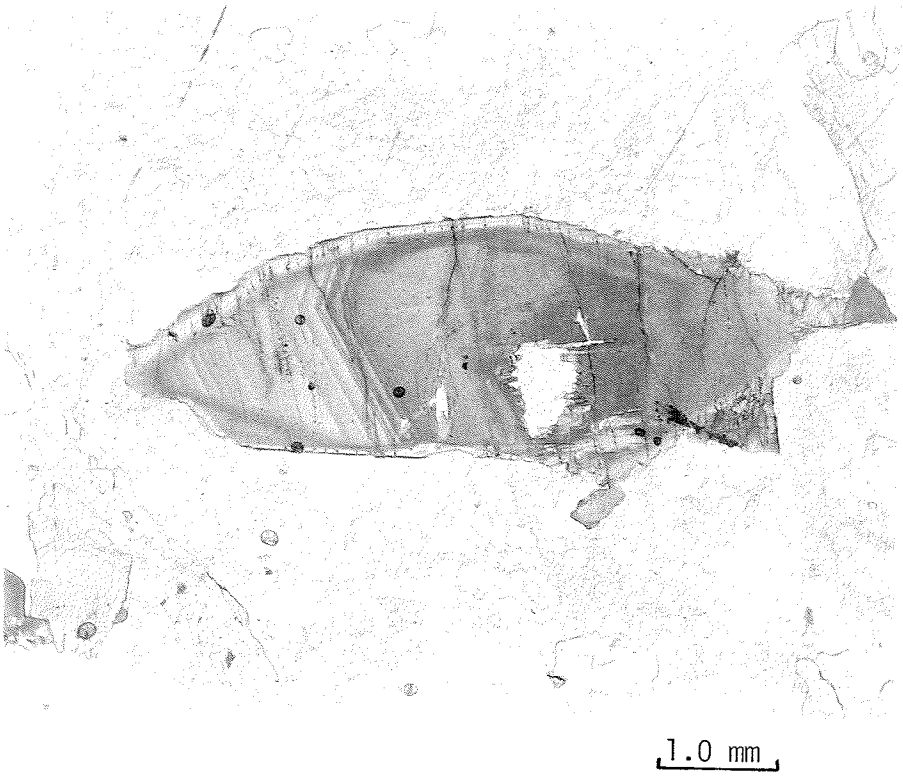

Fig. 5-38 A small crystal of black tourmaline from the B zone. Note the complex color zoning and corroded form. Thin section in plane polarized light.

Fig. 5-39 Large tapering columnar blue-black tourmalines growing perpendicular to the hanging wall contact (top of photograph). The surrounding matrix is platy pinkish albite, quartz and muscovite. Note how the crystals are broken along the basal parting and veins of quartz and albite injected to separate the fragments. The grip on the hammer is 15 cm long.

to 3 by 5 cm. They are randomly oriented floating in a fine grained quartz-albite-muscovite matrix (Fig. 5-40).

(3) Prismatic and bladed crystals of green and yellow-green tourmaline are included in plates of muscovite through much of the intermediate zones. Verdelite crystals up to 0.5 by 3 cm commonly form flattened blades parallel to the basal cleavage of the mica plates in which they are included.

(4) Irregular aggregates of indigo blue tourmaline occur in fractures in the country rock up to 10 m from the pegmatite.

No chemical analyses were done for the tourmalines so the names are based on the color and on variations in the unit cell parameters and refractive indices.

X-ray studies

Unit cell parameters were refined by x-ray powder diffraction techniques for 11 samples covering types 1, 2 and 3 above (Table 5-13). Figures 5-41 and 5-42 both show a separation of the 3 principal types of tourmaline into 3 fields. While there are distinct trends from dravite toward elbaite shown on these two figures corresponding to the position of the tourmaline in the pegmatite from the edge toward the core the exact chemical change is uncertain. The data used to determine the end member cell parameters and trend lines show a high level of scatter (Foord, 1976). The figures are meant to differentiate Fe, Mg and Li rich tourmalines and thus do not take into account other substitutions such as Al, Mn and Ca. Thus the trend of Mg depletion and Li enrichment indicated is at best an approximation of the compositional changes involved.

Fig. 5-40 Irregular shaped black tourmaline crystals in quartz-albite matrix of the lower wall zone. The greenish-black material to the right of the coin is an xenolith of amphibolite.

Table 5-13 Refined unit cell dimensions for tourmalines of the Buck dike.

Sample No.	Type/Location		a_o (Å)	c_o (Å)
BC 86	1	B	15.965±0.003	7.155±0.002
BC 97	1	LW	15.961±0.002	7.151±0.001
BC 98	1	LW	15.967±0.002	7.148±0.001
BC 56A	2	UW	15.983±0.007	7.146±0.002
BC 56B	2	UW	15.969±0.005	7.145±0.003
BC 58A	2	UW	15.969±0.003	7.123±0.003
BC 58B	2	UW	15.964±0.002	7.135±0.001
BC 56D	2	UW	15.963±0.004	7.135±0.009
BC 42	3	UI	15.891±0.003	7.117±0.001
BC 53	3	UI	15.911±0.003	7.121±0.001
BC 99	3	LI	15.916±0.002	7.116±0.001

Fig. 5-41 The ratio of cell parameters c/a as a function of c shows a distinct separation of the 3 tourmaline types. The end member parameters plotted are those of Epprecht (1953).

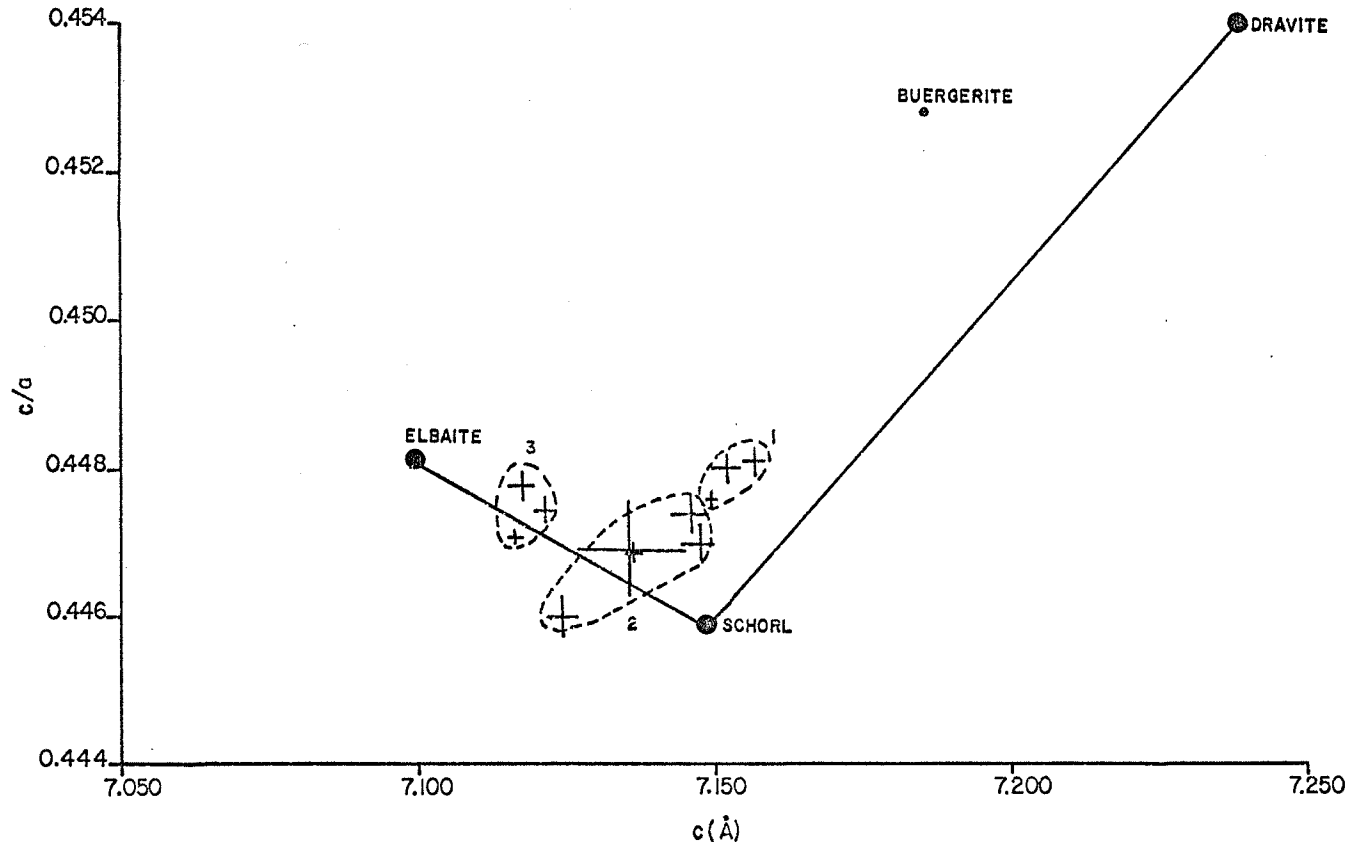

Fig. 5-42 A plot of the cell dimensions c versus a for the tourmalines. Note that the separation of the three types is better than in Fig. 5-41. The cell parameters for the end members are from Epprecht (1953).

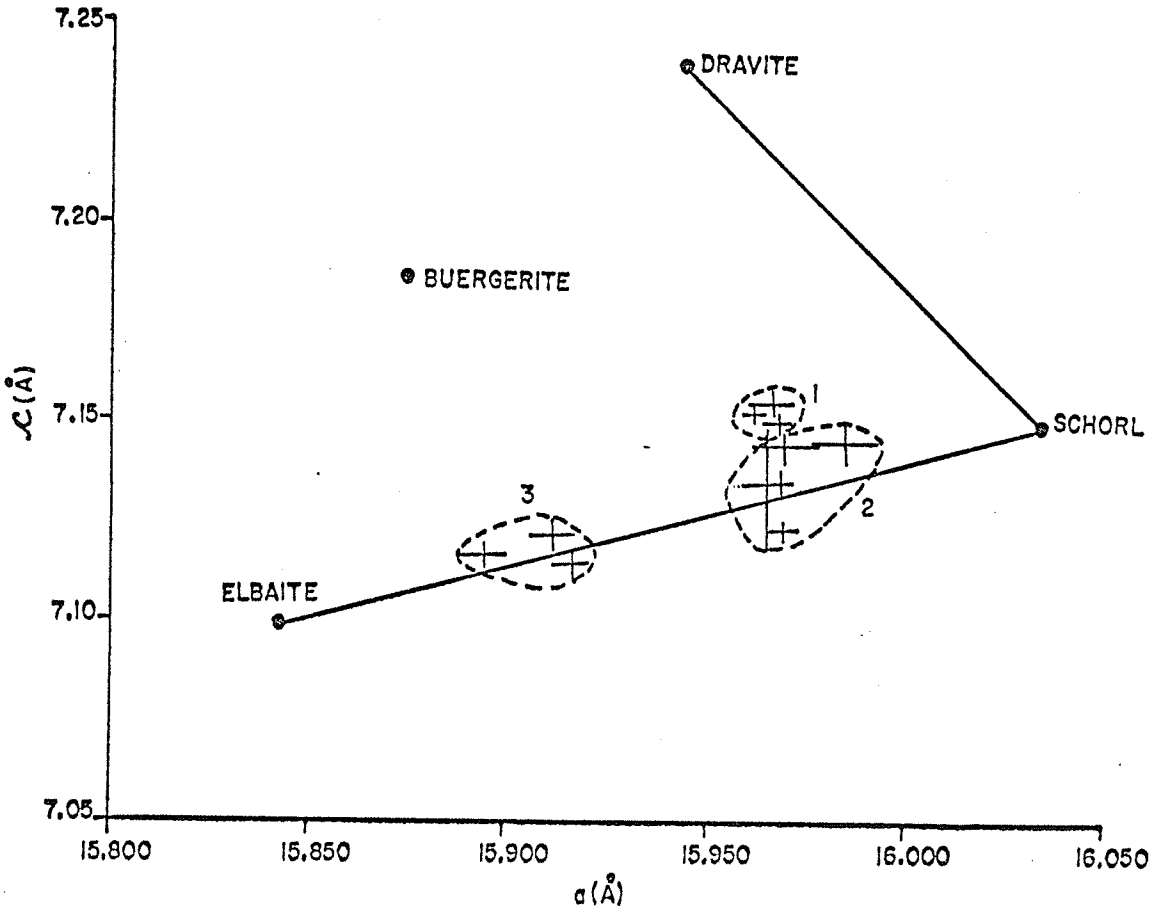

Optical studies

Attempts to make a detailed study of optical variations in the tourmalines of the Buck dike were severely hampered by the extensive chemical zoning of the crystals. The chemical variation and the optical zoning is often on such a fine scale (see Fig. 5-38) that repeated attempts to determine the refractive indices of the tourmalines by immersion oil techniques produced erratic and often contradictory results.

Zoning in small crystals is easily visible in thin section. To check the zoning in the large columnar crystals of type 2, chip samples were taken across 2 large columnar crystals. Repeated determination of n_ω produced relatively consistent data for each chip sample. The absorption color of the tourmalines was determined in polarized light, but showed no consistency and as Figures 5-43 and 5-44 show, n_ω has no obvious relation to color.

The only consistent optical property of the tourmalines noted was the n_ω value was lowest for the verdelite samples (cf. Fig 5-45).

Summary

(1) All tourmaline samples examined showed extensive zonation. This chemical variation is probably responsible for the high standard errors obtained on the refinement of unit cell parameters.

(2) The unit cell dimensions show a shift in chemistry of the tourmalines from the edges toward the middle of the dike. This should be caused, at least in part, by a decrease in Mg and an increase in Li.

Fig. 5-43 A profile of n_ω across a 6 cm wide type-2 tourmaline. The absorption colors are indicated by the letters with the color in the ω direction first and the color in the ε direction following in brackets. The colors are: G-green, B-blue, Br-brown, P-pink, V-violet, C-colorless; p indicates a pale tint.

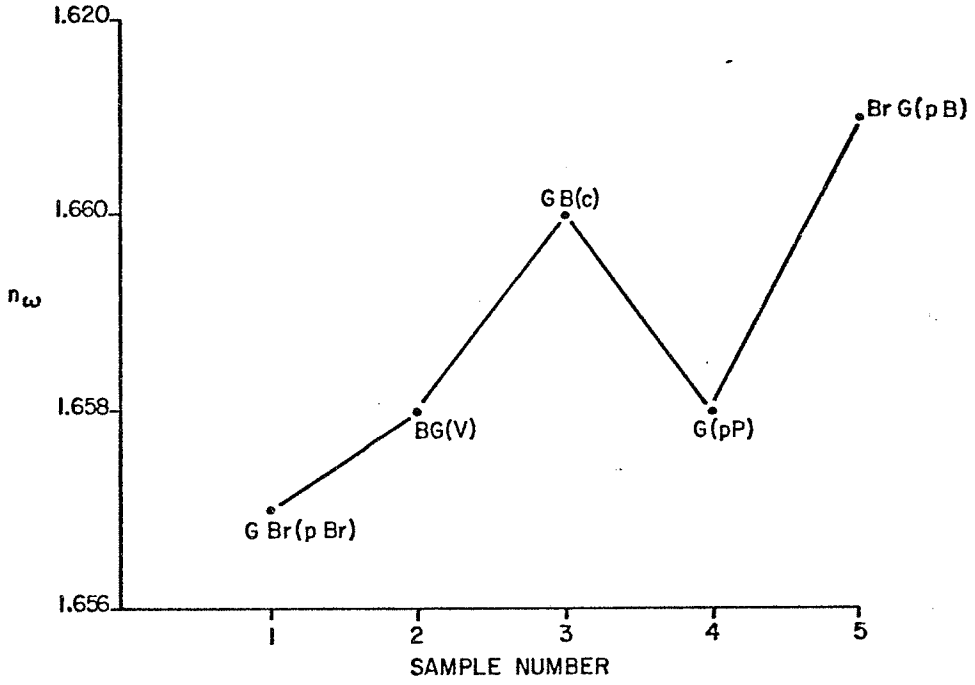

Fig. 5-44 A profile of n_ω across an 8 cm wide type-2 tourmaline. The absorption colors are abbreviated as in Fig. 5-43.

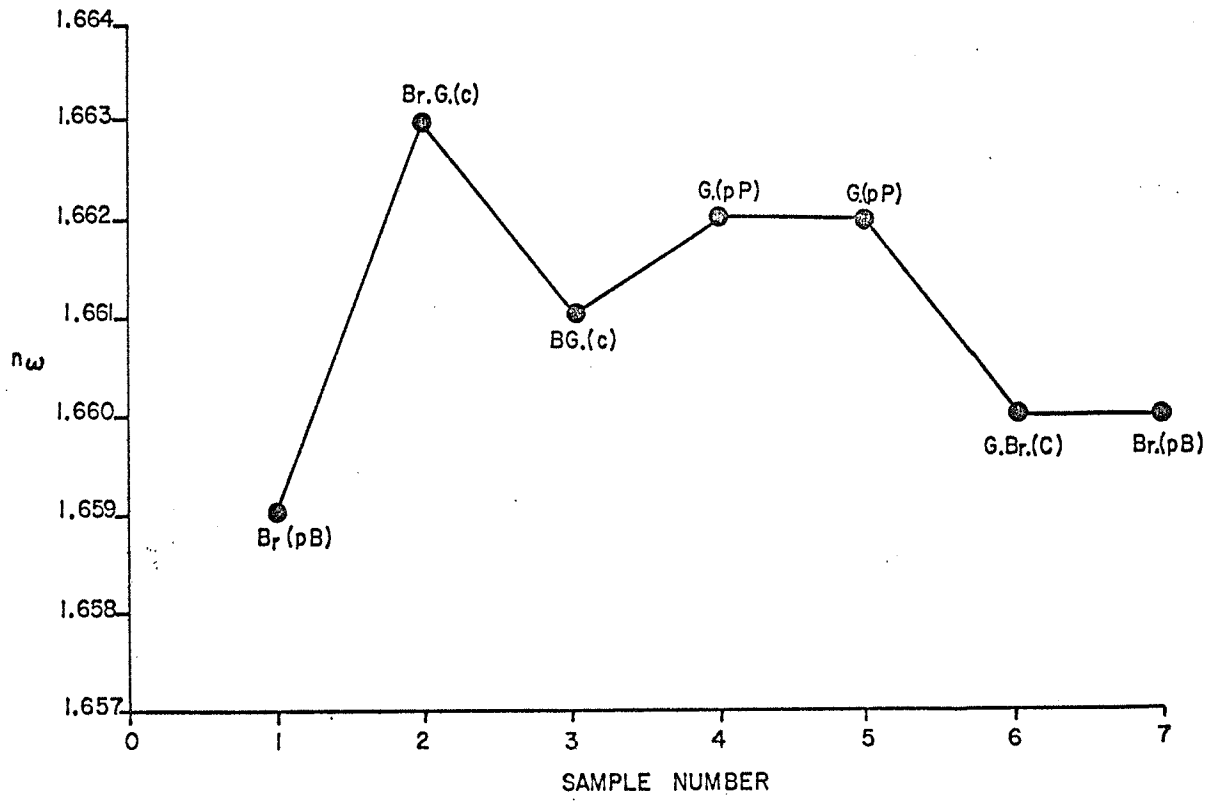

Fig. 5-45 Frequency plot of n_ω for 23 tourmalines. The cross-hatched area is the ω range of type 3 tourmaline (verdelite).

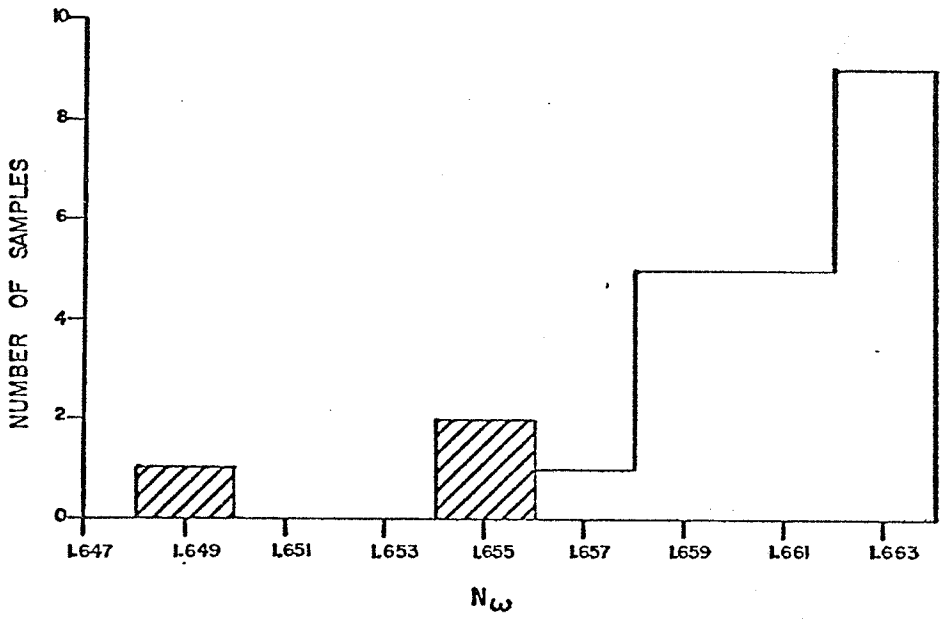

(3) There is no obvious relationship between n_ω and absorption color. Manning (1969) and Faye, et al. (1974) have shown that optical absorption spectra of tourmalines are governed by charge transfer and can be influenced by very minor fluctuations in chemistry.

(4) While absorption colors are not necessarily significant in determining chemistry, the extensive data of Foord (1976), Chaudhry and Howie (1976) and Deer et al. (1962) show a general correlation. In the schorlite-elbaite series, with gradual decrease of Fe^{+2} and increase of of Mn and Li the colors change from brown through blue, green to pink and then, with decrease in Mn, to colorless. The Buck tourmalines belong to the first half of this color sequence, the Fe rich up to Mn - and partly Li - enriched members.

J Spodumene

Spodumene, $LiAlSi_2O_6$, is present in two forms in the dike. The most common occurrence is in pseudomorphs after petalite, $LiAlSi_4O_{10}$. The blocky pseudomorphs, Fig. 5-46, consist of flat blades of greyish-white or beige spodumene separated by sheets of quartz. These aggregates are not abundant, occurring only along the contacts of the core zone with the UI and LI zones.

Two sizeable samples were ground and homogenized, then analysed for Li_2O and Al_2O_3 (Table 5-14). These show a close agreement with the composition of petalite. Sample BC-33 has lower Li_2O and

Fig. 5-46 A blocky aggregate of spodumene and quartz (elongate beige block, center) pseudomorphous after petalite. The "petalite" crystal is at the base of the quartz core. The hammer head is resting on the top of the LI zone.

Table 5-14 Comparison of the lithia-alumina contents of petalite and the spodumene-quartz aggregates.

	Wt. % Li_2O	Wt. % Al_2O_3
BC-32	4.69	16.94
BC-33	3.96	15.29
petalite (calculated)	4.88	16.64

Al_2O_3 contents than would be expected. This is probably a result of inhomogeneous distribution of quartz and spodumene in the pseudomorph which make representative sampling difficult.

Primary spodumene is rare in the Buck pegmatite. It was found only in small amounts associated with triphylite in the centre of the core zone. It occurs as small greenish yellow bladed crystals, rarely more than 5 mm long or as small yellow granular patches. Primary spodumene is often intergrown with quartz, triphylite, apatite and rarely with albite (Fig. 5-47).

K Tantalite-columbite

Tantalum-niobium oxide minerals are rare in the Buck pegmatite with only three samples discovered to date. Two samples were found in the cleavelandite masses of the upper intermediate zone and one in the upper border zone. Tantalite-columbite in the upper border zone occurs as needles 0.5 mm wide and up to 1 cm long included in large crystals of black tourmaline. The needle-like crystals show some reaction with the tourmaline in that pleochroic haloes surround the crystals. The tantalite-columbite was identified by x-ray photography using a Gandolfi camera, but the amount of sample available was insufficient for any further analysis.

Of the samples from the intermediate zone one is a single crystal approximately 4 cm wide. The length of the crystal is unknown as only about 5 cm of crystal was removed from the trench wall. The crystal shows a distinct color zoning, with a dark resinous brown core

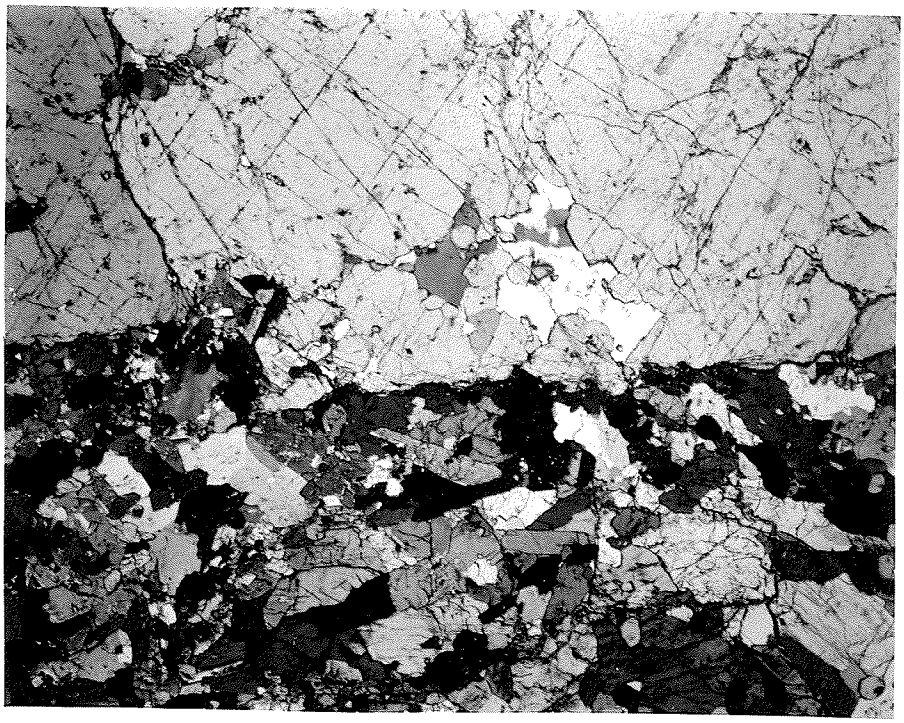

1.0 mm

Fig. 5-47 Microphotograph of crystals of primary yellow-green spodumene in a mass of triphylite. The large white and grey mass at the top of the photograph is triphylite, the lower granular mass is a mixture of spodumene, quartz and apatite. The photograph was taken in cross polarized light.

and a black rim. Three chip samples were taken, one from the black rim and 2 from the brown core zone. Unit cell dimensions were determined for the 3 samples, the results summarized in Table 5-15. Table 5-16 is a listing of x-ray powder diffraction data for the outer rim sample with data listings for tantalite and pseudo-ixiolite from the Tanco mine (Grice et al., 1972) for comparison. Pseudo-ixiolite is the structurally disordered form of tantalite-columbite. Heating of pseudo-ixiolite to 800°C in air for several hours will cause the structure to invert to the ordered tantalite structure. Comparison of the listings in Table 5-16 shows that the Buck sample corresponds to the ordered tantalite structure. The five peaks that were broader and ragged may indicate some small degree of disordering. A plot of $\underline{c}$ versus $1/3\underline{a}$, Fig. 5-48, shows that despite the obvious color zoning there is no significant variation in the cell parameters. The work of Grice, et al. (1972) with color changes in tantalites heated in oxidizing and reducing atmospheres has shown that tantalite will darken in a reducing atmosphere. Thus, the color difference could be caused by a change in fO_2 during crystallization, with the change being to a more reducing atmosphere.

Tantalite normally occurs as a late phase in pegmatite crystallization. The major occurrences in the Buck pegmatite are in the late albite masses of the intermediate zone, which agrees with this observation.

L Tetrahedrite

Tetrahedrite found as small grains near the center of the pegmatite is the only sulfosalt mineral identified in the Buck body.

Table 5-15 Unit cell dimensions of 3 samples of a tantalite crystal.

Core

a	14.427±.003 Å
b	5.761±.001 Å
c	5.095±.001 Å
V	423.467±.121 Å^3

Intermediate

a	14.430±.003 Å
b	5.762±.002 Å
c	5.095±.001 Å
V	423.626±.138 Å^3

Rim

a	14.424±.002 Å
b	5.760±.001 Å
c	5.093±.001 Å
V	423.101±.083 Å^3

Table 5-16 A comparison of the x-ray powder diffraction patterns for the dark rim material with data for tantalite and pseudo-ixiolite from Tanco (Grice et al. 1972).

Buck tantalite-columbite			Tanco tantalite			Tanco pseudo-ixiolite		
hkl	dÅ	I	hkl	dÅ	I	hkl	dÅ	I
200	7.211	8	200	7.227	6			
110	5.349	5	110	5.352	4			
310	3.692	51	310	3.687	35	110	3.673	30
400	3.605	13	400	3.604	8			
311	2.989	100	311	2.991	100	111	2.991	100
020	2.880	7	020	2.877	10	020	2.877	10
*002	2.546	5	002	2.560	11	002	2.579	11
021	2.507	13	021	2.508	16	021	2.512	19
600	2.404	17	600	2.404	15	200	2.381	6
*420	2.250	2	420	2.247	2			
312	2.096	6	312	2.102	2	112	2.110	6
*022	1.9076	6	022	1.9106	8	022	1.9198	8
620	1.8455	8	620	1.8442	6	220	1.8340	5
*512,711	1.8130	3	512,711	1.8140	8			
330	1.7831	12	330	1.7812	15	130	1.7792	19
602	1.7480	16	602	1.7500	20	202	1.7490	22
621	1.7351	25	621	1.7333	20	221	1.7288	23
313	1.5422	8	313	1.5421	10	113	1.5578	8
*622	1.4943	5	622	1.4930	5	222	1.4953	6

Table 5-16 A comparison of the x-ray powder diffraction patterns for the dark rim material with data for tantalite and pseudo-ixiolite from Tanco (Grice et al. 1972). (Cont'd.)

Buck tantalite-columbite			Tanco tantalite			Tanco pseudo-ixiolite		
hkl	dÅ	I	hkl	dÅ	I	hkl	dÅ	I
911	1.4776	11	911	1.4763	15	311	1.4670	20
			802	1.4708	3			
332	1.4606	15	332	1.4600	15			
						041	1.3861	3

* These five reflections formed broader ragged peaks on the diffractograms.

Fig. 5-48 A plot of cell dimensions c and 1/3a for 3 samples from a tantalite-columbite crystal. The field defining Mn/Fe relation is after Černý and Turnock (1971). The field is for ordered phases only. The dimension 1/3a represents the basic sub-cell of the tantalite structure type. The crosses represent double standard errors.

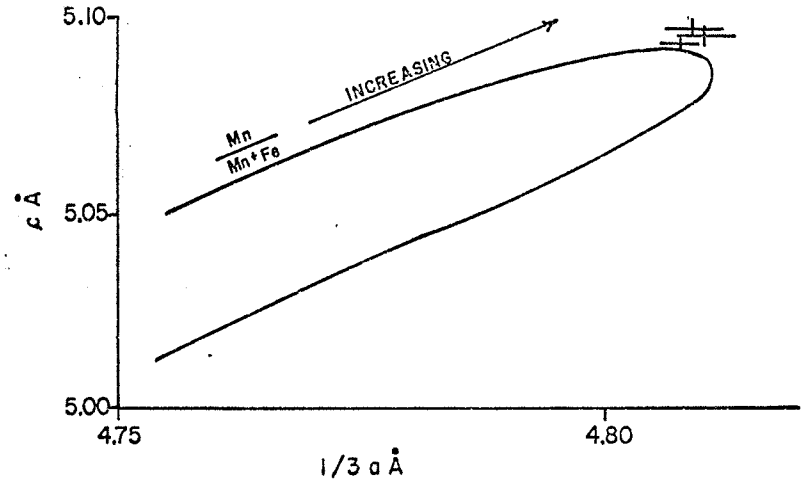

It occurs in veins of apatite up to 10 cm thick filling fractures as the edges of the quartz core. Occurrences of tetrahedrite are rare, the grains rarely exceeding 1 mm in size. Often the grains are surrounded by a thin coating of porous limonite. Other minerals in the apatite veins with the tetrahedrite include white muscovite and lithiophilite-triphylite and its alteration products.

One grain of tetrahedrite was analysed by microprobe and the cell edge determined. The data are summarized in Table 5-17. On the basis of this analyses a formula was calculated for the tetrahedrite based on 29 atoms per formula as $(Cu_{9.94}Ag_{0.06})(Fe_{1.00}Zn_{0.76}Cu_{0.20})(Sb_{3.47}As_{0.53}Bi_{0.02})S_{13}$. The type formula $(Cu,Ag)_{10}(Fe,zn,Cu)_2(Sb,As,Bi)_4S_{13}$ where charge balance is maintained by the distribution of monovalent and divalent Cu is based on the work of Charlat and Lévy (1974). The presence of Se, Hg and Cd was not detected during analyses.

Because its occurrence is restricted to late veins in the quartz core the tetrahedrite must have crystallized during a late stage hydrothermal event.

M Clay alterations of pollucite

Pods of green to buff colored clay are found along the contacts of the core zone and the intermediate zones. The clay pods show no significant form or texture (Fig. 5-49). The clay is cut by fine vein networks composed of microcrystalline quartz and mica. The surrounding minerals, chiefly quartz, cleavelandite and amblygonite show no alteration that can be related to the clay pods other than thin coatings of grey quartz, mica and occasionally apatite along the contacts

Table 5-17 The mean and deviation for elements of 8 spot microprobe analyses of a tetrahedrite grain.

Element	Weight Percent	Atomic Content Per 13 S
Zn	3.06 ± 0.05	0.76
Fe	3.45 ± 0.10	1.00
Ag	0.40 ± 0.02	0.06
Cu	39.84 ± 0.36	10.14
Sb	26.09 ± 0.29	3.47
Bi	0.23 ± 0.10	0.02
As	2.45 ± 0.18	0.53
S	25.82 ± 0.39	13.00
Total	101.34	
Cell edge	a_o = 10.369 Å ± 0.001 Å	

Analysis by T. T. Chen, CANMET, Ottawa, 1977.

Fig. 5-49 A large mass of pollucite altered to green clay at the edge of the quartz core. Note the friable character of the clay and the irregular fine grey veins throughout it. The bright white minerals along the edges of the clay pods are blocky amblygonites. The lens cap is 52 mm wide.

with the clay pods.

Samples of the green clay from the Buck dike were included in a study by P. Černý (1978) of similar clay pods in the neighbouring Tanco and Odd West pegmatites and at Luolamaki, Finland. The results indicate the green clay is an alteration product of pollucite.

A summary of the data obtained by Černý for the clay sample from the Buck dike follows:

(1) Partial chemical analysis of the clay yielded Li_2O, 0.11; Na_2O, 0.05; K_2O, 4.64; Rb_2O, 0.08; Cs_2O, 0.05; MgO, 3.72; CaO, 0.13.

(2) X-ray powder diffraction data indicate the presence of kaolinite, an illite-type mica and smectite minerals.

(3) Differential thermal analysis records confirm the presence of the above minerals but did not detect additional phases.

(4) Textural studies show that the quartz-mica veining of the clay pods is closely analogous to muscovite veining in fresh pollucite in general appearance and pattern.

Černý makes the following conclusions to support the thesis that the clay represents pseudomorphous alteration after pollucite:

(1) While no fresh pollucite is present in the dike, other consanguineous pegmatites of the area contain pollucite.

(2) The clay pods occur mainly in the middle and upper portions of the core zone, which is the most common location for pollucite in zoned Li,Rb,Cs enriched pegmatites.

(3) Kaolinite and montmorillonite are the common alteration products of pollucite.

(4) A Cs_2O content of 0.05 % is equal to the average contents for microcline and muscovite in the dikes. Only beryl and the lithian micas contain more Cs_2O. This makes it unlikely that the clay is either an alteration of feldspar or that the Cs_2O was concentrated in the clay during late hydrothermal activity. In addition, no other phases show an alteration to clay including the quartz, albite, microcline and amblygonite in direct contact with the clay pods.

Summary

Pollucite was formed during the crystallization of the pegmatite and was subsequently totally altered to clay minerals. The presence of kaolinite, montmorillonite and illite as alteration products indicates a low temperature alteration.

N Cassiterite

Cassiterite, SnO_2, is a minor phase in the dike. It has been identified only in thin sections of the lower aplitic wall zone. It forms stubby irregularly shaped crystals of 0.4 mm by 0.2 mm maximum size or as radiating rosette aggregates of crystals up to 0.6 mm wide. It is associated with lath-shaped albite, skeletal crystals of complexly zoned tourmaline, pale blue apatite and very small acicular crystals of an unidentified silver-grey opaque mineral.

The cassiterite is pleochroic, with the color ranging from brown to a deep reddish-brown, and with irregularly distributed darker patches.

Because the cassiterite is so rare and occurs only as tiny grains no detailed work was possible on it.

CHAPTER 6

PETROLOGY AND GEOCHEMISTRY

A Petrology

Introduction

The internal crystallization processes of pegmatites have been studied by many authors. The most recent work of Jahns and Burnham (1969) has taken the process classifications of previous authors such as Niggli, Fersman and Smith and provided experimental proof supporting the classic model of pegmatite crystallization. This model consists of four successive stages descriptive of the evolution of a water-rich granitic melt. In summary these stages are:

(1) Magmatic stage. Crystallization takes place from a volatile-rich, but undersaturated silicate melt. Typically, the products of this stage are anhydrous silicates with or without OH-bearing phases. The textures produced during this process are phaneritic and can be fine to coarse grained. Because crystallization is taking place from a granitic magma the products should have a granitic minimum composition. Products related to this stage are fine-grained border zones and graphic zones of granitic minimum bulk composition.

(2) Magma/aqueous fluid stage. As mainly anhydrous phases crystallize in the magmatic stage the residual melt becomes progressively enriched in volatiles. As the volatile content increases the viscosity of the melt decreases (Burnham, 1964) and when the melt reaches the saturation point for water it

separates into two immiscible fluids, a silicate melt and a supercritical aqueous fluid* (Smith, 1948). Crystallization can take place simultaneously from the silicate melt and the aqueous fluid. Because of the very low viscosity of the aqueous fluid ionic migration is very fast so crystal growth is rapid and the typical "giant crystals" associated with pegmatites can form. Typical products of this process are the large crystals of the blocky crystal zones and finer grained aplitic material formed directly from the melt. Zoned crystals are common because rapid growth will not allow solids and fluids to equilibrate.

(3) Aqueous fluid stage. When progressive crystallization has exhausted the silicate melt, the residual aqueous supercritical fluid can continue to crystallize minerals and to react with earlier precipitates and alter them. Typical products of this stage are the precipitation of the quartz core and the extensive albitization of earlier precipitates.

(4) Hydrothermal stage. In the late stage of formation, the last residual hot water circulates in fissures in the dike. This hot solution can leach solid phases and precipitate minerals typical of alpine-vein-types of parageneses.

---

* The term "aqueous fluid" is used here to indicate a mixture of alkalies, silica and alumina in suspension in a medium of supercritical water. While water, above the critical temperature, is not a fluid but gaseous in nature, the term aqueous fluid has been retained in this discussion to remain consistent with the terminology of recent literature. A more complete discussion of the problems of terminology concerning supercritical water can be found in Jahns and Burnham, 1969.

Associated with some of these stages is the process of exomorphism, or the alteration of the country rock. As this is caused by outward migration of aqueous fluids this can be of significance in steps 2 to 4.

All pegmatites do not necessarily have to form as a result of all the above processes. Some pegmatites may be dominantly magmatic in origin, while others show no indication of crystallization from a melt.

Textural relationships of zones

Examination of the textures and zones of the Buck dike has shown that, in the section of the pegmatite exposed, there is no zone that corresponds to a granitic minimum composition. Similarly, there are no zones with a typical phaneritic texture. Because of this it must be assumed that the magmatic process of the Jahns and Burnham model is absent in the Buck dike. The earliest formed crystals visible in the exposed portion of the dike appear to be the large blocky crystals of the core and intermediate zones. Because of the size of these crystals they must have crystallized from an aqueous fluid. There is no evidence of finer grained products likely to have crystallized from the silicate melt in contact with the aqueous fluid. The presence of two liquid phases cannot be ruled out however, because the portion of the dike examined is small compared to the known extent of the body. While the water saturated silicate melt is more fluid than a dry melt, its viscosity and density is much higher than the exsolved mobile aqueous fluid. Gravitational settling and filter pressing can segregate the

aqueous fluid and force it into the apical portion of the dike as documented on many examples of gently to steeply dipping pegmatites (e.g. Beus, 1948, 1960). Thus, as only the most apical portion of the dike is exposed, the textural evidence suggesting the pegmatite crystallized only from the aqueous fluid does not preclude the possibility of products of simultaneous crystallization from two fluid mediums existing at greater depth in the dike.

Precipitation along a thermal gradient produces inward crystallization as heat is lost to the country rock. Under this situation the minerals of the border zone should be the earliest formed solids and the quartz core the last to solidify. The following textural evidence suggests that the majority of the dike formed by late stage alteration and replacement of early precipitates by albitizing fluids.

(1) The thin upper border zone (which should have a granite minimum composition if formed from a silicate melt) consists of only platy albite with numerous tiny inclusions of round quartz grains. Occasional remnants of tourmaline are present, usually altered to micas.

(2) The tourmalines of the upper wall zone are broken apart and veined with albite and quartz. The lower wall zone consists mainly of saccharoidal albite containing corroded crystals of tourmaline and rare highly altered remnants of microcline. Minerals such as cassiterite and tantalite, which should be among the last phases to precipitate, occur in the albite very near the contact of the dike.

(3) Blocky microcline crystals in the intermediate zones are cut by veins of albite and muscovite. The surfaces of the crystals are corroded by masses of cleavelandite and coated with lithian muscovite (see Fig. 5-2). Quartz masses in the intermediate zones are veined by networks of fine albite stringers.

(4) Large blocky crystals of amblygonite, where they are in contact with the radiating fans of cleavelandite have siliceous reaction rims coating them. Occasionally the amblygonite crystals are penetrated by veins of muscovite, quartz, albite and apatite. The amblygonite is altered to montebrasite along these veins.

(5) Blocky quartz-spodumene pseudomorphs after petalite are cut by veins of a fine grey-green sugary mica.

Textural evidence suggests that only the core zone and the relictic blocky material of the intermediate zones belong to the primary inward crystallization. The border, wall and much of the intermediate zones consist largely of late replacement products.

The last precipitate from the supercritical fluid, or possibly the hydrothermal solution, appears to be the veins of massive apatite containing some mica, alluaudite and tetrahedrite that occur in the quartz core. These apatite veins crosscut the late albite veins so they appear to postdate the albitization.

The final stage in the development of the pegmatite, the alteration by, and precipitation from the hydrothermal fluids, appears restricted to the fractures in the quartz core. This resulted in precipitation of adularia, euhedral apatite and flaky white muscovite

in the fractures. The hydrothermal solutions may have been also responsible for altering the pollucite to green clay.

Because so much of the early precipitated material has been albitized the original composition of the wall and intermediate zones can only be speculated on. Černý (pers. comm. 1976) has suggested it consisted largely of microcline and quartz. This hypothesis is supported by the presence of "petalite" in the intermediate zones. Many authors have shown (see summary in Černý and Ferguson, 1972) that petalite forms preferentially in association with primary microcline and is not cogenetic with albite replacement units. This suggests that when petalite precipitated, microcline was the predominant phase in the dike. It clearly is predominant in the western drill hole intersection (Canol Metal Mines, 1961) where the metasomatic processes are much less developed. Relictic microcline is a fairly common phase in the dike as are fairly extensive masses of muscovite likely to have formed from microcline. A small exposure of the dike north of the main trench is composed almost exclusively of muscovite, suggesting it can form much larger masses locally in the dike.

Conditions of formation

No specific studies were made to determine the pressure-temperature conditions under which the pegmatite formed. Some estimate of the pressure can be made, however, because of the presence of petalite pseudomorphed by spodumene and quartz. Černý (1975b, Fig. 11) shows the stability field of petalite superposed on the liquidus-solidus of the Li-bearing Harding pegmatite. The minimum pressure under

which petalite can form is approximately 2.0 Kbars and the maximum about 4.0 Kbars. The corresponding temperature interval for the formation of petalite between the liquidus and solidus is 650°C to 550°C. However, as no silicate melt was involved in the formation of the dike, the solidus temperature does not represent a meaningful lower limit of crystallization.

Exomorphism

Loss of volatiles into the country rocks can cause alteration haloes to form around pegmatites. The only evidences of exomorphism around the Buck dike are the local alteration of hornblende to biotite and in rare instances the development of holmquistite along fractures in the amphibolite near the dike. Traces of tourmaline have been found in the narrow alteration fractures.

B Geochemistry

Introduction

Chemical variation in mineral phases in pegmatites can be used to study fractionation within the bodies and to classify pegmatites according to the degree of enrichment of rare elements. The relationship of geochemistry of minerals to zonal structure can help in defining the processes involved in the formation of the zones and the sequence of formation of the zones.

Geochemical variations

During crystallization of a pegmatite some elements will

decrease in concentration in the fluid phases while other elements will be progressively enriched in the fluid phases and thus will concentrate in minerals formed at the later stages of crystallization or alteration. In general Ca, Fe, Ti, Ba, Sr, Mg, Sc and Zn will decrease progressively while Pb, Li, Rb, Cs, Ga, Sn, Be, Ta, Nb, Hf, F, B and Ca will accumulate during crystallization (Ginzburg 1960, and Burnham and Jahns 1961). Relational parameters are also of significance, such as Fe/Mn, K/Rb, K/Cs, Ti/(Ta+Nb) and Nb/Ta which decrease progressively with fractionation.

Ginzburg (1960) established a series of geochemical stages characterizing the stages of crystallization of a pegmatite. These stages can be related directly to the previously described processes of Jahns and Burnham (1969). The first three stages are primary stages equivalent to the primary crystallization from melt and melt plus aqueous fluid. The final three stages are replacement stages corresponding to the crystallization and alteration from an aqueous fluid. In summary, Ginzburg's stages are:

(1) Ca-Na (plagioclase) stage. This stage typically shows high Ca, Fe, Mg, Ti, Zn, Sc and rare earth elements. The plagioclase stage is characteristic of deep seated pegmatites that have reacted extensively with the country rock and thus is not present in the Buck dike.

(2) K (microcline/muscovite) stage. Microcline forms extensively while muscovite forms later in the stage, possibly at the expense of microcline. Late in this stage Ca, Mg, Fe and Ti are depleted with schorl crystallizing. Some beryl can form.

In the Buck dike this stage corresponds to the formation of the primary minerals of the wall and intermediate zones such as microcline and muscovite. As Figures 6-1 and 6-2 show, the microcline and muscovite in the dike became progressively enriched inward in Cs and Rb.

(3) Li (spodumene) stage. This develops along with the K-stage in pegmatites highly enriched in Li. The principal feature of this stage is the crystallization of Li-Cs bearing minerals such as spodumene, petalite, amblygonite and triphylite. According to evidence assembled by P. Černý most pollucite occurrences in pegmatites belong to this stage. In the Buck dike, this stage corresponds to the formation of the core zone with its blocky crystals of Li-minerals. The triphylite formed in the Buck dike is iron rich with an Fe/Mn ratio of approximately 3:1.

(4) Na (albitization) stage. In this stage albite forms at the expense of earlier precipitates, particularly microcline. As the microcline and spodumene is albitized considerable amounts of Rb, Cs, Li and Pb are released into solution again, further increasing their concentrations. This is evident in the Buck dike in that the lithian and lithian-lepidolitic micas associated with the albitized zones are much richer in Li, Rb and Cs than the earlier muscovite (cf. Chapter 5, section D). As Na concentration increases, Fe decreases in solution and Ta, Nb, Mn, Sn and Be reach concentrations suitable for forming minerals (see Solodov, 1965). Thus the minerals beryl,

Fig. 6-1 Plots of K/Cs vs. Cs and K/Rb for microcline crystals of the upper half of the dike. The arrows indicate inward enrichment in the dike.

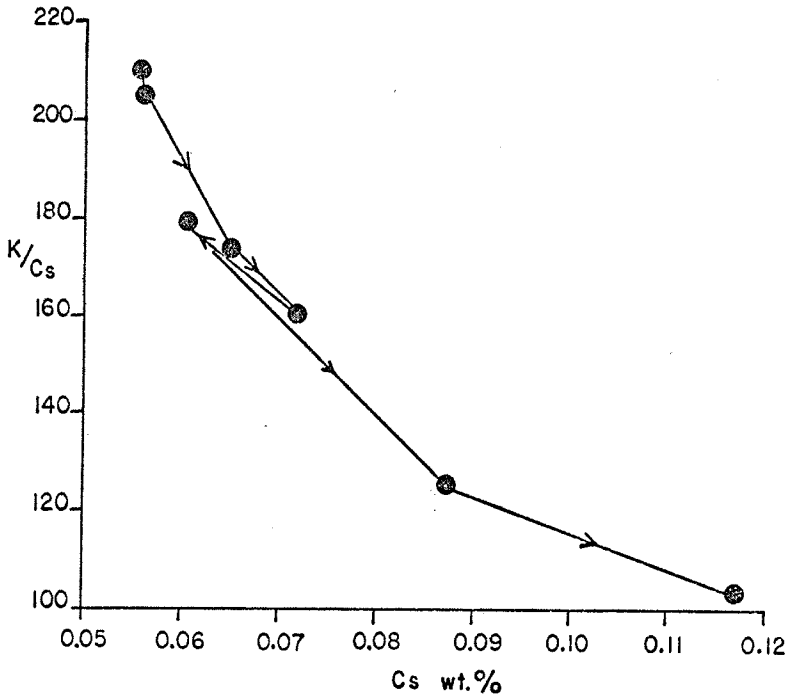

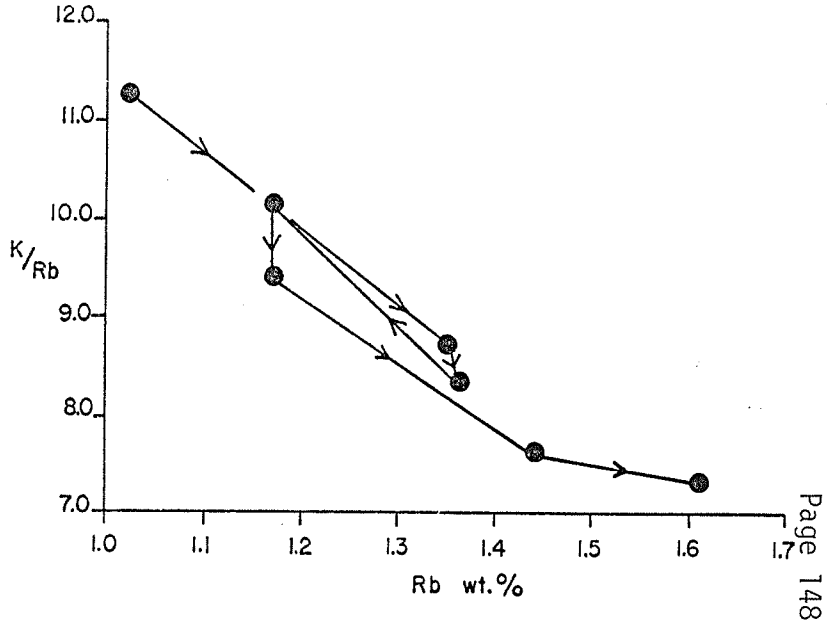

Fig. 6-2 Plots of K/Cs vs. Cs and K/Rb for muscovites. The arrows indicate inward enrichment in the dike.

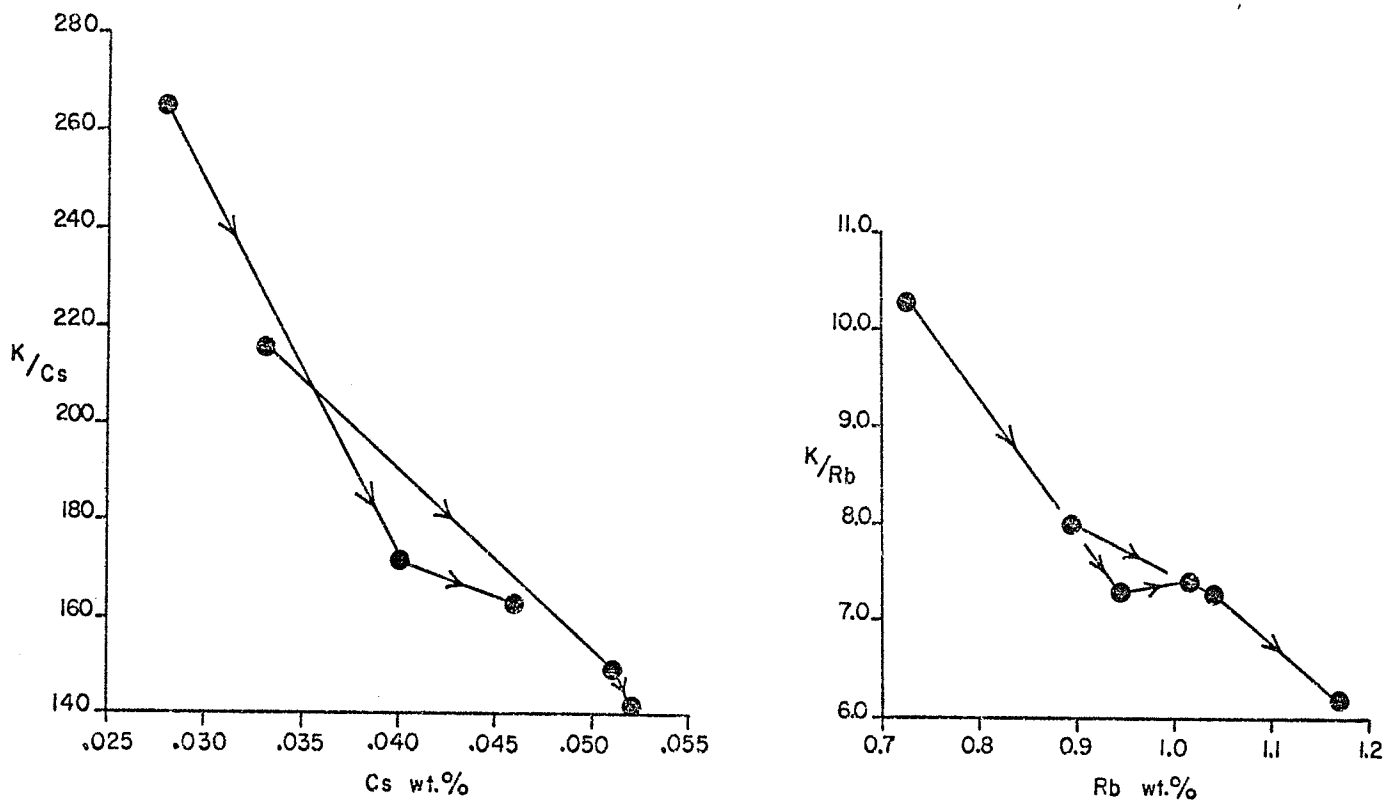

tantalite-columbite and cassiterite are found associated with the albitized zones in the dike. The tantalite formed has a low Fe/Mn ratio (cf. Fig. 5-48), $\approx$1:9 as compared to the earlier formed triphylite.

(5) Cs-Rb-Li-K (lepidolite) stage. This stage is a characteristic development of late stage fluids very rich in Li and volatiles, particularly F. It can occur instead of or immediately after the Na-stage. High concentrations of Li, Rb, Cs, Ta and volatiles are typical as well as the appearance of Sb and Bi bearing minerals. Iron is generally extremely depleted. In the Buck dike, no extensive development of lepidolite took place, so this stage cannot be distinguished from the Na-stage. This is indicated by the close association of Li-rich micas and albite in the metasomatized K-feldspars. Tetrahedrite rich in Cu and Sb and containing some Bi occurs in small amounts in the veins of coarse fluorapatite, so the volatile-rich apatite veins could tentatively be assigned to this stage. This type of massive late apatite veins is very rare in granitic pegmatites (pers. comm. A. A. Beus to P. Černý).

(6) Hydrothermal stage. Late stage hot aqueous fluids circulating in fractures in the pegmatite is the main feature of this stage. The hot fluids leach the surrounding minerals so geochemical parameters are variable for this stage. Typical developments of this stage are alpine-vein-type coatings of adularia, tabular apatite and flaky micas in open fractures as are found in the core of the Buck pegmatite.

Geochemical classification

During crystallization and differentiation of a magma, some elements will concentrate in residual magmas and other elements will be depleted in the residual. Heier and Taylor (1959) have shown that the alkali elements are particularly suitable for studying differentiation in granitic rocks. As Li, Rb and Cs concentrate in pegmatitic fluids the concentration of rare alkalies in pegmatitic minerals can be used to classify pegmatites by the degree of enrichment. Using this as a basis Gordiyenko (1971) set up a classification of rare element enrichment in pegmatites based on the indicator parameters of the concentration of Li, Rb and Cs in microcline and muscovite. The classification is essentially industry-oriented, being based on the type of economic mineralization present. Gordiyenko defined his classes of pegmatites as: Ia-barren feldspathic pegmatites of non-mineralized mica-ceramic provinces, Ib-barren feldspathic pegmatites of rare metal pegmatite provinces, II muscovite-feldspathic pegmatites with Be, Nb and Ta mineralization, III spodumene pegmatites with Li, Be, Ta, Nb and Sn mineralization and IV spodumene-lepidolite pegmatites with Li, Cs, Ta, Be, Nb and Sn mineralization. Thus each class is successively more enriched in rare metal elements. Comparing the mean contents of Li, Rb and Cs in the micas and microclines of the Buck dike to the limiting values of Gordiyenko, Table 6-1 shows the Buck dike falls between type III spodumenic and type IV spodumene-lepidolitic classes. Thus the Buck dike can be classified as a spodumene pegmatite highly enriched in Li, Cs (Rb) and with a possible Ta enrichment.

The chemical variations of beryl can also be used to

Table 6-1 Geochemical classification of Gordiyenko with the Buck pegmatite type indicated. The values are the mean and standard deviation in weight percent for the elements in microcline and muscovite.

Type	Mineralization	Li	Rb	Cs
Muscovite				
Ia	barren	0.006±0.0005	0.037±0.002	0.0007±0.00003
Ib	barren	0.063±0.008	0.260±0.004	0.0094±0.0030
II	Be, Nb (Ta)	0.058±0.001	0.360±0.040	0.0250±0.0060
III	Li, Be, Ta (Nb,Sn)	0.065±0.006	0.790±0.080	0.0298±0.0034
Buck Dike		0.230±0.03	0.960±0.15	0.0420±0.010
IV	Li,Cs,Ta(Be,Nb,Sn)	0.137±0.035	1.920±0.360	0.2270±0.038
Microcline				
Ia		0.0004±0.00005	0.029±0.003	0.0003±0.00007
Ib		0.0015±0.0003	0.102±0.029	0.0053±0.0022
II		0.0080±0.0008	0.312±0.064	0.0058±0.0014
III		0.0190±0.0031	0.870±0.054	0.0380±0.0024
Buck Dike			1.290±0.21	0.0750±0.022
IV		0.0226±0.0026	1.610±0.360	0.1480±0.0033

classify the degree of rare element enrichment in pegmatites. Beus (1960) presents extensive data on the chemistry of beryl from many types of pegmatites. Černý (1975a) summarized the classifications of Beus and of Feklitchev (1964) for a classification of beryl-bearing pegmatites based on the Na, Li and Cs contents of the beryl. The beryls of the Buck pegmatite would be classed as sodic-lithian beryls with moderate cesium contents, typical of lithium enriched differentiated bodies. Černý uses the plot Na/Li vs. Cs in beryls to differentiate pegmatite groups of varying degrees of enrichment in rare elements (cf. Fig. 5-36 for the trend line and the position of the Buck beryls on this plot). The beryls of the Buck dike correspond to the class of beryls from Li, Rb and Cs enriched differentiated pegmatites. It must be pointed out that Černý included the Buck beryl data in his original plot for the Bernic-Rush Lake group (as defined by Černý and Turnock, 1971), but the position of the Buck beryls in the above class of pegmatites has been confirmed by additional data accumulated since the 1975 publication from other pegmatite districts (P. Černý, pers. comm., 1979).

In terms of mineralogy alone the Buck pegmatite dike falls within classifications such as Fersman's (1931) as the most Li, Rb and Cs enriched type of pegmatite.

CHAPTER 7

ECONOMIC ASPECTS

The Buck pegmatite contains several minerals of potential economic interest (Table 7-1). These are minerals for which an established market exists. The dike, because it is thin and contains low grades of these particular minerals is unlikely to become an economic deposit.

Lithium content would be the obvious reason for mining this particular body, however as Table 7-2 shows, the bulk Li_2O values for core samples are generally quite low with erratic occurrences of high values. The erratic nature of the assays can be caused by two factors:

(1) The drill core used for the assay determination represents a 3 cm wide sample through an inhomogeneous body containing large crystals of lithium bearing minerals scattered in a lithium poor matrix.

(2) Drilling data seems to indicate greater than expected lateral inhomogeneity in the dike. Drill log descriptions indicate that pods of minerals such as spodumene exist atdepth in the dike. The drill logs for hole number 29 (Table 7-2) describe the 2.4 m section containing 2.92 wt. % Li_2O as comprising 75% green spodumene (by visual estimates). The fact that the green primary spodumene is so abundant at depth while it occurs only in very small amounts in the open trench accentuates the inhomogeneity of the dike.

Table 7-1 Minerals of the Buck pegmatite dike for which economic uses exists.

Mineral	Element	Uses
spodumene, micas	Li	high temperature greases nuclear weapons high yield storage batteries high temperature ceramics
lithian micas	Rb,Ga	semiconductor industry magnetic bubble computer memories chemical catalysts laser generators
beryl	Be	refractory materials Be-Cu alloys for springs control elements for nuclear reactors
tantalite	Ta	high potential electronic capacitors corrosion resistant alloys
pollucite	Cs	magnetohydrodynamic power generators ion engines for space research
amblygonite		ceramic glazes

Table 7-2 Assay values for total lithia content in diamond drill core. The zone positions were estimated from drill hole logs of the Lithium Corporation of Canada. The drilling was done in 1956.

Hole No.	Wt. % Li_2O	Sample length (m)	Zones sampled
18	trace	3.8	B, UW, UI
	trace	2.1	C, LI, LW
21	0.38	1.5	lower C,LI
22	0.16	2.6	all
23	0.11	1.2	B, UW, UI
	0.18	2.1	C?, LI
	0.02	1.7	LI, LW
24	0.19	2.1	B,UW,UI,part C
	1.06	2.0	part C, LI, LW
25	0.13	2.5	B, UW, UI
	0.24	2.7	C, LI
	0.12	2.4	LI, LW
27	0.12	2.1	UW, UI
	0.11	2.3	UI, C
	0.13	2.3	C, LI
	0.12	2.8	LW
28	0.16	2.3	B, UW, UI
	0.90	2.4	C, LI
	0.35	2.4	LI, LW
29	2.92	2.4	C, LI
30	1.14	2.5	UI? C
	0.15	2.6	LI, LW ?
31	0.44	2.1	C, LI ?

Because of the inhomogeneity, certain areas of the dike may contain material of economic grade, but it is unlikely that sufficient tonnage exists to support a mining operation.

The other minerals of economic interest occur in even lower concentrations than spodumene. Tantalite, of economic interest because of the close proximity of the Tanco tantalum mining and milling operations, has only been noted in three small locations with the dike. Tantalite received no mention in the drill logs, but may have been present but not identified.

The most significant economic aspect of the Buck pegmatite dike is as a regional indicator of economic potential. The Buck dike indicates that the Tanco type of rare element enriched pegmatites have a continuity to the east of the mine. As no satisfactory geophysical method exists for locating pegmatite deposits, surface geology and geochemistry are the only reliable tools in locating these bodies. Locating a subeconomic pegmatite deposit can reduce the search from a regional scale operation to the restricted vicinity of the occurrence to locate cogenetic bodies of possible economic size and grade.

The larger dike below the Buck pegmatite (see Fig. 4-3) is richer in lithia. Reserves of 800,000 tons of 2.13% Li_2O have been reported (B. Bannatyne, pers. comm.). Mineralogically the dike differs from the Buck dike in that it contains large masses of primary petalite.

REFERENCES

Bambauer, H. U., Corlett, M., Eberhard, E. and Viswanathan, K., 1967. Diagrams for the determination of plagioclases using X-ray powder methods. Schweiz. Miner. Petr. Mitt., 47, 333-349

Bannatyne, B. B., 1972. Pegmatite project. In Manitoba Mines Br. Geol. Paper 3/72, 50-53.

Beakhouse, G., 1976. The English River Subprovince. In Centre for Precambrian studies, 1975 Annual Report, University of Manitoba, 51-66.

Beus, A. A., 1960. Geochemistry of beryllium and genetic types of beryllium deposits. English translation, 1966, W. H. Freeman and Co., San Francisco.

Beus, A. A., 1948. Vertical zoning of pegmatites on the example of the pegmatite field Aksu-Pushtiru (Turkestan Range) (in Russian). Doklady Acad. Sci. U. S. S. R., 60, 1235-1238.

Burnham, C. W., 1964. Viscosity of a water-rich pegmatite melt at high pressure. Geol. Soc. Am., Spec. paper 76, p. 26 (abst.).

Burnham, C. W. and Jahns, R. H., 1961. Experimental studies of pegmatite genesis; the composition of pegmatite fluids. Geol. Soc. Am., Spec. Paper 68, 143-144 (abst.).

Černá, I., Černý, P. and Ferguson, R. B., 1972. The Tanco pegmatite at Bernic Lake. Manitoba. III Amblygonite-montebrasite. Can. Mineral. 11, 643-659.

Černá, I., Černý, P., and Ferguson, R. B., 1973. The fluorine content and some physical properties of the amblygonite-montebrasite minerals. Am. Mineral., 58, 291-301.

Černý, P., 1975a. Alkali variations in pegmatitic beryl and their petrogenetic implications. Neues. Jahrb. Mineral. Abh., 123, 198-212.

Černý, P., 1975b. Granitic pegmatites and their minerals; selected examples of recent progress. Fortschr. Miner., 52, 225-240.

Černý, P. 1976. Pegmatite studies. Centre for Precambrian Studies, University of Manitoba, Annual Report 1976, 22-44.

Černý, P., 1978. Alteration of pollucite in some pegmatites of southeastern Manitoba. Can. Mineral., 16, 89-95.

Černý, P. and Ferguson, R. B., 1972. The Tanco pegmatite at Bernic Lake, Manitoba. IV Petalite and spodumene relations. Can. Mineral., 11, 660-678.

Černý, P., Goad, B. E. and Trueman, D. L., 1978. Petrogenetic relations in the Winnipeg River pegmatite district, southeastern Manitoba. Geol. Assoc. Can., Min. Assoc. Can. General Meeting Abstracts, p. 378.

Černý, P. and Hawthorne, F. C., 1976. Refractive indices versus alkali contents in beryl: general limitations and applications to some pegmatitic types. Can. Mineral., 14, 491-497.

Černý, P. and Simpson, F. M. 1977. The Tanco pegmatite at Bernic Lake, Manitoba. IX Beryl. Can. Mineral., 15, 489-499.

Černý, P. and Simpson, F. M., 1978. The Tanco pegmatite at Bernic Lake, Manitoba. X Pollucite. Can. Mineral., 16, 325-333.

Černý, P. and Trueman, D. L., 1978. Distribution and petrogenesis of lithium pegmatites in the western Superior Province of the Canadian shield. Energy, 3, 365-377.

Černý, P. and Turnock, A. C., 1971. Pegmatites of southeastern Manitoba. Geol. Assoc. Can., Spec. Paper 9, 119-127.

Chapman, C. A., 1943. Large magnesia-rich triphylite crystals in pegmatites. Am. Mineral., 28 p. 90.

Charlat, M. and Lévy, C., 1974. Substitutions multiples dans la série tennatite-tetrahédrite. Bull. Soc. fr. Minéral. Crystallogr., 97, 241-250.

Chaudhry, M. N. and Howie, R. A., 1976. Lithium tourmalines from the Meldon aplite, Devonshire, England. Min. Mag., 40, 747-751.

Crouse, R. A., Černý, P., Trueman, D. L. and Burt, R. O., 1979. The Tanco pegmatite, southeastern Manitoba. Can. Mining Met. Bull., 72, No. 802, 142-150.

Davies, J. F., 1957. Geology of the Winnipeg River area (Shatford Lake-Ryerson Lake). Manitoba Mines Br., Publ. 56-1.

Deer, W. A., Howie, R. A. and Zussman, J., 1962. Rock-forming minerals, 1, ortho-and ring-silicates. Longmans London.

Epprecht, W., 1953. Die Gitterkonstanten der Turmalin. Schweiz. Min. Petr. Mitt., 33, p. 481.

Evans, H. T. Jr., Appleman, D. E. and Handwerker, S. S., 1963. The least squares refinement of crystal unit cells with powder diffraction data by an automatic computer indexing method. Amer. Cryst. Ass. Meeting Cambridge, Mass., Abstr. 42.

Farquharson, R. R., 1975. Revised Rb-Sr age of the Lac du Bonnet quartz monzonite, southeastern Manitoba. Can. J. Earth Sci., 12, 115-118.

Faye, G. H., Manning, P. G., Gosselin, J. R. and Tremblay, R. J., 1974. The optical absorption spectra of tourmaline; importance of charge-transfer processes. Can. Mineral., 12, 370-380.

Fersman, A. E., 1931 Ueber die Geochemisch-genetische Klassification der Granitpegmatite. Mineral. Petrog. Mitteil., 41, 64-83.

Foord, E. E., 1976. Mineralogy and petrogenesis of layered pegmatite-aplite dikes in the Mesa Grande District, San Diego County, California. Unpubl. PhD thesis, Stanford University, 326 pp.

Foster, M. D., 1960. Interpretation of the composition of lithium micas. U. S. Geol. Survey, Prof. Paper 354-E.

Ginsburg, A. I., 1960. Specific geochemical features of the pegmatitic process. Rept. XXI, Int. Geol. Congr., Norden, Pt. 17, 111-121.

Gordiyenko, V. V., 1971. Concentration of Li, Rb and Cs in potash feldspars and muscovite as criteria for assessing the rare metal mineralization in granitic pegmatites. Int. Geol. Rev. 2, 13, 134-142.

Grice, J. D., Černý, P. and Ferguson, R. B., 1972. The Tanco pegmatite at Bernic Lake, Manitoba: II Wodginite, pseudo-ixiolite and related minerals. Can. Mineral., 11, 609-642.

Heier, K. S. and Taylor, S. R., 1959. Distribution of Li, Na, K, Rb, Cs, Pb and Tl in southern Norwegian pre-Cambrian Alkali-feldspars. Geochim. Cosmochim. Acta, 15, 284-304.

Heinrich, E. Wm. and Corey, A. S., 1955. Montebrasite from Eight Mile Park, Fremont County, Colorado. Am. Mineral., 40, 1141-1145.

Jahns, R. H. and Burnham, C. W., 1969. Experimental studies of pegmatite genesis: I A model for the derivation and crystallization

of granitic pegmatites. Econ. Geol., 64, 843-864.

Levinson, A. A., 1953. Studies in the mica group; relationship between polymorphism and composition in the muscovite-lepidolite series. Am. Mineral., 38, 88-107.

Loh, S. E. and Wise, W. S., 1976. Synthesis and fluorine-hydroxyl exchange in the amblygonite series. Can. Mineral., 14, 357-363.

Manning, P. G., 1969. An optical absorption study of the origin of colour and pleochroism in pink and brown tourmalines. Can. Mineral., 9, 678-690.

McRitchie, W. D., 1971. The petrology and environment of the acidic plutonic rocks of the Wannipigow-Winnipeg Rivers region, S.E. Manitoba. In Geology and geophysics of the Rice Lake region, S.E. Manitoba. Manitoba Mines Br. Publ. 71-1, 7-62.

Moore, P. B., 1973. Pegmatite phosphates: descriptive mineralogy and crystal chemistry. Mineral. Record, 4, 103-136.

Morse, S.A., 1968. Revised dispersion method for low plagioclase. Am. Mineral., 53, 105-115.

Orville, P. M., 1967. Unit cell parameters of the microcline-low albite and the sanidine-high albite solid solution series. Am. Mineral., 52, 55-86.

Penner, A. P. and Clark, G. S., 1971. Rb-Sr age determinations from the Bird River area, southeastern Manitoba. In Geoscience Studies in Manitoba, A. C.Turnock (ed.), Geol. Assoc. Can. Spec. Paper 9, 105-109.

Rinaldi, R., Černý, P. and Ferguson, R. B., 1972. The Tanco pegmatite at Bernic Lake, Manitoba., VI Lithium-rubidium-cesium micas. Can. Mineral., 11, 690-707.

Smith, F. G., 1948. Transport and deposition of the non-sulphide vein minerals. III Phase relations at the pegmatitic stage. Econ. Geol., 43, 535-546.

Solodov, N. A., 1965. Relationship between ionization potential of elements and the concentration necessary for the formation of their own minerals. Doklady Akad. Nauk S. S. S. R., 165, 190-193.

Springer, G. D., 1950. Mineral deposits of the Cat Lake-Winnipeg River area. Manitoba Mines Br. Publ. 49-7.

Stewart, D. B., 1974. Optic axial angle and extinction angles of alkali feldspars related by cell parameters to Al/Si order and composition. In the feldspars, proceedings of a NATO Advanced Study Institute, Manchester, 1972; ed. W. S. MacKenzie and J. Zussman, Manchester University Press.

Stewart, D. B. 1978. Petrogenesis of lithium rich pegmatites. Am. Mineral., 63, 970-980.

Thomssen, R. W. and Anthony, J. W., 1977. Lithiophilite crystals from the Foote Mine. Mineral. Record, 8, no. 2., 95-99.

Trueman, D. L. and Macek, J. J., 1971. Geology of the Bird River sill. Manitoba Mines Br. Prelim. Map series 1971-A-1.

Wilson, H. D. B., Morrice, M. G., Ziehlke, D. V. and Beakhouse, G. P., 1976. Development of greenstone-granite and gneissie terrains in Archean shields. Centre for Precambrian Studies, University of Manitoba, Annual Report 1976, 2-21.

Winchell, A. N., 1951. Elements of optical mineralogy. Part II. Descriptions of minerals: John Wiley and Sons, New York.

Wright, T. L. and Stewart, D. B., 1968. X-ray and optical study of alkali feldspars: I Determination of composition and structural state from refined unit cell parameters 2V. Am. Mineral., 53, 38-87.